מכון ויצמן למדע

WEIZMANN INSTITUTE OF SCIENCE

Thesis for the degree
Doctor of Philosophy

חבור לשם קבלת התואר
דוקטור לפילוסופיה

By
Limor Landsman

מאת
לימור לנדסמן

חקר מערכת התאים הבלעניים החד-גרעיניים: תפקיד קולטן הכימוקין CX_3CR1 ומקורם של תאים דנדריטיים ומאקרופאג'ים ריאתיים

Studies on the Mononuclear Phagocyte System: the Role of the CX_3CR1 Chemokine Receptor and the Origin of Pulmonary Dendritic Cells and Macrophages

Published papers format

Advisor
Dr. Steffen Jung

מנחה
ד"ר סטפן יונג

September 2007

תשרי, תשס"ח

Submitted to the Scientific Council of the
Weizmann Institute of Science
Rehovot, Israel

מוגש למועצה המדעית של
מכון ויצמן למדע
רחובות, ישראל

Summary

The mononuclear phagocyte system, which plays a central role in innate immune responses, is comprised of macrophages (MΦ), dendritic cells (DC) and monocytes. This PhD thesis aims to study the origin of MΦ and DC, focusing on the pulmonary system. In addition it includes studies on the chemokine receptor requirement of mononuclear phagocyte, focusing on the CX_3CR1 chemokine receptor.

We could show blood monocytes to give rise to both DC and MΦ in the lung parenchyma. Murine blood monocytes are however not a homogenous population, and similarly to human, can be divided into two main $Gr1^{high}$ and $Gr1^{low}$ subsets. Adoptive transfers of fractionated blood monocytes to recipient mice allow the study of their differential contribution to DC and MΦ population. Using this system we found both monocyte subsets to give rise to pulmonary DC under steady state and inflammatory conditions. However, only $Gr1^{low}$ monocytes harbored the immediate potential to give rise to lung MΦ. Our results therefore suggest a distinct differentiation potential of monocyte subsets in the lung, and imply differential requirements for MΦ and DC generation.

The lung comprises the lung parenchyma and the alveolar space, both seeded with MΦ. The origin of alveolar MΦ, the main cell type found in quiescence alveolar space, was for many years a matter of debate. Whereas some studies suggest that these cells rely on a local proliferating precursor for their renewal, other suggested a reliance on BM-derived precursor. In the frame of this PhD thesis we could show that alveolar MΦ originate from blood monocytes. This process is however an indirect one, and requires a lung parenchymal MΦ intermediate. In addition, we found MΦ to proliferate in both lung parenchyma and alveolar space. We therefore suggest that lung parenchymal MΦ serve as a reservoir from which the alveolar MΦ population is renewed whenever needed.

MΦ, DC and monocytes can be divided into subsets, differ in location, activity and gene expression profile. Accordingly, they express distinct repertoire of chemokine receptors, allowing them to differentially respond to environmental signals. One of these chemokine receptors is CX_3CR1, which has a sole ligand, the membrane-tethered CX_3CL1 (Fractalkine).

In the small intestinal lamina propria, CX_3CR1 is mainly expressed by DC. Those cells are marked by their ability to send dendrites that cross the epithelial layer

and can therefore directly sample the intestinal lumen content. Interestingly, the formation of trans epithelial dendrites (TED) is CX_3CR1-depended. Here we show that in the absence of CX_3CR1, and therefore of TED, pathogen uptake from the small intestinal lumen is not impaired. Our result therefore suggest other routes, such as the one involve villous M cell, to play a dominant role in this process. TED formation might however be required for proper response to intestinal pathogens.

All blood monocytes express CX_3CR1, but the chemokine receptor is differentially expressed by the two subsets, in both human and mouse. Murine $Gr1^{high}$ monocytes express low levels of CX_3CR1, while $Gr1^{low}$ are CX_3CR1^{high}. In the frame of this thesis we could show that absence of either CX_3CR1 or it ligand, CX_3CL1, resulted in a significant reduction of $Gr1^{low}$ monocyte levels. Enforced monocyte survival, however, restored this phenotype. In addition, CX_3CL1 specifically rescued cultured monocytes from serum-deprivation induced cells death. Our results therefore suggest a role CX_3CL1-CX_3CR1 in monocyte survival during homeostasis.

CX_3CL1-CX_3CR1 interactions play a role in atherogenesis. Thus, polymorphisms in human CX_3CR1 are associated with protection from this disease, and mice lacking either CX_3CL1 or CX_3CR1 do not develop atherosclerosis in the murine disease model. Here we show that CX_3CL1 provides an essential survival signals for CX_3CR1-expressing monocytes and foam cells, a MΦ population unique to atherosclerotic plaques. Our results suggest that in absence of CX_3CL1-CX_3CR1 interactions, monocyte and foam cell death prevent disease progression.

To conclude, the work presented in this thesis furthers our understanding on the origin of mononuclear phagocytes, and the role blood monocyte play in this process. In addition we defined unique requirements for CX_3CR1 expression by mononuclear phagocytes, which are notably distinct from involvement in cell migration. Our findings therefore shed a light on the differential roles this chemokine receptor plays during steady state and disease.

תקציר

מערכת התאים הבולעניים החד גרעיניים, המשחקת תפקיד מרכזי בתגובה החיסונית המולדת, מורכבת ממקרופאג'ים, תאים דנדריטיים ומונוציטים. מטרתה של תזת דוקטורט זו היא חקר מקורם של מקרופאג'ים ותאים הדנדריטיים, תוך התמקדות במערכת הריאתית כמודל. מטרה נוספת היא חקר התלות של תאים בלעניים חד-גרעיניים בקולטני כימוקינים, תוך התמקדות בקולטן לכימוקין CX_3CL1, הוא CX_3CR1.

ביכולתנו להראות כי מונוציטים ממקור דמי יכולים להתמיין למאקרופאג'ים ולתאים דנדריטיים ברקמת הריאה. מונוציטים עכבריים אינם אוכלוסיה הומוגנית, אלא, בדומה לאלה באדם, יכולים להתחלק לשני תתי-סוגים, $Gr1^{high}$ ו-$Gr1^{low}$. הזרקת סוגי מונוציטים מופרדים לעכברים מקבלים מאפשרת את חקר תרומתם היחסית לאוכלוסיות המאקרופאג'ים והתאים הדנדריטיים. באמצעות מערכת זו מצאנו כי שני סוגי המונוציטים תורמים ליצירת תאים דנדריטיים במצב מנוחה ובזמן דלקת, אבל רק מונוציטים מסוג $Gr1^{low}$ הם בעלי יכולת ישירה ליצירת מקרופאג'ים בריאות. עם כן, תוצאותינו אלה מציאות יכולת התמיינות שונה של סוגי המונוציטים בריאות, ומרמזת על דרישות שונות ליצירת מקרופאג'ים ותאים דנדריטיים.

הריאות מורכבות מרקמת- ומנאדיות-הריאה, המלאים במקרופאג'ים. מקורם של המקרופאג'ים של נאדיות הריאה, המהווים את רוב ההרכב התאי של החלל הריאתי, היה במשך שנים רבות שנוי במחלוקת. בעוד מחקרים מסוימים הראו כי התחדשותם של אוכלוסיית תאים זו תלויה בשגשוג מקומי של תאי מקור, מחקרים אחרים הצביעו על תלות בתא מקור שמוצאו במוח-העצם. במסגרת תזה זו ביכולתנו להראות כי מקור מקרופאג'ים אלה הוא המונוציטים, אך תהליך זה אינו ישיר ודורש שלב ביניים של התמיינות מונוציטים למקרופאג'ים ברקמת הריאה. בנוסף, הראינו שגשוג מקרופאג'ים ברקמת ובנאדיות הריאה. לפי כך, אנחנו מציעים כי מקרופאג'ים ברקמת הריאה משמשים מאגר ממנו מחדשת אוכלוסיית המקרופאג'ים בנאדיות הריאה.

מאקרופאג'ים, תאים דנדריטיים ומונוציטים יכולים להיות ממוינים לתתי סוגים, השונים זה מזה במיקומם, פעילותם ודגם ביטוי הגנים שלהם. בהתאמה, הם שונים בדגם ביטוי קולטני כימוקינים, מה שמאפשר להם להגיב באורך שונה לאותות סביבתיים. קולטן כזה הוא CX_3CR1, בעל ליגנד בודד, הכימוקין CX_3CL1 (Fractalkine).

בלאמינה פרופריה של המעי הדק CX_3CR1 מבוטא בעיקר על ידי תאים דנדריטיים. תאים אלה מאופיינים ביכולתם לשלוח שלוחות החוצות את שכבת האפיתל, המאפשרות דגימה ישירה של תכולת חלל המעי. יצירת שלוחות חוצות-אפיתל אלו היא תלויית CX_3CR1. כאן אנו מראים כי בחוסר של CX_3CR1, ולכן של שלוחות חוצות אפיתל, הכנסת פטוגנים מחלל המעי אינה נפגעת. תוצאות אלה מציעות, עם כן, כי למסלולים חלופיים, כמו זה המערב תאי M המצויים על ה-villi , תפקיד מכריע

בהכנסת פטוגנים. למרות זאת, יתכן ויצירת שלוחות חוצות-אפיתל חיונית לתגובה חיסונית נאותה כנגד פתוגני-המעיים.

כל המונוציטים בדם מבטאים CX_3CR1, אך רמת ביטוייו שונה בין שני תתי הסוגים, הן באדם והן בעכבר. מונוציטים עכבריים מסוג $Gr1^{high}$ מבטאים רמות נמוכות של CX_3CR1, בעוד מונוציטים מסוג $Gr1^{low}$ הם בעלי רמות CX_3CR1 גבוהות. במסגרת תזת דוקטורט זו הראנו כי חסר של CX_3CR1 או הליגנד שלו, CX_3CL1 , גורם לירידה משמעותית ברמות מונוציטים מסוג $Gr1^{low}$. הישרדות כפויה של מונוציטים תיקנה מופע זה. בנוסף, CX_3CL1 הציל באופן ספציפי תרבית מונוציטים ממות הנגרם ממחסור בסרום. לכן, תוצאותינו מציעות תפקיד לCX_3CR1 ו-CX_3CL1 בהישרדות מונוציטים.

מעורבות של CX_3CR1 ו-CX_3CL1 בהתפתחותה של טרשת עורקים (Atherosclerosis) הוצעה בעבר. בהתאם, פולימורפיזם ב-CX_3CR1 הומני קשור להגנה מפני מחלה זו, ועכברים חסרי CX_3CR1 או CX_3CL1 אינם מפתחים טרשת עורקים במודל העכברי שלה. כאן אנו מראים כי CX_3CL1 מספק אותות הישרדות למונוציטים ותאי Foam, אוכלוסיית מאקרופאג'ים ייחודית לטרשת עורקים, המבטאים CX_3CR1. כשחלבונים אלה חסרים, מוות של מונוציטים ותאי Foam מונע התקדמות המחלה.

לסיכום, עבודתנו, כמוצגת בתזה זו, מרחיבה את הבנתנו על מקורם של תאים בלעניים חד-גרעיניים, ועל התפקיד שמונוציטים ממלאים בתהליך זה. כמוכן, עבודתנו מציעה מגוון תפקידים לביטויו של CX_3CR1 על ידי בלעניים חד-גרעיניים, תפקידים שאינם קשורים בנדידת תאים. ממצאינו לפיכך שופכים אור על התפקידים השונים שקולטני כימוקינים ממלאים בזמן מנוחה ודלקת.

Table of Contents

1. Introduction

The mononuclear phagocyte system (MPS) plays an important role in host protection against pathogens, participating in both innate and adaptive immune defense. The MPS can be divided into three main cell subsets: monocytes, macrophages (MΦ) and dendritic cells (DC). MΦ and DC are characterized by the existence of specialized tissue specific representatives, and blood monocytes were also shown to be heterogeneous population (Gordon and Taylor, 2005; Steinman, 1999). Highlighting their functional specialization, monocytes, DC and MΦ subtypes differ in cell surface marker expression, including integrins and chemokine receptors (Gordon, 1999; Gordon and Taylor, 2005; Shortman and Liu, 2002). One such chemokine receptor is the CX_3CL1 (Fractalkine) receptor, CX_3CR1 (Combadiere et al., 1998), which is differentially expressed by blood monocyte and DC subsets (Geissmann et al., 2003; Jung et al., 2000; Landsman et al., 2007; Niess et al., 2005).

1.1. *In Vivo* origins of mononuclear phagocytes

1.1.1. Monocyte origin

Monocytes are non-dividing circulating phagocytes with a short half-life (van Furth and Cohn, 1968). They are characterized by typical morphological features, such as irregular cell shape, bean shaped nuclei and high cytoplasm-to-nucleus ratio (Ziegler-Heitbrock et al., 1988). Monocytes are generated in the BM and are released to the bloodstream, from which they can extravasate to tissues (van Furth and Cohn, 1968). Importantly, we could recently show that monocyte circulate between the BM and the blood under steady state conditions (Varol et al., 2007). Their circulating behavior allows monocytes to rapidly respond to challenges. In addition to their ability to phagocytose blood pathogens, such as *Listeria monocytogenes* (Drevets et al., 2004), monocytes are considered circulating precursors of tissue MΦ and DC, as will elaborated below (van Furth et al., 1973; Randolph, 1999; Geissmann et al., 2003; Landsman et al., 2007). In addition, monocytes were shown to contribute to atherogenesis (Gerrity, 1981) and angiogenesis (De Palma et al., 2005; Grunewald et al., 2006; Landsman, Avraham et al., manuscript in preparation), suggesting their involvement also in non-immunological settings.

Monocytes are not a homogenous population. Human monocytes can be divided into two $CD14^{++}$ and $CD14^{+}CD16^{+}$ subsets {Passlick, 1989 #54}. More recently, monocyte dichotomy has also been established in mice and rats (Palframan et al., 2001; Yrlid et al., 2006). Circulating murine monocytes encompass two main $Gr1^{hi}CX_3CR1^{int}CCR2^{+}$ and $Gr1^{low}CX_3CR1^{hi}CCR2^{-}$ subsets (Palframan et al., 2001; Geissmann et al., 2003), which based on their chemokine receptor expression correlate to human $CD14^{++}$ and $CD14^{+}CD16^{+}$ monocytes, respectively (Geissmann et al., 2003; Gordon and Taylor, 2005). The identification of the murine monocyte subsets allowed studies into their differential function and fates (see below).

Monocytes are BM-derived (van Furth, 1989; van Furth and Cohn, 1968). Recently, Fogg et al. reported the identification of a novel clonotypic BM precursor that gives rise to DC and MΦ, named "MΦ and DC Precursor" (MDP) (Fogg et al., 2006). We could show that MDP are also precursors of BM and blood monocytes (Varol et al., 2007). Interestingly, the kinetics of the monocyte subset generation from MDP differ, with $Gr1^{hi}$ monocytes preceding the appearance of MDP-derived $Gr1^{low}$ monocytes (Varol et al., 2007). Both subsets can be found in BM and blood (Varol et al., 2007), although in different ratios. In wt mice $Gr1^{low}$ monocytes comprise around 40% of blood monocytes, but only 5% of the BM monocyte population (Landsman, Bar-On et al., submitted manuscript). Importantly, $Gr1^{hi}$ monocytes have been shown to convert into $Gr1^{low}$ monocyte (Qu et al., 2004; Sunderkotter et al., 2004; Varol et al., 2007). It remains however unclear where this conversion takes place, i.e. blood, BM or both. To conclude, it MDP-derived $Gr1^{hi}$ monocytes seem to act as precursors for $Gr1^{low}$ monocytes (summarized in Fig. 1).

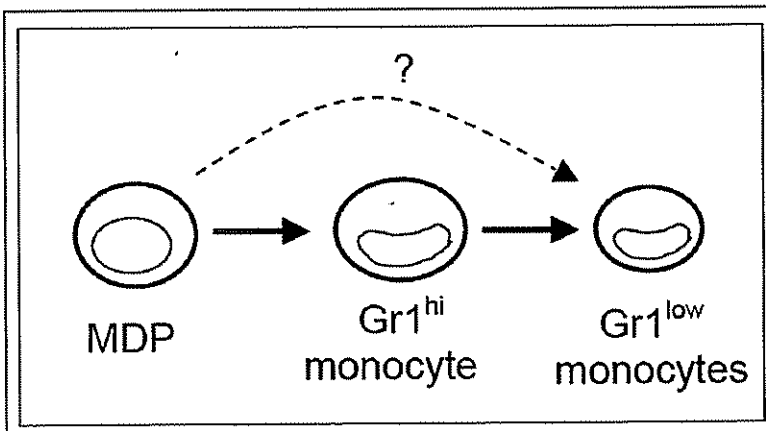

Figure 1: Origin of monocyte subsets

MDP give rise to $Gr1^{hi}$ monocytes in the BM, which can be further converted into $Gr1^{low}$ monocytes. $Gr1^{hi}$ might serve as the sole $Gr1^{low}$ precursor. Alternatively, $Gr1^{low}$ might also originate directly from MDP.

1.1.2. Dendritic cell origin

DC, first identified in 1973 (Steinman and Cohn, 1973), are considered professional antigen-presenting cells (APC), together with MΦ and B cells (Steinman and Cohn, 1974). They are unrivaled in their potency to stimulate naïve T cells and believed to be required to prime most naïve T cells responses (Jung et al., 2002; Steinman and Witmar, 1978). DC are specialized to capture antigens and initiate T-cell immunity, having both antigen-presenting and co-stimulatory functions (Banchereau and Steinman, 1998; Steinman, 1999). Antigen presenting DC can induce either priming of T cells to foreign antigens, or T cell tolerance to self-antigens. Upon antigen uptake DC change their chemokine receptor profile; leave the tissues and home to lymph nodes (LN), where they encounter naïve T cells (Banchereau and Steinman, 1998; Steinman, 1999). Mature DC are typically short-lived cells, even though distinct DC subsets may differ in their life span (Steinman, 1999).

The first evidence suggesting monocytes as origin of DC came from *in vitro* studies, showing the generation of DC from monocytes upon addition of granulocytes-MΦ colony stimulating factor (GM-CSF) (Sallusto and Lanzavecchia, 1994). Subsequently, it was established that monocyte differentiation into DC could also be induced by trans-endothelial trafficking (Randolph et al., 1998). *In vivo*, recent studies implicated a differential reliance of DC subsets on monocytes, as described below.

$CD11c^{hi}$ conventional DC (cDC) can be mainly found in lymphoid tissues, such as spleen and LN. All splenic DC arise from BM-derived precursors (Manz et al., 2001). Monocytes were shown to give rise to cDC under inflammatory conditions (Randolph, 1999; Geissmann et al., 2003; Naik et al., 2006). However, in steady state the renewal of splenic DC population seems not to rely on circulating monocytes (Kabashima et al., 2005; Naik et al., 2006; Varol et al., 2007). Rather, their renewal is dependent on either local proliferating precursor (Naik et al., 2006) or rare circulating cells, distinct from monocytes, such as the MDP (Liu et al., 2007; Varol et al., 2007).

Langerhans cells (LC) are a unique DC subset that resides in skin epidermis. LC maturation results in migration to draining lymph node and was believed to culminate in the activation of antigen-specific T cells (Steinman, 1999). More recent data however challenge this model as it was shown that LC might not directly prime T cells (Allan et al., 2003; Zhao et al., 2003). LC are not replaced by donor cells upon

BM transfer into lethally irradiated recipients, and arise in steady state from radio-resistant, tissue-resident proliferating precursor cells (Krueger et al., 1983; Merad et al., 2002). Interestingly, however, UV-induced skin inflammation results in their replacement by BM donor-derived cells (Merad et al., 2002). More recent work showed these BM-derived cells to be monocytes (Ginhoux et al., 2006).

Intestinal mucosal surfaces are in continuous contact with the endogenous flora and food antigens, as well as foreign microorganisms (Martin and Frevert, 2005). The small intestinal lamina propria is seeded with DC (Niess and Reinecker, 2006), and the role those cells play in pathogen uptake will be discussed elsewhere in this summary. As for their origin, DC in rat intestinal draining LN were shown to originate from grafted monocytes under steady state (Yrlid et al., 2006). In addition, we recently reported that murine monocytes differentiate into lamina propria DC (lpDC) under non-inflammatory conditions (Varol et al., 2007). To conclude, small intestinal DC steady state replenishment seems to dependent on monocytic precursors.

In the lung, a network of airway DC is located immediately above and beneath the basement membrane of respiratory epithelium. Inflammatory conditions result in the recruitment of DC to the alveolar space and lung parenchyma (Gonzalez-Juarrero et al., 2003; Julia et al., 2002). Alveolar DC are strong stimulators of T cell activation (Julia et al., 2002; Lambrecht and Hammad, 2003), and hence thought to play a major role in initiation and maintenance of chronic inflammatory conditions such as asthma (Eisenbarth et al., 2002; Fainaru et al., 2004; Lambrecht et al., 1998). In the frame of this PhD thesis, the role of monocytes as origin of pulmonary DC has been studied. We showed that grafted blood monocytes can give rise to lung and alveolar DC under both steady state and inflammation (Landsman et al., 2007), and established that pulmonary DC do not proliferate (Landsman and Jung, 2007). Our results therefore indicate blood monocytes as pulmonary DC precursor.

To conclude, the origin of DC is organ-dependent. Mucosal DC, such as the ones found in the intestinal and respiratory tract, originate from blood monocytes under non-inflammatory conditions (Landsman et al., 2007; Varol et al., 2007; Yrlid et al., 2006). LC, on the other hand, rely in steady state on local proliferating precursors, but can originate from blood monocytes under inflammation (Ginhoux et al., 2006; Krueger et al., 1983; Merad et al., 2002). Similarly, cDC might originate from blood monocytes under inflammatory condition (Geissmann et al., 2003; Naik et

al., 2006; Randolph, 1999), but seem not to rely on monocytic precursors under steady state (Kabashima et al., 2005; Liu et al., 2007; Naik et al., 2006; Varol et al., 2007) (summarized in Fig. 2).

Figure 2: Context- and tissue-dependent origin of DC

Under steady state conditions, monocytes give rise to mucosal DC (i.e., intestinal and pulmonary DC). Replenishment of cDC, on the other hand, relies on non-monocytic proliferating precursors. Inflammatory conditions allow the generation of both DC types from blood monocytes.

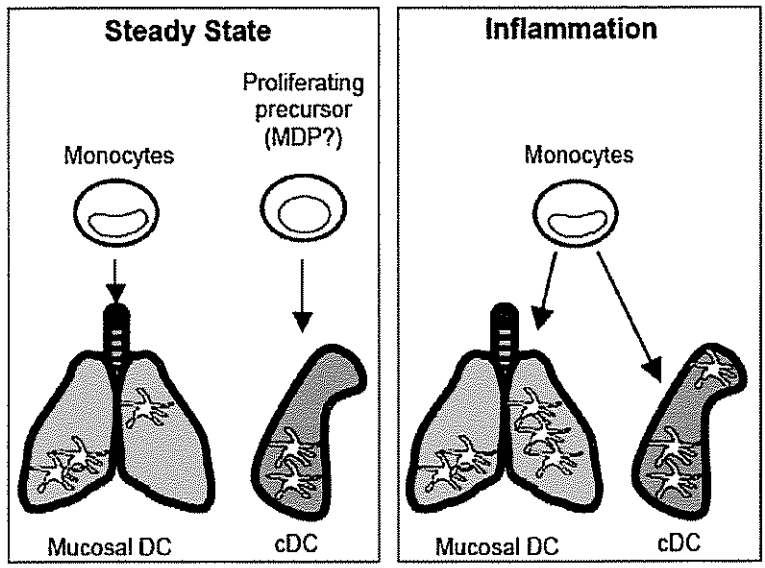

1.1.3. Macrophage Origin

MΦ play a major role in tissue remodeling and as innate enhancers of anti-microbial resistance. First identified by Metchnikoff at the end of the 19th century, MΦ are highly phagocytotic cells, involved in the clearance and destruction of bacteria, non-microbial foreign materials and damaged tissue cells (Gordon, 1999). Even though MΦ express both MHC class I and class II, and are therefore able to present antigen to T cells, they are poor primary stimulators of adaptive immunity. The latter is believed to result from their lack of co-stimulatory molecules (Gordon, 1999; Steinman, 1999). MΦ are widely distributed throughout the body and are generally long-lived cells. However, their life span and phenotype varies depending on their microenvironment (Gordon and Taylor, 2005).

MΦ in the adult are considered to originate from circulating monocytes, which constitutively replenish tissue-resident MΦ populations. This notion is mainly based on studies carried by van Furth *et al.*, showing replenishment of inflammatory peritoneal MΦ by circulating cells (van Furth and Cohn, 1968; van Furth et al., 1973). *In vitro*, addition of MΦ colony stimulating factor (MCSF) can drive cultured

monocytes to acquire a MΦ phenotype (Wiktor-Jedrzejczak and Gordon, 1996). However, studies on the origin of many tissue resident MΦ populations have shown that local proliferation contributes considerably to the renewal and maintenance of different MΦ types, as summarized below.

Osteoclasts are a bone-resident MΦ population reside responsible for bone resorption. Murine monocytes are defined by the expression of the MCSF receptor (MCSF-R), and MCSF-R deficient *op/op* mice show a considerable monocyte reduction (Lagasse and Weissman, 1997; Wiktor-Jedrzejczak et al., 1982). Interestingly, these mice suffer from osteoporosis resulting from a severe reduction of osteoclast numbers (Marks and Lane, 1976), pointing at a role of monocyte as origin of this MΦ subset. The *in vitro* differentiation of blood monocytes into osteoclasts further supports this notion (Matsuzaki et al., 1998; Udagawa et al., 1990). However, a direct *in vivo* connection between monocytes and osteoclasts remains to be shown.

Microglia, the brain-resident MΦ population, is believed to rely on local proliferation during steady state (de Groot et al., 1992; Lawson et al., 1992). Accordingly, microglial cells are not replaced by donor cells upon BM transplantation (de Groot et al., 1992). Inflammatory conditions result however in a rapid recruitment of blood-borne monocytes to the sites of brain injury (Lawson et al., 1992; Priller et al., 2006), and recent work further suggests their differentiation into *bona fide* microglia (Djukic et al., 2006).

Kupffer cells are an important component of the MPS found in the liver. Their origin has been suggested to involve two mechanisms: replenishment by local proliferation, and recruitment of circulating precursors (Bouwens et al., 1986b; Crofton et al., 1978). Although the Kupffer cell population has been shown to depend on BM-derived cells (Naito et al., 1997), they seem not to directly rely on circulating blood monocytes (Bouwens et al., 1986a). To date, the immediate precursor of Kupffer cells remains elusive.

Splenic MΦ are a heterogeneous population, and can be further divided according to their anatomical location. As for their origin, at least some splenic MΦ subsets, such as white-pulp and metallophilic MΦ are replenished by local proliferation under steady state conditions (van Furth and Diesselhoff-den Dulk, 1984; van Rooijen et al., 1989). In addition, circulating precursors contribute to

splenic MΦ populations (van Furth and Diesselhoff-den Dulk, 1984), but the connection to monocytes was never established.

The lung is comprised of the lung parenchyma and the alveolar space both of which are seeded with MΦ. Alveolar MΦ are a unique type of mononuclear phagocytes that populate the external surface of the lung cavity (Martin and Frevert, 2005). Early studies have suggested that alveolar MΦ originate from tissue-resident, local precursors (Bowden and Adamson, 1980; Sawyer et al., 1982; Tarling et al., 1987), while others reported their derivation from circulating cells (Godleski and Brain, 1972; Thomas et al., 1976). BM transfer studies show that even though they can be replaced by donor BM-derived cells, this process takes considerably longer as compared to other cell types (Tarling et al., 1987; Matute-Bello et al., 2004). Although their replacement by BM-derived cells suggests the presence of circulating precursors, the role of monocytes in this process was never directly shown. In the frame of my PhD thesis the origin of alveolar and lung parenchymal MΦ was investigated. Our results showed that blood monocytes could give rise to both lung and alveolar MΦ, albeit with distinct kinetics (Landsman and Jung, 2007; Landsman et al., 2007). We further provided evidence that alveolar MΦ do not directly originate from blood monocytes, but require a parenchymal lung MΦ intermediate (Landsman and Jung, 2007). In addition, we showed that both lung and alveolar MΦ could undergo proliferation (Landsman and Jung, 2007). We therefore suggested lung MΦ to serve as a reservoir from which alveolar MΦ can be generated whenever needed. This model is in line with the results of most previous studies on alveolar MΦ origin. Importantly, it offers a connection between works reporting local precursor and those indicating blood-borne precursor for alveolar MΦ, previously thought to be contradictory.

To conclude, for most MΦ populations a dual origin was suggested, i.e. their derivation from both proliferating precursor and blood circulating precursor. However, the relationship between the two types of precursors, as well as their identities, remain largely unknown. Our work on pulmonary MΦ suggests that monocytes give rise to MΦ, which further divide *in situ* to replenish MΦ population (Landsman and Jung, 2007). This results in reduced dependency of MΦ population on monocyte recruitment. It is therefore possible that the reliance on local proliferation

of monocyte-derived MΦ is true also for other MΦ subsets, such as liver Kupffer cells, osteoclasts and splenic MΦ (summarized in Fig. 3).

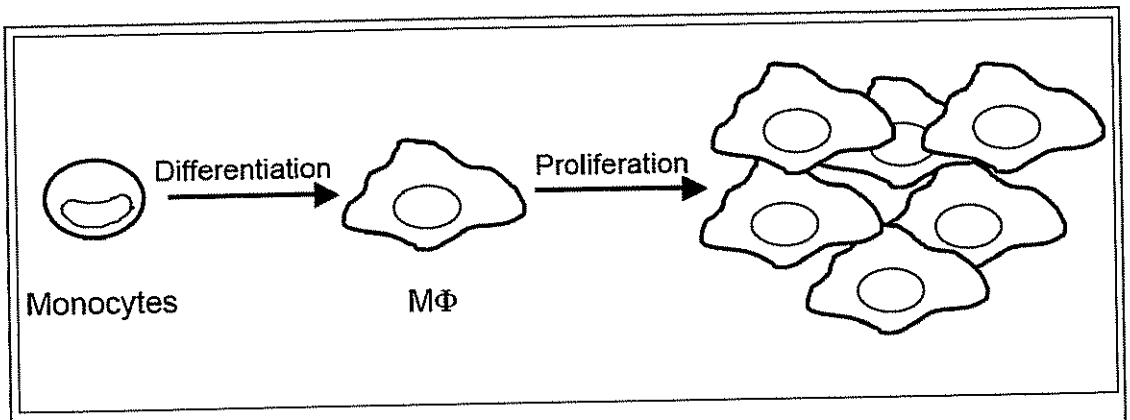

Figure 3: A model for MΦ origin

Blood monocytes give rise to tissue MΦ, which proliferate to replenish the MΦ population.

1.1.4. Differentiation of monocyte subsets

As mentioned above, human and rodent monocytes can be divided into main subsets, with distinct migration properties (Geissmann et al., 2003; Gordon and Taylor, 2005). The identification of these two subsets raised the question whether they are also functionally distinct.

The contribution of the two monocyte subsets to DC populations remains poorly defined. Both the rat counterpart of $Gr1^{low}$ monocytes and mouse $Gr1^{hi}$ monocytes were shown to give rise to DC in the small intestine under non-inflammatory conditions (Yrlid et al., 2006; Varol et al., 2007). Our comparative study in the lung revealed that the two monocyte subsets can differentiate into pulmonary DC under non-inflammatory and inflammatory conditions (Landsman et al., 2007). However, it seems that under challenge $Gr1^{hi}$ are more efficient in this process (Landsman et al., 2007). LC and cDC originate from monocytes only under inflammatory condition, and both were shown to originate from $Gr1^{hi}$ monocytes (Geissmann et al., 2003; Ginhoux et al., 2006). The contribution of $Gr1^{low}$ monocyte to this process was however not directly tested. $Gr1^{hi}$ monocytes express inflammatory chemokine receptors such as CCR2 and CD62L, which are not expressed by $Gr1^{low}$ monocytes, and are therefore more likely to respond to state of inflammation by rapid migration to site of injury (Geissmann et al., 2003). To

conclude, although both monocyte subsets can give rise to DC, they might have differential contributions under inflammation.

The data accumulated on monocytes subsets as MΦ origin are even more scarce. When transferring fractionated blood monocytes to recipient mice we could observe that only $Gr1^{low}$ monocyte could give rise to lung MΦ under both non-inflammatory and inflammatory conditions. Conversion into $Gr1^{low}$ monocytes, however, enabled $Gr1^{hi}$ monocytes to differentiate into lung MΦ (Landsman et al., 2007). We therefore concluded that only the $Gr1^{low}$ monocyte subset harbored the immediate potential to become pulmonary MΦ. In addition, $Gr1^{low}$ monocytes have been implicated as MΦ origin in an inflammatory setting of muscle injury (Arnold et al., 2007). Under these conditions $Gr1^{hi}$ monocytes are recruited to site of injury and convert *in situ* into $Gr1^{low}$ monocytes, which subsequently differentiate into MΦ. Therefore, MΦ generation seems to solely rely on $Gr1^{low}$ monocytes.

To conclude, monocyte subsets seem to differ in their differentiation properties. Only $Gr1^{low}$ monocytes seem to harbor the immediate potential of becoming MΦ. This scenario further suggests distinct requirements for the differentiation into DC and MΦ (summarized in Fig.4).

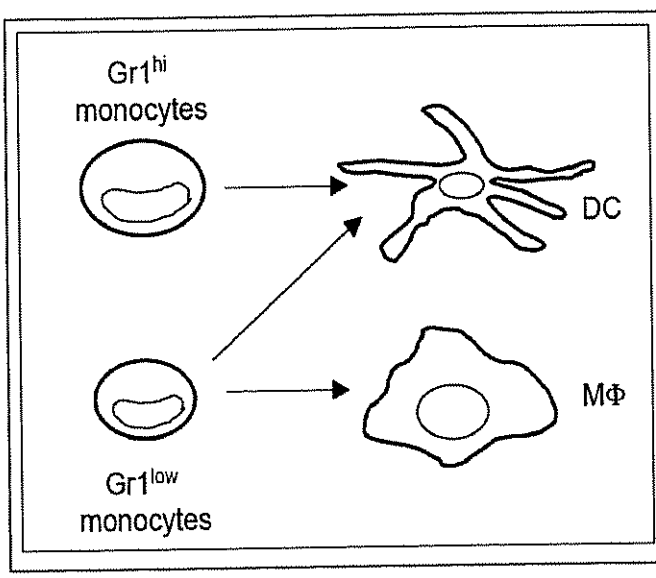

Figure 4: distinct differentiation potential of blood monocyte subsets

Both monocyte subsets can give rise to DC. MΦ can only directly originate from $Gr1^{low}$ monocytes. Upon conversion into $Gr1^{low}$ monocytes, $Gr1^{hi}$ monocytes gain the potential to differentiate into MΦ.

1.2. CX_3CR1 requirement by mononuclear phagocytes

Chemokines are a family of chemotactic cytokines that bind G-protein-coupled, 7-transmembrane receptors. Based on the spacing of N-terminal conserved cysteines, they have been categorized into C, CC, CXC, and CX_3C families (Zlotnik and Yoshie, 2000). CX_3CL1, also known as Fractalkine, is the only known CX_3C chemokine (Bazan et al., 1997; Zlotnik and Yoshie, 2000). CX_3CL1 is synthesized as a transmembrane protein with its chemokine domain presented on an extended mucin-like stalk (Bazan et al., 1997; Pan et al., 1997), which can be released from the cell membrane upon cleavage by metalloproteases (Garton et al., 2001; Hundhausen et al., 2003; Ludwig and Weber, 2007). To date, CX_3CL1 shares this unique membrane-anchorage only with one other chemokine, CXCL16 (Matloubian et al., 2000). CX_3CL1 thus potentially acts as adhesion molecule and chemoattractant, but the importance of these activities for its physiological role remains to be determined. CX_3CL1 expression was reported for activated vascular endothelial cells (Bazan et al., 1997), neurons (Harrison et al., 1998), epithelial cells (Lucas et al., 2001; Muehlhoefer et al., 2000), smooth muscle cells (Ludwig et al., 2002), dendritic cells (DC) (Papadopoulos et al., 1999) and macrophages (Greaves et al., 2001).

CX_3CL1 has one known receptor, CX_3CR1 (Combadiere et al., 1998), which is expressed by T and NK cell subsets (Combadiere et al., 1998; Imai et al., 1997), brain microglia (Harrison et al., 1998; Nishiyori et al., 1998; Jung et al., 2000), DC subsets (Jung et al., 2000; Niess et al., 2005; Landsman et al., 2007) as well as blood monocytes (Imai et al., 1997; Jung et al., 2000). Mice deficient for either CX_3CR1 or CX_3CL1 do not exhibit gross changes in leukocyte migration as compared to their wild type littermates (Cook et al., 2001; Jung et al., 2000). For instance, absence of CX_3CR1 interfered neither with monocyte extravasation nor with DC migration under inflammatory settings (Jung et al., 2000). As will be elaborated below, CX_3CR1 deficiency was however shown to be associated with other phenotypes, including reduced atherosclerosis in men and mice (Combadiere et al., 2003; Lesnik et al., 2003; McDermott et al., 2001; Moatti et al., 2001; Teupser et al., 2004), reduced cardiac allograft rejection (Robinson et al., 2000) and lack of trans-epithelial dendrite formation by small intestinal lamina propria DC (Niess et al., 2005). A part of this PhD thesis focused on the functional role of CX_3CR1 expression by mononuclear phagocytes, in order to better understand its *in vivo* function.

1.2.1. CX_3CR1 requirement by small intestinal lamina propria dendritic cell

Intestinal mucosal surfaces are in continuous contact with the endogenous flora and food antigens as well as foreign microorganisms. The decision whether to respond to environmental antigens by active suppression or protective immune responses, appears to depend, in part, on initial recognition by the innate immune system (Didierlaurent et al., 2002). Three pathways can mediate transport of antigens across epithelial barriers: absorptive epithelial cells (enterocyte), M cell and DC (summarize in Fig. 5). Enterocytes can present processed antigens to intraepithelial lymphocytes (IEL), but since they lack co-stimulatory functions, they are thought to induce suppression, rather than activation, of naïve T cells (Didierlaurent et al., 2002). M cells are specialized epithelial cells with the ability to efficiently deliver foreign material samples from the intestinal lumen (Neutra et al., 2001). M cells were originally shown to be localized above the sub-epithelial dome of the Peyers's patches, but recently a population of villous M cells have been identified (Jang et al., 2004). Antigens transported by M cells are then being captured by immature DC, which in turn initiate T cell response (Didierlaurent et al., 2002).

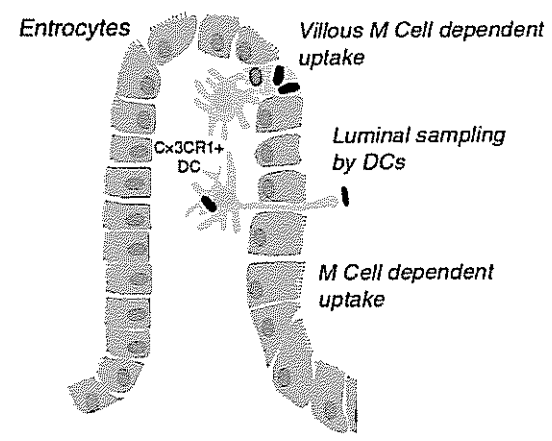

Figure 5: Routes of sampling the small intestinal lumen
(Adopted from Niess and Reinecker, 2006)

A third pathway of antigen sampling and presentation in the small intestine is formed by DC themselves (Niess and Reinecker, 2006). Lamina propria DC (lpDC) were shown to have the capacity to directly sample the small intestinal content by sending dendrites that cross the epithelial barrier into the lumen (Niess et al., 2005; Rescigno et al., 2001)(Figure 5). Penetration of the epithelial barrier is achieved by the ability of DC to open epithelial tight junctions (Rescigno et al., 2001). The projection of transepithelial dendrites (TED) seems to be induced by the presence of gut pathogens (Niess et al., 2005; Vallon-Eberhard, Landsman et al., 2006).

LpDC express CX_3CR1, and are the main CX_3CR1-expressing cells localized in the intestinal villi (Niess et al., 2005; Vallon-Eberhard, Landsman et al., 2006). Surprisingly, we found, in collaboration with a group at Harvard, that lpDC of CX_3CR1 KO mice are unable to form TED (Niess et al., 2005). We therefore investigated how lack of CX_3CR1, and therefore of TED, effects pathogen uptake into the small intestine. Uptake of non-invasive *Aspergillus fumigatus* conidia into the small intestinal lamina propria was unaffected by the absence of CX_3CR1 and TED (Vallon-Eberhard, Landsman et al., 2006). Moreover, depletion of both lamina propria MΦ and DC also did not affect pathogen uptake. This suggests that alternative routes, such as the one mediated by villous M cells, play a major role in the active uptake of pathogens into the small intestine lamina propria (Vallon-Eberhard, Landsman et al., 2006). It however might as well be that TED are required to initiate appropriate immune responses without actively participating in pathogen uptake. The role of the CX_3CR1-dependent TED therefore remains an open question.

1.2.2. CX_3CR1 requirement by blood monocytes

All blood monocyte express CX_3CR1, but the level of receptor expression differs between the two subsets: mouse $Gr1^{hi}$ and human $CD14^{++}CD16^{-}$ monocytes are CX_3CR1^{int}, whereas mouse $Gr1^{low}$ and human $CD14^{+}CD16^{+}$ are CX_3CR1^{hi} (Geissmann et al., 2003; Jung et al., 2000). In the frame of this PhD thesis the role of CX_3CR1 expression by monocytes has been studied (summarized in Landsman, Bar-On et al., submitted manuscript).

CX_3CL1 mice were reported to have a reduction in their blood monocyte levels (Cook et al., 2001). We could show that this specifically affects the levels of $Gr1^{low}$ monocytes, both in the blood of CX_3CL1 and CX_3CR1-deficient mice. However, enforced monocytic expression of the anti-apoptotic factor Bcl2 (Lagasse and Weissman, 1994) reverted the phenotype, providing genetic evidence that this reduction results from impaired monocyte survival. In support of the *in vivo* data, recombinant CX_3CL1 specifically rescued cultured human monocytes from serum deprivation-induced death (Landsman, Bar-On et al., submitted manuscript). These result are in agreement with earlier reports showing that CX_3CR1-CX_3CL1 interactions trigger the PI3K/Akt signaling pathway in cell lines and cultured brain microglia, resulting in cell survival and proliferation (Boehme et al., 2000; Brand et

al., 2002; Chandrasekar et al., 2003; Davis and Harrison, 2006). Our data therefore offer *in vivo* evidence for the role of the CX_3C chemokine family in providing survival signals required for monocyte homeostasis.

1.2.3. CX_3CR1 requirement during atherosclerosis

Atherosclerosis is characterized by accumulation of lipids and fibrous elements in the large arteries (Libby, 2002). One of the first events in the disease progression is the migration of monocytes into the arterial intima, where they are believed to give rise to foam cells (Bobryshev, 2006). Foam cell are a specialized MΦ subset found in atherosclerotic plaques, which accumulate large amounts of intracellular cholesterol and are considered to play a central role in the disease development (Libby, 2002). Accordingly, increased apoptosis of foam cell during early stages of atherogenesis impaired disease progression (Tabas, 2005).

In humans, a polymorphism of the chemokine receptor CX_3CR1 was reported to be associated with reduced susceptibility to atherosclerosis and coronary artery disease (McDermott et al., 2001; Moatti et al., 2001). Accordingly, mice deficient for CX_3CR1 or its ligand CX_3CL1 are protected from atherogenesis in the respective murine disease models (Combadiere et al., 2003; Lesnik et al., 2003; Teupser et al., 2004). Furthermore, CX_3CL1 was found to be abundantly expressed in atherosclerotic plaques, mainly by smooth muscle cells and endothelial cells (Lesnik et al., 2003). CX_3CR1, on the other hand, is expressed by monocytes and foam cell in the plaques (Barlic et al., 2006; Landsman, Bar-On et al., submitted manuscript). The mechanism through which CX_3CL1-CX_3CR1 interaction controls atherogenesis is however yet to be revealed.

CX_3CL1 acts as monocyte survival factor during steady state, and could play a similar role during atherogenesis. We therefore investigated the role CX_3CL1-CX_3CR1 interaction plays in a murine atherosclerosis model; $ApoE^{-/-}$ mice that develop atherosclerotic plaques when subjected to high fat diet (Plump et al., 1992). As mentioned above, CX_3CR1 KO mice show reduced atherogenesis in this model, as compared to their wt littermates (Combadiere et al., 2003; Lesnik et al., 2003). However, enforced survival of monocytes and foam cells in CX_3CR1 KO mice by human Bcl2 transgene expression restored their atherogenesis levels to those found in wt mice (Landsman, Bar-On et al., submitted manuscript). This suggests that

CX_3CL1-CX_3CR1 interaction provides essential survival signals to monocyte and foam cells for disease progression (summarized in Fig. 6).

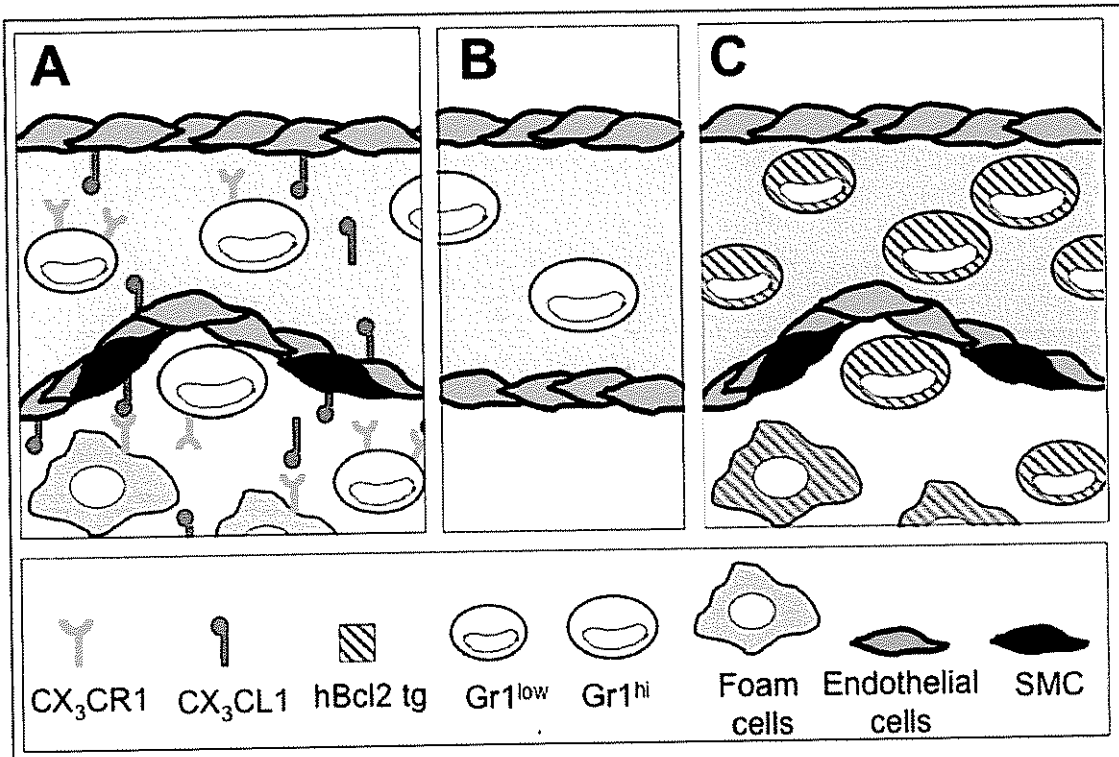

Figure 6: CX_3CL1-CX_3CR1 interaction provides survival signals essential for monocyte homeostasis and atherogenesis

A) CX_3CL1, expressed by endothelial cells, provides survival signals for blood $Gr1^{low}CX_3CR1^{hi}$ monocytes. During atherogenesis, CX_3CL1 is expressed by endothelial and smooth muscle cells, and acts as survival factor for CX_3CR1-expressing cells in the plaque, including monocytes and foam cells.
B) In the absence of either CX_3CL1 or CX_3CR1, the numbers of blood $Gr1^{low}$ monocytes are reduced. Increased death of plaque foam cells and monocytes inhibits atherosclerosis progression.
C) Enforced survival of blood monocytes, by human Bcl2 transgene expression, allows high $Gr1^{low}$ monocyte levels in the absence of CX_3CL1-CX_3CR1 interaction. Such enforced survival of monocytes and foam cells in the plaque allows also atherosclerosis development in CX_3CR1 and CX_3CL1 absence.

To conclude, despite its chemotactic potential, the main phenotypes associated with CX_3CR1-deficiency do not support its role in cell migration. Rather CX_3CL1-CX_3CR1 interactions promote the activation of intracellular signaling pathways that result in cell survival and the formation of membranal extensions.

1.3. Concluding remarks

The Jung laboratory aims to investigate the origin and function of mononuclear phagocytes, on both cellular and molecular levels. To this end we make use of a novel and cell type-specific cell ablation system, in combination with adoptive precursor cell transfers. Better understanding of mononuclear phagocyte function further requires the identification of molecular components expressed by these cells, and the definition of their role in proper cell function. Here our laboratory focuses on the CX_3CR1 chemokine receptor, which is broadly expressed by mononuclear phagocytes, but whose function remains unknown.

In this PhD thesis I studied the role of monocytes as origin of DC and MΦ, focusing on the pulmonary system as a model. In addition I investigated CX_3CR1 chemokine receptor requirement by monocyte, MΦ and DC subsets, and investigated how it absence effects their function and fate.

Using a conditional cell ablation system allowing the specific depletion of $CD11c^{high}$ DC, we were able to show a differential requirement of DC subsets, including cDC and plasmacytoid DC, for T cell priming (Jung et al., 2002; Sapoznikov et al., 2007). cDC, however, are not a homogeneous population, and can be divided to functionally distinct subsets based on surface marker expression (Shortman and Liu, 2002). Accordingly, studying CX_3CR1 expression by splenic cDC allowed us to identify a novel and new DC subset (Birnberg, Bar-On et al., manuscript in preparation). Besides considerable heterogeneity in the spleen, we have defined DC in the lamina propria (lpDC) of the lung and the small intestine according to their CX_3CR1 expression (Niess et al., 2005; Vallon-Eberhard, Landsman et al., 2006). In order to investigate the role of CX_3CR1 expression by these cells, we studied their function in its absence, and found that CX_3CR1 deficiency prevented the formation of trans-epithelial dendrites (TED) by lpDC (Niess et al., 2005). The absence of TED allowed us to probe for the function of these unique structures. Surprisingly, we found - despite the prevailing claims – that they were dispensable for pathogen sampling from the intestinal lumen. Thus pathogen uptake was unimpaired in the absence of TED formation by lpDC, and even in absence of lpDC (Vallon-Eberhard, Landsman et al., 2006). These studies highlight how the combination of cellular and molecular studies can further our understanding of DC and DC subset functions.

In addition to its expression by DC subsets, CX_3CR1 is also prominently expressed by circulating blood monocytes (Jung et al., 2000; Geissmann et al., 2003) and certain terminally differentiated macrophages (Jung et al., 2000; Landsman, Bar-On et al., submitted manuscript). Using the CX_3CR1^{GFP} system, we could show that the chemokine receptor is required for the survival of one of the main blood monocyte subsets ($Gr1^{low}CX_3CR1^{hi}$) during homeostasis (Landsman, Bar-On et al., submitted manuscript). We could further demonstrate that CX_3CR1 interactions with its ligand promote survival of monocyte and/or MΦ population (i.e., foam cell) within atherosclerotic plaques (Landsman, Bar-On et al., submitted manuscript). Interestingly, CX_3CR1 deficiency resulted in the reduction of the plaque areas and the prevention of disease progression, thus potentially providing the mechanistic explanation for CX_3CR1 function, and highlighting the important role monocytes and MΦ play in this process.

A better understanding of the *in vivo* origins of monocytes, DC and MΦ might eventually allow the development of protocols for their future manipulation. We were able to identify the BM precursor of blood monocytes, and directly show that the $Gr1^{high}CX_3CR1^{int}$ cells can *in vivo* give rise to $Gr1^{low}CX_3CR1^{hi}$ monocytes (Varol et al., 2007). As for their fate in the periphery, we showed that under non-inflammatory conditions blood monocytes give rise to mucosal DC and MΦ (Landsman et al., 2007; Landsman and Jung, 2007; Varol et al., 2007). Moreover, focusing on the respiratory tract we demonstrated the two blood monocyte subsets to harbor a distinct differentiation potential to become either MΦ or DC (Landsman et al., 2007). Given the distinct fates of monocytes in different tissues, these studies highlight the importance of elucidating the differential potential of monocytes *in vivo*. Importantly, a key for better understanding of monocyte biology is likely to lie in the revelation of the molecular differences between the two monocyte subsets, which eventually might allow the control of their fate.

Cells of the mononuclear phagocytes system play a role in almost all aspects of the immune response. The combined efforts to study mononuclear biology, on the molecular and cellular level, allowed us to better understand the physiological roles of these cells. They also enabled us to further dissect known cell populations into unique subsets. Future efforts to identify cell subsets within the mononuclear phagocyte system, including the understanding of their different function and molecular

requirement, will allow a full mapping of this unique system. Finally, the understanding of their origin, including the definition of the molecular cues that govern differentiation, might allow the *in vivo* manipulation of mononuclear phagocytes. Given their central role in innate and adaptive immune responses, such manipulation might allow a "costume-made" immune system, preventing conditions such as allergic and autoimmune responses.

1.4. References

Allan, R. S., Smith, C. M., Belz, G. T., van Lint, A. L., Wakim, L. M., Heath, W. R., and Carbone, F. R. (2003). Epidermal viral immunity induced by CD8alpha+ dendritic cells but not by Langerhans cells. Science *301*, 1925-1928.

Arnold, L., Henry, A., Poron, F., Baba-Amer, Y., van Rooijen, N., Plonquet, A., Gherardi, R. K., and Chazaud, B. (2007). Inflammatory monocytes recruited after skeletal muscle injury switch into antiinflammatory macrophages to support myogenesis. J Exp Med *204*, 1057-1069.

Banchereau, J., and Steinman, R. M. (1998). Dendritic cells and the control of immunity. Nature *392*, 245-252.

Barlic, J., Zhang, Y., Foley, J. F., and Murphy, P. M. (2006). Oxidized lipid-driven chemokine receptor switch, CCR2 to CX3CR1, mediates adhesion of human macrophages to coronary artery smooth muscle cells through a peroxisome proliferator-activated receptor gamma-dependent pathway. Circulation *114*, 807-819.

Bazan, J. F., Bacon, K. B., Hardiman, G., Wang, W., Soo, K., Rossi, D., Greaves, D. R., Zlotnik, A., and Schall, T. J. (1997). A new class of membrane-bound chemokine with a CX3C motif. Nature *385*, 640-644.

Bobryshev, Y. V. (2006). Monocyte recruitment and foam cell formation in atherosclerosis. Micron *37*, 208-222.

Boehme, S. A., Lio, F. M., Maciejewski-Lenoir, D., Bacon, K. B., and Conlon, P. J. (2000). The chemokine fractalkine inhibits Fas-mediated cell death of brain microglia. J Immunol *165*, 397-403.

Bouwens, L., Baekeland, M., De Zanger, R., and Wisse, E. (1986a). Quantitation, tissue distribution and proliferation kinetics of Kupffer cells in normal rat liver. Hepatology *6*, 718-722.

Bouwens, L., Knook, D. L., and Wisse, E. (1986b). Local proliferation and extrahepatic recruitment of liver macrophages (Kupffer cells) in partial-body irradiated rats. J Leukoc Biol *39*, 687-697.

Bowden, D. H., and Adamson, I. Y. (1980). Role of monocytes and interstitial cells in the generation of alveolar macrophages I. Kinetic studies of normal mice. Lab Invest *42*, 511-517.

Brand, S., Sakaguchi, T., Gu, X., Colgan, S. P., and Reinecker, H. C. (2002). Fractalkine-mediated signals regulate cell-survival and immune-modulatory responses in intestinal epithelial cells. Gastroenterology *122*, 166-177.

Chandrasekar, B., Mummidi, S., Perla, R. P., Bysani, S., Dulin, N. O., Liu, F., and Melby, P. C. (2003). Fractalkine (CX3CL1) stimulated by nuclear factor kappaB (NF-kappaB)-dependent inflammatory signals induces aortic smooth muscle cell proliferation through an autocrine pathway. Biochem J *373*, 547-558.

Combadiere, C., Potteaux, S., Gao, J. L., Esposito, B., Casanova, S., Lee, E. J., Debre, P., Tedgui, A., Murphy, P. M., and Mallat, Z. (2003). Decreased atherosclerotic lesion formation in CX3CR1/apolipoprotein E double knockout mice. Circulation *107*, 1009-1016.

Combadiere, C., Salzwedel, K., Smith, E. D., Tiffany, H. L., Berger, E. A., and Murphy, P. M. (1998). Identification of CX3CR1. A chemotactic receptor for the human CX3C chemokine fractalkine and a fusion coreceptor for HIV-1. J Biol Chem *273*, 23799-23804.

Cook, D. N., Chen, S. C., Sullivan, L. M., Manfra, D. J., Wiekowski, M. T., Prosser, D. M., Vassileva, G., and Lira, S. A. (2001). Generation and analysis of mice lacking the chemokine fractalkine. Mol Cell Biol *21*, 3159-3165.

Crofton, R. W., Diesselhoff-den Dulk, M. M., and van Furth, R. (1978). The origin, kinetics, and characteristics of the Kupffer cells in the normal steady state. J Exp Med *148*, 1-17.

Davis, C. N., and Harrison, J. K. (2006). Proline 326 in the C terminus of murine CX3CR1 prevents G-protein and phosphatidylinositol 3-kinase-dependent stimulation of Akt and extracellular signal-regulated kinase in Chinese hamster ovary cells. J Pharmacol Exp Ther *316*, 356-363.

De Palma, M., Venneri, M. A., Galli, R., Sergi Sergi, L., Politi, L. S., Sampaolesi, M., and Naldini, L. (2005). Tie2 identifies a hematopoietic lineage of proangiogenic monocytes required for tumor vessel formation and a mesenchymal population of pericyte progenitors. Cancer Cell *8*, 211-226.

de Groot, C. J., Huppes, W., Sminia, T., Kraal, G., and Dijkstra, C. D. (1992). Determination of the origin and nature of brain macrophages and microglial cells in mouse central nervous system, using non-radioactive in situ hybridization and immunoperoxidase techniques. Glia *6*, 301-309.

Didierlaurent, A., Sirard, J. C., Kraehenbuhl, J. P., and Neutra, M. R. (2002). How the gut senses its content. Cell Microbiol *4*, 61-72.

Djukic, M., Mildner, A., Schmidt, H., Czesnik, D., Bruck, W., Priller, J., Nau, R., and Prinz, M. (2006). Circulating monocytes engraft in the brain, differentiate into microglia and contribute to the pathology following meningitis in mice. Brain *129*, 2394-2403.

Drevets, D. A., Dillon, M. J., Schawang, J. S., Van Rooijen, N., Ehrchen, J., Sunderkotter, C., and Leenen, P. J. (2004). The Ly-6Chigh monocyte subpopulation transports Listeria monocytogenes into the brain during systemic infection of mice. J Immunol *172*, 4418-4424.

Eisenbarth, S. C., Piggott, D. A., Huleatt, J. W., Visintin, I., Herrick, C. A., and Bottomly, K. (2002). Lipopolysaccharide-enhanced, toll-like receptor 4-dependent T helper cell type 2 responses to inhaled antigen. J Exp Med *196*, 1645-1651.

Fainaru, O., Woolf, E., Lotem, J., Yarmus, M., Brenner, O., Goldenberg, D., Negreanu, V., Bernstein, Y., Levanon, D., Jung, S., and Groner, Y. (2004). Runx3 regulates mouse TGF-beta-mediated dendritic cell function and its absence results in airway inflammation. Embo J *23*, 969-979.

Fogg, D. K., Sibon, C., Miled, C., Jung, S., Aucouturier, P., Littman, D. R., Cumano, A., and Geissmann, F. (2006). A clonogenic bone marrow progenitor specific for macrophages and dendritic cells. Science *311*, 83-87.

Garton, K. J., Gough, P. J., Blobel, C. P., Murphy, G., Greaves, D. R., Dempsey, P. J., and Raines, E. W. (2001). Tumor necrosis factor-alpha-converting enzyme (ADAM17) mediates the cleavage and shedding of fractalkine (CX3CL1). J Biol Chem *276*, 37993-38001.

Geissmann, F., Jung, S., and Littman, D. R. (2003). Blood monocytes consist of two principal subsets with distinct migratory properties. Immunity *19*, 71-82.

Gerrity, R. G. (1981). The role of the monocyte in atherogenesis: I. Transition of blood-borne monocytes into foam cells in fatty lesions. Am J Pathol *103*, 181-190.

Ginhoux, F., Tacke, F., Angeli, V., Bogunovic, M., Loubeau, M., Dai, X. M., Stanley, E. R., Randolph, G. J., and Merad, M. (2006). Langerhans cells arise from monocytes in vivo. Nat Immunol *7*, 265-273.

Godleski, J. J., and Brain, J. D. (1972). The origin of alveolar macrophages in mouse radiation chimeras. J Exp Med *136*, 630-643.

Gonzalez-Juarrero, M., Shim, T. S., Kipnis, A., Junqueira-Kipnis, A. P., and Orme, I. M. (2003). Dynamics of macrophage cell populations during murine pulmonary tuberculosis. J Immunol *171*, 3128-3135.

Gordon, S. (1999). Macrophages and the immune response. In Fundomental Immunology, W. E. Paul, ed. (Philadelphia, Lippincott-Raven), pp. 533-545.

Gordon, S., and Taylor, P. R. (2005). Monocyte and macrophage heterogeneity. Nat Rev Immunol *5*, 953-964.

Greaves, D. R., Hakkinen, T., Lucas, A. D., Liddiard, K., Jones, E., Quinn, C. M., Senaratne, J., Green, F. R., Tyson, K., Boyle, J., *et al.* (2001). Linked chromosome 16q13 chemokines, macrophage-derived chemokine, fractalkine, and thymus- and activation-regulated chemokine, are expressed in human atherosclerotic lesions. Arterioscler Thromb Vasc Biol *21*, 923-929.

Grunewald, M., Avraham, I., Dor, Y., Bachar-Lustig, E., Itin, A., Jung, S., Chimenti, S., Landsman, L., Abramovitch, R., and Keshet, E. (2006). VEGF-induced adult neovascularization: recruitment, retention, and role of accessory cells. Cell *124*, 175-189.

Harrison, J. K., Jiang, Y., Chen, S., Xia, Y., Maciejewski, D., McNamara, R. K., Streit, W. J., Salafranca, M. N., Adhikari, S., Thompson, D. A., *et al.* (1998). Role for neuronally derived fractalkine in mediating interactions between neurons and CX3CR1-expressing microglia. Proc Natl Acad Sci U S A *95*, 10896-10901.

Hundhausen, C., Misztela, D., Berkhout, T. A., Broadway, N., Saftig, P., Reiss, K., Hartmann, D., Fahrenholz, F., Postina, R., Matthews, V., *et al.* (2003). The disintegrin-like metalloproteinase ADAM10 is involved in constitutive cleavage of CX3CL1 (fractalkine) and regulates CX3CL1-mediated cell-cell adhesion. Blood *102*, 1186-1195.

Imai, T., Hieshima, K., Haskell, C., Baba, M., Nagira, M., Nishimura, M., Kakizaki, M., Takagi, S., Nomiyama, H., Schall, T. J., and Yoshie, O. (1997). Identification and molecular characterization of fractalkine receptor CX3CR1, which mediates both leukocyte migration and adhesion. Cell *91*, 521-530.

Jang, M. H., Kweon, M. N., Iwatani, K., Yamamoto, M., Terahara, K., Sasakawa, C., Suzuki, T., Nochi, T., Yokota, Y., Rennert, P. D., *et al.* (2004). Intestinal villous M cells: an antigen entry site in the mucosal epithelium. Proc Natl Acad Sci U S A *101*, 6110-6115.

Julia, V., Hessel, E. M., Malherbe, L., Glaichenhaus, N., O'Garra, A., and Coffman, R. L. (2002). A restricted subset of dendritic cells captures airborne antigens and remains able to activate specific T cells long after antigen exposure. Immunity *16*, 271-283.

Jung, S., Aliberti, J., Graemmel, P., Sunshine, M. J., Kreutzberg, G. W., Sher, A., and Littman, D. R. (2000). Analysis of fractalkine receptor CX(3)CR1 function by targeted deletion and green fluorescent protein reporter gene insertion. Mol Cell Biol *20*, 4106-4114.

Jung, S., Unutmaz, D., Wong, P., Sano, G., De los Santos, K., Sparwasser, T., Wu, S., Vuthoori, S., Ko, K., Zavala, F., *et al.* (2002). In vivo depletion of CD11c(+)

dendritic cells abrogates priming of CD8(+) T cells by exogenous cell-associated antigens. Immunity *17*, 211-220.

Kabashima, K., Banks, T. A., Ansel, K. M., Lu, T. T., Ware, C. F., and Cyster, J. G. (2005). Intrinsic lymphotoxin-beta receptor requirement for homeostasis of lymphoid tissue dendritic cells. Immunity *22*, 439-450.

Krueger, G. G., Daynes, R. A., and Emam, M. (1983). Biology of Langerhans cells: selective migration of Langerhans cells into allogeneic and xenogeneic grafts on nude mice. Proc Natl Acad Sci U S A *80*, 1650-1654.

Lagasse, E., and Weissman, I. L. (1994). bcl-2 inhibits apoptosis of neutrophils but not their engulfment by macrophages. J Exp Med *179*, 1047-1052.

Lagasse, E., and Weissman, I. L. (1997). Enforced expression of Bcl-2 in monocytes rescues macrophages and partially reverses osteopetrosis in op/op mice. Cell *89*, 1021-1031.

Lambrecht, B. N., and Hammad, H. (2003). Taking our breath away: dendritic cells in the pathogenesis of asthma. Nat Rev Immunol *3*, 994-1003.

Lambrecht, B. N., Salomon, B., Klatzmann, D., and Pauwels, R. A. (1998). Dendritic cells are required for the development of chronic eosinophilic airway inflammation in response to inhaled antigen in sensitized mice. J Immunol *160*, 4090-4097.

Landsman, L., and Jung, S. (2007). Lung Macrophages Serve as Obligatory Intermediate between Blood Monocytes and Alveolar Macrophages. J Immunol *179*, 3488-3494.

Landsman, L., Varol, C., and Jung, S. (2007). Distinct differentiation potential of blood monocyte subsets in the lung. J Immunol *178*, 2000-2007.

Lawson, L. J., Perry, V. H., and Gordon, S. (1992). Turnover of resident microglia in the normal adult mouse brain. Neuroscience *48*, 405-415.

Lesnik, P., Haskell, C. A., and Charo, I. F. (2003). Decreased atherosclerosis in CX3CR1-/- mice reveals a role for fractalkine in atherogenesis. J Clin Invest *111*, 333-340.

Libby, P. (2002). Inflammation in atherosclerosis. Nature *420*, 868-874.

Liu, K., Waskow, C., Liu, X., Yao, K., Hoh, J., and Nussenzweig, M. (2007). Origin of dendritic cells in peripheral lymphoid organs of mice. Nat Immunol *8*, 578-583.

Lucas, A. D., Chadwick, N., Warren, B. F., Jewell, D. P., Gordon, S., Powrie, F., and Greaves, D. R. (2001). The transmembrane form of the CX3CL1 chemokine fractalkine is expressed predominantly by epithelial cells in vivo. Am J Pathol *158*, 855-866.

Ludwig, A., Berkhout, T., Moores, K., Groot, P., and Chapman, G. (2002). Fractalkine is expressed by smooth muscle cells in response to IFN-gamma and TNF-alpha and is modulated by metalloproteinase activity. J Immunol *168*, 604-612.

Ludwig, A., and Weber, C. (2007). Transmembrane chemokines: versatile 'special agents' in vascular inflammation. Thromb Haemost *97*, 694-703.

Manz, M. G., Traver, D., Akashi, K., Merad, M., Miyamoto, T., Engleman, E. G., and Weissman, I. L. (2001). Dendritic cell development from common myeloid progenitors. Ann N Y Acad Sci *938*, 167-173; discussion 173-164.

Marks, S. C., Jr., and Lane, P. W. (1976). Osteopetrosis, a new recessive skeletal mutation on chromosome 12 of the mouse. J Hered *67*, 11-18.

Martin, T. R., and Frevert, C. W. (2005). Innate immunity in the lungs. Proc Am Thorac Soc *2*, 403-411.

Matloubian, M., David, A., Engel, S., Ryan, J. E., and Cyster, J. G. (2000). A transmembrane CXC chemokine is a ligand for HIV-coreceptor Bonzo. Nat Immunol *1*, 298-304.

Matsuzaki, K., Udagawa, N., Takahashi, N., Yamaguchi, K., Yasuda, H., Shima, N., Morinaga, T., Toyama, Y., Yabe, Y., Higashio, K., and Suda, T. (1998). Osteoclast differentiation factor (ODF) induces osteoclast-like cell formation in human peripheral blood mononuclear cell cultures. Biochem Biophys Res Commun *246*, 199-204.

Matute-Bello, G., Lee, J. S., Frevert, C. W., Liles, W. C., Sutlief, S., Ballman, K., Wong, V., Selk, A., and Martin, T. R. (2004). Optimal timing to repopulation of resident alveolar macrophages with donor cells following total body irradiation and bone marrow transplantation in mice. J Immunol Methods *292*, 25-34.

McDermott, D. H., Halcox, J. P., Schenke, W. H., Waclawiw, M. A., Merrell, M. N., Epstein, N., Quyyumi, A. A., and Murphy, P. M. (2001). Association between polymorphism in the chemokine receptor CX3CR1 and coronary vascular endothelial dysfunction and atherosclerosis. Circ Res *89*, 401-407.

Merad, M., Manz, M. G., Karsunky, H., Wagers, A., Peters, W., Charo, I., Weissman, I. L., Cyster, J. G., and Engleman, E. G. (2002). Langerhans cells renew in the skin throughout life under steady-state conditions. Nat Immunol *3*, 1135-1141.

Moatti, D., Faure, S., Fumeron, F., Amara Mel, W., Seknadji, P., McDermott, D. H., Debre, P., Aumont, M. C., Murphy, P. M., de Prost, D., and Combadiere, C. (2001). Polymorphism in the fractalkine receptor CX3CR1 as a genetic risk factor for coronary artery disease. Blood *97*, 1925-1928.

Muehlhoefer, A., Saubermann, L. J., Gu, X., Luedtke-Heckenkamp, K., Xavier, R., Blumberg, R. S., Podolsky, D. K., MacDermott, R. P., and Reinecker, H. C. (2000). Fractalkine is an epithelial and endothelial cell-derived chemoattractant for intraepithelial lymphocytes in the small intestinal mucosa. J Immunol *164*, 3368-3376.

Naik, S. H., Metcalf, D., van Nieuwenhuijze, A., Wicks, I., Wu, L., O'Keeffe, M., and Shortman, K. (2006). Intrasplenic steady-state dendritic cell precursors that are distinct from monocytes. Nat Immunol *7*, 663-671.

Naito, M., Hasegawa, G., and Takahashi, K. (1997). Development, differentiation, and maturation of Kupffer cells. Microsc Res Tech *39*, 350-364.

Neutra, M. R., Mantis, N. J., and Kraehenbuhl, J. P. (2001). Collaboration of epithelial cells with organized mucosal lymphoid tissues. Nat Immunol *2*, 1004-1009.

Niess, J. H., Brand, S., Gu, X., Landsman, L., Jung, S., McCormick, B. A., Vyas, J. M., Boes, M., Ploegh, H. L., Fox, J. G., *et al.* (2005). CX3CR1-mediated dendritic cell access to the intestinal lumen and bacterial clearance. Science *307*, 254-258.

Niess, J. H., and Reinecker, H. C. (2006). Dendritic cells in the recognition of intestinal microbiota. Cell Microbiol *8*, 558-564.

Nishiyori, A., Minami, M., Ohtani, Y., Takami, S., Yamamoto, J., Kawaguchi, N., Kume, T., Akaike, A., and Satoh, M. (1998). Localization of fractalkine and CX3CR1 mRNAs in rat brain: does fractalkine play a role in signaling from neuron to microglia? FEBS Lett *429*, 167-172.

Palframan, R. T., Jung, S., Cheng, G., Weninger, W., Luo, Y., Dorf, M., Littman, D. R., Rollins, B. J., Zweerink, H., Rot, A., and von Andrian, U. H. (2001). Inflammatory chemokine transport and presentation in HEV: a remote control

mechanism for monocyte recruitment to lymph nodes in inflamed tissues. J Exp Med *194*, 1361-1373.

Pan, Y., Lloyd, C., Zhou, H., Dolich, S., Deeds, J., Gonzalo, J. A., Vath, J., Gosselin, M., Ma, J., Dussault, B., *et al.* (1997). Neurotactin, a membrane-anchored chemokine upregulated in brain inflammation. Nature *387*, 611-617.

Papadopoulos, E. J., Sassetti, C., Saeki, H., Yamada, N., Kawamura, T., Fitzhugh, D. J., Saraf, M. A., Schall, T., Blauvelt, A., Rosen, S. D., and Hwang, S. T. (1999). Fractalkine, a CX3C chemokine, is expressed by dendritic cells and is up-regulated upon dendritic cell maturation. Eur J Immunol *29*, 2551-2559.

Plump, A. S., Smith, J. D., Hayek, T., Aalto-Setala, K., Walsh, A., Verstuyft, J. G., Rubin, E. M., and Breslow, J. L. (1992). Severe hypercholesterolemia and atherosclerosis in apolipoprotein E-deficient mice created by homologous recombination in ES cells. Cell *71*, 343-353.

Priller, J., Prinz, M., Heikenwalder, M., Zeller, N., Schwarz, P., Heppner, F. L., and Aguzzi, A. (2006). Early and rapid engraftment of bone marrow-derived microglia in scrapie. J Neurosci *26*, 11753-11762.

Qu, C., Edwards, E. W., Tacke, F., Angeli, V., Llodra, J., Sanchez-Schmitz, G., Garin, A., Haque, N. S., Peters, W., van Rooijen, N., *et al.* (2004). Role of CCR8 and other chemokine pathways in the migration of monocyte-derived dendritic cells to lymph nodes. J Exp Med *200*, 1231-1241.

Randolph, G. J. (1999). Differentiation of phagocytic monocytes into lynph node dendritic cells in vivo. Immunity *11*, 753-761.

Randolph, G. J., Beaulieu, S., Lebecque, S., Steinman, R. M., and Muller, W. A. (1998). Differentiation of monocytes into dendritic cells in a model of transendothelial trafficking. Science *282*, 480-483.

Rescigno, M., Urbano, M., Valzasina, B., Francolini, M., Rotta, G., Bonasio, R., Granucci, F., Kraehenbuhl, J. P., and Ricciardi-Castagnoli, P. (2001). Dendritic cells express tight junction proteins and penetrate gut epithelial monolayers to sample bacteria. Nat Immunol *2*, 361-367.

Robinson, L. A., Nataraj, C., Thomas, D. W., Howell, D. N., Griffiths, R., Bautch, V., Patel, D. D., Feng, L., and Coffman, T. M. (2000). A role for fractalkine and its receptor (CX3CR1) in cardiac allograft rejection. J Immunol *165*, 6067-6072.

Sallusto, F., and Lanzavecchia, A. (1994). Efficient presentation of soluble antigen by cultured human dendritic cells is maintained by granulocyte/macrophage colony-stimulating factor plus interleukin 4 and downregulated by tumor necrosis factor alpha. J Exp Med *179*, 1109-1118.

Sapoznikov, A., Fischer, J.A., Zaft, T., Krauthgamer, R., Dzionek, A., and Jung, S. (2007). Organ-dependent in vivo priming of naive CD4+, but not CD8+, T cells by plasmacytoid dendritic cells. J Exp Med *204*, 1923-1933.

Sawyer, R. T., Strausbauch, P. H., and Volkman, A. (1982). Resident macrophage proliferation in mice depleted of blood monocytes by strontium-89. Lab Invest *46*, 165-170.

Shortman, K., and Liu, Y. J. (2002). Mouse and human dendritic cell subtypes. Nat Rev Immunol *2*, 151-161.

Steinman, R. M. (1999). Dendritic cells. In Fundamental Immunology, W. E. Paul, ed. (Philadelphia, Lippincott-Raven), pp. 547-573.

Steinman, R. M., and Cohn, Z. A. (1973). Identification of a novel cell type in preipheral lymphoid organs of mice. I. Morphology, quantitiation, tissues distribution. J Exp Med *137*, 1142-1162.

Steinman, R. M., and Cohn, Z. A. (1974). Identification of a novel cell type in preipheral lymphoid organs of mice. II.Functinal properties in vitro. J Exp Med *139*, 380-397.

Steinman, R. M., and Witmar, M. D. (1978). Lymphoid dendritic cells are potent stimulators of the primary mixed leukocyte reaction in mice. Proc Natl Acad Sci USA *75*, 5132-5136.

Sunderkotter, C., Nikolic, T., Dillon, M. J., Van Rooijen, N., Stehling, M., Drevets, D. A., and Leenen, P. J. (2004). Subpopulations of mouse blood monocytes differ in maturation stage and inflammatory response. J Immunol *172*, 4410-4417.

Tabas, I. (2005). Consequences and therapeutic implications of macrophage apoptosis in atherosclerosis: the importance of lesion stage and phagocytic efficiency. Arterioscler Thromb Vasc Biol *25*, 2255-2264.

Tarling, J. D., Lin, H. S., and Hsu, S. (1987). Self-renewal of pulmonary alveolar macrophages: evidence from radiation chimera studies. J Leukoc Biol *42*, 443-446.

Teupser, D., Pavlides, S., Tan, M., Gutierrez-Ramos, J. C., Kolbeck, R., and Breslow, J. L. (2004). Major reduction of atherosclerosis in fractalkine (CX3CL1)-deficient mice is at the brachiocephalic artery, not the aortic root. Proc Natl Acad Sci U S A *101*, 17795-17800.

Thomas, E. D., Ramberg, R. E., Sale, G. E., Sparkes, R. S., and Golde, D. W. (1976). Direct evidence for a bone marrow origin of the alveolar macrophage in man. Science *192*, 1016-1018.

Udagawa, N., Takahashi, N., Akatsu, T., Tanaka, H., Sasaki, T., Nishihara, T., Koga, T., Martin, T. J., and Suda, T. (1990). Origin of osteoclasts: mature monocytes and macrophages are capable of differentiating into osteoclasts under a suitable microenvironment prepared by bone marrow-derived stromal cells. Proc Natl Acad Sci U S A *87*, 7260-7264.

Vallon-Eberhard, A., Landsman, L., Yogev, N., Verrier, B., and Jung, S. (2006). Transepithelial pathogen uptake into the small intestinal lamina propria. J Immunol *176*, 2465-2469.

van Furth, R. (1989). Origin and turnover of monocytes and macrophages. Curr Top Pathol *79*, 125-150.

van Furth, R., and Cohn, Z. A. (1968). The origin and kinetics of mononuclear phagocytes. J Exp Med *128*, 415-435.

van Furth, R., Diesselhoff-den Dulk, M. C., and Mattie, H. (1973). Quantitative study on the production and kinetics of mononuclear phagocytes during an acute inflammatory reaction. J Exp Med *138*, 1314-1330.

van Furth, R., and Diesselhoff-den Dulk, M. M. (1984). Dual origin of mouse spleen macrophages. J Exp Med *160*, 1273-1283.

van Rooijen, N., Kors, N., and Kraal, G. (1989). Macrophage subset repopulation in the spleen: differential kinetics after liposome-mediated elimination. J Leukoc Biol *45*, 97-104.

Varol, C., Landsman, L., Fogg, D. K., Greenshtein, L., Gildor, B., Margalit, R., Kalchenko, V., Geissmann, F., and Jung, S. (2007). Monocytes give rise to mucosal, but not splenic, conventional dendritic cells. J Exp Med *204*, 171-180.

Wiktor-Jedrzejczak, W., and Gordon, S. (1996). Cytokine regulation of the macrophage (M phi) system studied using the colony stimulating factor-1-deficient op/op mouse. Physiol Rev *76*, 927-947.

Wiktor-Jedrzejczak, W. W., Ahmed, A., Szczylik, C., and Skelly, R. R. (1982). Hematological characterization of congenital osteopetrosis in op/op mouse. Possible mechanism for abnormal macrophage differentiation. J Exp Med *156*, 1516-1527.

Yrlid, U., Jenkins, C. D., and Macpherson, G. G. (2006). Relationships between Distinct Blood Monocyte Subsets and Migrating Intestinal Lymph Dendritic Cells In Vivo under Steady-State Conditions. J Immunol *176*, 4155-4162.

Zhao, X., Deak, E., Soderberg, K., Linehan, M., Spezzano, D., Zhu, J., Knipe, D. M., and Iwasaki, A. (2003). Vaginal submucosal dendritic cells, but not Langerhans cells, induce protective Th1 responses to herpes simplex virus-2. J Exp Med *197*, 153-162.

Ziegler-Heitbrock, H. W., Passlick, B., and Flieger, D. (1988). The monoclonal antimonocyte antibody My4 stains B lymphocytes and two distinct monocyte subsets in human peripheral blood. Hybridoma *7*, 521-527.

Zlotnik, A., and Yoshie, O. (2000). Chemokines: a new classification system and their role in immunity. Immunity *12*, 121-127.

2. Publications

Distinct Differentiation Potential of Blood Monocyte Subsets in the Lung[1]

Limor Landsman, Chen Varol, and Steffen Jung[2]

Peripheral blood monocytes are a population of circulating mononuclear phagocytes that harbor potential to differentiate into macrophages and dendritic cells. As in humans, monocytes in the mouse comprise two phenotypically distinct subsets that are $Gr1^{high}CX_3CR1^{int}$ and $Gr1^{low}CX_3CR1^{high}$, respectively. The question remains whether these populations contribute differentially to the generation of peripheral mononuclear phagocytes. In this study, we track the fate of adoptively transferred, fractionated monocyte subsets in the lung of recipient mice. We show that under inflammatory and noninflammatory conditions, both monocyte subsets give rise to pulmonary dendritic cells. In contrast, under the conditions studied, only $Gr1^{low}CX_3CR1^{high}$ monocytes, but not $Gr1^{high}CX_3CR1^{int}$ cells, had the potential to differentiate into lung macrophages. However, $Gr1^{high}CX_3CR1^{int}$ monocytes could acquire this potential upon conversion into $Gr1^{low}CX_3CR1^{high}$ cells. Our results therefore indicate an intrinsic dichotomy in the differentiation potential of the two main blood monocyte subsets. *The Journal of Immunology,* **2007, 178: 2000–2007.**

Blood monocytes are considered circulating precursors of macrophages (MΦ)[3] and dendritic cells (DC) and, together with the latter, have collectively been termed mononuclear phagocytes (1, 2). Accordingly, when cultured in vitro in the presence of the cytokines M-CSF or GM-CSF, monocytes can be driven to differentiate into MΦ and DC, respectively (3, 4). Furthermore, in vivo studies also provide evidence that blood monocytes can act as precursors of MΦ (1, 5, 6). More recent reports have shown that monocytes can under inflammatory conditions differentiate in vivo into conventional $CD11c^{high}$ DC (cDC) (7, 8) and Langerhans cells (9). However, interestingly, blood monocytes seem not to contribute to the generation of splenic cDC (10–12).

Monocytes are, however, not a homogeneous cell population, but rather comprise at least two discrete subsets. Human monocytes consist of a $CD14^{2+}CD16^{-}$ population, which is $CCR2^{+}CD62L^{+}CX_3CR1^{int}$, and a $CD14^{+}CD16^{+}$ subset, which can be further characterized as being $CX_3CR1^{high}CCR2^{-}CD62L^{-}$ (8, 13, 14). In vitro culture and expression analysis of the human monocyte subsets suggest a particular role of $CD14^{+}CD16^{+}$ monocytes in inflammatory settings (15). More recently, monocyte dichotomy has also been established in mice and rats (8, 16, 17). Circulating murine $CD115^{+}$ monocytes encompass two main $Gr1^{high}CX_3CR1^{int}$ and $Gr1^{low}CX_3CR1^{high}$ subsets (8, 16), which based on their chemokine receptor expression correlate to human $CD14^{+/+}CD16^{-}$ and $CD14^{+}CD16^{+}$ monocytes, respectively (2, 8). Results of adoptive transfers of fractionated murine monocytes suggest that these cells are also functionally distinct: $Gr1^{low}$ monocytes were found to be recruited to resting tissues, whereas the $Gr1^{high}$ monocytes shuttle between the blood and the bone marrow (BM) unless recruited to sites of inflammation (8, 12). With regard to their differential fates, $Gr1^{high}$ monocytes were shown in mice to differentiate into cDC and Langerhans cells under inflammation (8, 9), and both $Gr1^{high}$ and $Gr1^{low}$ rat monocytes were reported to give rise to intestinal DC in steady state (17). However, for neither of the subsets the in vivo potential to become MΦ has been investigated. Furthermore, monocyte fate studies are complicated by the recent finding that $Gr1^{high}$ monocytes can convert in vivo into $Gr1^{low}$ monocytes (12, 18, 19). In addition, a comprehensive evaluation of the in vivo differentiation potential of monocytes has to consider that the monocyte fate is likely to be dictated by the tissue environment encountered upon their extravasation. Comparison of the differentiation potential of $Gr1^{high}$ and $Gr1^{low}$ monocytes therefore requires that the two subsets will be exposed to the same microenvironment and studied side by side.

Lymphoid and nonlymphoid organs often harbor tissue-specific mononuclear phagocyte members. In this study, we investigate the differentiation potential of adoptively transferred fractionated blood monocyte subsets into DC and MΦ, focusing on the pulmonary mononuclear phagocyte system as a nonlymphoid tissue model. The lung hosts well-defined MΦ and DC populations, which are believed to play opposing roles in the initiation and maintenance of lung inflammations (20–22). Importantly, expression of the β integrin CD11c discriminates both of these cell types from undifferentiated $CD11c^{-}$ monocytes found in this tissue (21, 23). Collectively, the pulmonary mononuclear phagocyte system is therefore particularly suited for a comparative monocyte differentiation study into either DC or MΦ.

In this study, we show that under both inflammatory and noninflammatory conditions, $Gr1^{high}CX_3CR1^{int}$ and $Gr1^{low}CX_3CR1^{high}$ monocytes give rise to pulmonary DC. In contrast, only $Gr1^{low}$, but not $Gr1^{high}$ monocytes harbor the immediate potential to differentiate into lung MΦ.

Department of Immunology, The Weizmann Institute of Science, Rehovot, Israel

Received for publication August 29, 2006. Accepted for publication December 1, 2006.

The costs of publication of this article were defrayed in part by the payment of page charges. This article must therefore be hereby marked *advertisement* in accordance with 18 U.S.C. Section 1734 solely to indicate this fact.

[1] This study was supported by the Minerva and the Pasteur-Weizmann Foundations. S.J. is the incumbent of the Pauline Recanati Career Development Chair and a scholar of the Benoziyo Center for Molecular Medicine.

[2] Address correspondence and reprint requests to Dr. Steffen Jung, Department of Immunology, The Weizmann Institute of Science, Rehovot 76100, Israel. E-mail address: s.jung@weizmann.ac.il

[3] Abbreviations used in this paper: MΦ, macrophage; DC, dendritic cell; BAL, bronchoalveolar lavage; BM, bone marrow; cDC, conventional $CD11c^{high}$ DC; DTx, diphtheria toxin; DTR, DTx receptor; FKN, fractalkine; int, intermediate; i.t., intratracheal; LN, lymph node; wt, wild type.

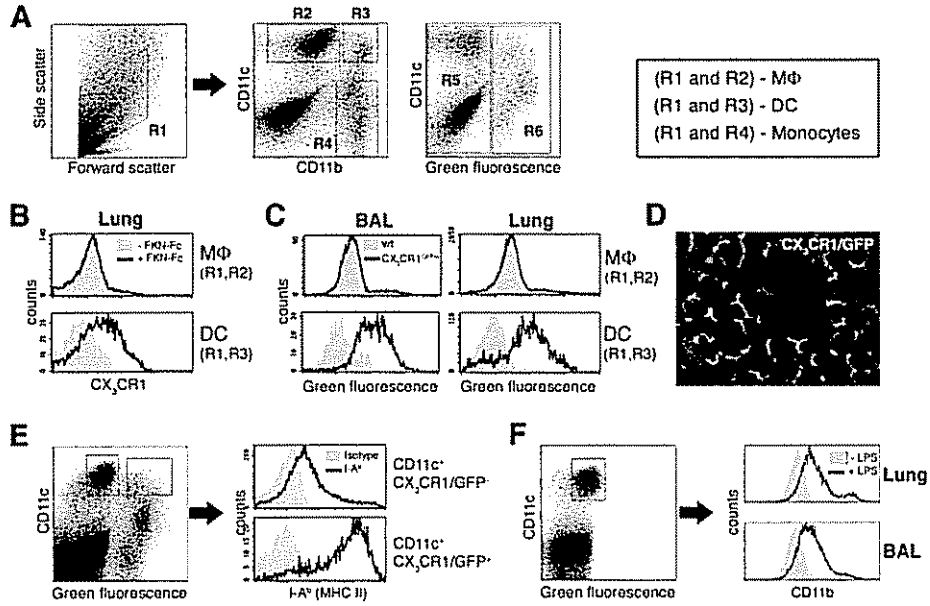

FIGURE 1. CX_3CR1/GFP expression by lung and alveolar mononuclear phagocytes. *A*, Flow cytometric analysis of lung cells of $cx_3cr1^{gfp/+}$ mouse. Cells were isolated and analyzed for expression of CD11c, CD11b, and green fluorescence. *Left panel*, Forward/side light scatter gate for living cells (R1). *Middle dot plot*, CD11c/CD11b expression pattern of cells of R1 gate and mononuclear phagocyte gates used in this study: $CD11c^+CD11b^-$ (R2, MΦ), $CD11c^+CD11b^+$ (R3, DC), and $CD11c^-CD11b^+$ (R4, monocytes) cells. *Right dot plot*, GFP expression of cells gated in R1 region and position of R5 (CX_3CR1/GFP negative) and R6 (CX_3CR1/GFP positive). Abs used were PE-coupled anti-CD11c and PerCP-conjugated anti-CD11b. *B*, FACS analysis of CX_3CR1 expression by lung MΦ (*upper panel*) and DC (*lower panel*) of $cx_3cr1^{gfp/+}$ mouse. Cells were either stained with Fc-coupled CX_3CR1 ligand (FKN-Fc), followed by Cy5-conjugated anti-Fc (+FKN-Fc, empty histogram), or with Cy5-conjugated anti-Fc alone (−FKN-Fc, gray filled histogram), followed by PE- and PerCP-coupled Abs against CD11c and CD11b, respectively. DC and MΦ were defined as cell gated in R1,R3 and R1,R2, respectively (as shown in *A*). *C*, FACS analysis of CX_3CR1/GFP expression by pulmonary MΦ and DC. Cells isolated from either BAL (*left panels*) or lungs (*right panels*) of $cx_3cr1^{gfp/+}$ (empty histogram) and wt (gray filled histogram) mice were analyzed for their green fluorescence intensity. DC and MΦ were defined as cells gated in (R1 and R3) and (R1 and R2), respectively (as shown in *A*). *D*, Live imaging of $cx_3cr1^{gfp/+}$;$rag1^{-/-}$ mouse lung by fluorescent microscopy showing GFP-labeled cells with DC morphology. *E*, FACS analysis of MHC class II ($I\text{-}A^b$) expression by $CD11c^+CX_3CR1/GFP^-$ (MΦ) and $CD11c^+$ CX_3CR1/GFP^+ cells (DC) (*upper* and *lower panels*, respectively). Cells were isolated from a lung of $cx_3cr1^{gfp/+}$ mouse, and stained with either anti $I\text{-}A^b$ Ab (empty histograms) or isotype control (gray filled histograms). Histograms show cells gated, as indicated in dot plot. *F*, CD11b expression by lung and alveolar MΦ of untreated and endotoxin-treated mice. Histograms show CD11b expression by $CD11c^+$ autofluorescent lung and BAL wt cells (MΦ) (gated as indicated in dot plot) of untreated (gray filled histograms) and LPS-treated (200 ng i.t. on day 1; empty histograms) wt mice.

Materials and Methods

Mice

This study involved the use of the C57BL/6 mouse strains *CD11c*: Diphtheria toxin (DTx) receptor (DTR) transgenic mice (B6.FVB-Tg(Itgax-DTR/GFP)57Lan/J; The Jackson Laboratory) that carry a human DTR transgene under the murine CD11c promotor (24); CX_3CR1^{GFP} mice harboring a targeted replacement of the cx_3cr1 gene by a GFP reporter (25); $rag1^{-/-}$ mice (B6.129S7-*Rag1tm1Mom*/J; The Jackson Laboratory) that lack mature lymphocytes; $cd80^{-/-}/cd86^{-/-}$ mice (B6.129S4-$Cd80^{tm1Shr}Cd86^{tm1Shr}$/J; The Jackson Laboratory) that lack expression of both CD80 and CD86 costimulatory molecules (26); and OT-II TCR transgenic mice (C57BL/6-Tg(TcraTcrb)425Cbn/J; The Jackson Laboratory) harboring $CD4^+$ T cells specific for OVA (27, 28). Animals were backcrossed to mice bearing the CD45.1 allotype (B6.SJL-$Ptprc^a$ $Pepc^b$/BoyJ; The Jackson Laboratory), when indicated. The wild-type (wt) C57BL/6 mice were purchased from Harlan Teklad. All mice were maintained under specific pathogen-free conditions and handled under protocols approved by the Weizmann Institute Animal Care Committee according to international guidelines.

Cell isolations

Mice were sacrificed, and blood was collected from the main artery. For bronchoalveolar lavage (BAL), the trachea was exposed to allow insertion of a catheter, through which the lung was filled and washed four times with 1 ml of PBS without Ca^{2+}/Mg^{2+}. Lung parenchyma and spleens were then collected, and tissues were digested with either 4 mg/ml (lung) or 1 mg/ml (spleen) collagenase D (Roche) for 1 h at 37°C, followed by incubation with ACK buffer to lyse erythrocytes. Following their isolation, mediastinal lymph nodes (LNs) were passed through a mesh and cells were collected. All isolated cells were suspended in PBS supplemented with 2 mM EDTA, 0.05% sodium azide, and 1% FCS.

Flow cytometric analysis

The following fluorochrome-labeled mAbs were purchased from BD Pharmingen or eBioscience and used according to manufacturers' protocols: PE-conjugated anti-CD11c, $I\text{-}A^b$, and CD115 Abs; allophycocyanin-conjugated anti-CD11c, CD11b, CD4, and Gr1 (Ly6C/G) Abs; PerCP-conjugated anti-CD11b Ab; biotin-conjugated anti-CD45.1 Ab; and allophycocyanin- and PE-conjugated streptavidin. CX_3CR1 staining using the CX_3CR1 ligand fractalkine (FKN) was performed, as previously described (25). Briefly, cells were incubated with a FKN-Fc fusion protein (provided by Millenium Biotherapeutics) or PBS, followed by incubation with Cy5-conjugated anti-human Fc Ab. After an intensive wash, cells were incubated with indicated Abs. Cells were analyzed on a FACSCalibur cytometer (BD Biosciences) using CellQuest software (BD Biosciences).

Cell transfers

For blood monocyte transfers, ~20 mice were sacrificed and blood was collected to obtain an average of 15 ml of blood for each experiment. Erythrocytes and neutrophils were removed by a Ficoll density gradient (Amersham). Cells were washed and exposed to biotin-conjugated anti-CD115 or anti-Gr1 Abs (eBioscience), followed by incubation with streptavidin-conjugated MACS beads (Miltenyi Biotec). Cells were then magnetically separated, according to manufacturer's protocol. Indicated fractions were collected and i.v. injected to recipient mice. For BM monocyte transfers, cells were isolated from donor femora and tibiae and enriched for mononuclear cells on a Ficoll density gradient, followed by immunostaining with PE-conjugated anti-CD115 and allophycocyanin-conjugated

anti-Gr1 Abs (eBioscience). BM monocytes were then purified by high speed sorting using FACSAria (BD Biosciences). For T cell transfers, $CD4^+$ T cells were isolated from OT-II;CD45.1 mice by enrichment using CD4-conjugated MACS beads (Miltenyi Biotec), according to manufacturer's protocol.

Intratracheal (i.t.) instillation

PBS (80 μl) containing either DTx (catalog 150; List Biological Laboratories), LPS (*Escherichia coli* 055:B5; Sigma-Aldrich catalog L4005), or OVA (Sigma-Aldrich; catalog A5503) was applied to mouse tracheae, as previously described, with modifications (29). Briefly, mice were lightly anesthetized using isoflurane and placed vertically, and their tongues were pulled out. Using a long-nasal tip, liquid was placed at trachea top and actively aspirated by the mouse. Gasping of treated mice verified liquid application to the alveolar space.

Microscopy of lung parenchyma

Lungs were filled with 2% low melting agarose (Sigma-Aldrich; catalog A0701), as previously described (30). Live tissues were cut and imaged with a Zeiss Axioskop II fluorescent microscope using Simple PCI software.

Results

CX_3CR1 expression discriminates between pulmonary MΦ and DC

Alveolar and lung MΦ and DC have been defined according to discrete surface marker expression. Both MΦ and DC express the β integrin CD11c, whereas DC are further characterized as $CD11b^+$ cells, and MΦ are $CD11b^-$ (21, 23, 31) (Fig. 1*A*). In addition, lung and alveolar MΦ, but not DC, are autofluorescent (31, 32). In this study, we show that lung MΦ and DC also differ in their expression of the chemokine receptor CX_3CR1. Thus, surface staining with an Fc fusion of the CX_3CR1 ligand FKN/CX_3CL1 (FKN-Fc) showed that $CD11c^+CD11b^+$ lung DC are CX_3CR1 positive, whereas $CD11c^+CD11b^-$ MΦ are CX_3CR1 negative (Fig. 1*B*). Accordingly, in CX_3CR1^{GFP} knockin mice, whose *cx_3cr1* gene was replaced by a GFP cassette (25), lung and BAL DC express GFP (Fig. 1, *C* and *D*), whereas lung and BAL MΦ do not (Fig. 1*C*).

Lung DC can be further characterized as $CD11c^+$MHC-II^{high} cells, whereas lung MΦ are $CD11c^+$MHC-II^{low} (21, 31). Staining for MHC-II revealed that $CD11c^+CX_3CR1/GFP^+$ cells also express high levels of MHC-II, whereas $CD11c^+CX_3CR1/GFP^-$ cells are MHC-II^{low} (Fig. 1*E*), supporting their definition as DC and MΦ, respectively (31). Interestingly, we recently reported the same CX_3CR1 expression pattern for small intestinal lamina propria DC and MΦ (33). CX_3CR1 is therefore a reliable marker allowing discrimination of $CD11c^+$ DC and MΦ in the lung and alveolar space. In contrast, we have observed that CD11b expression is significantly up-regulated on lung and alveolar MΦ under inflammation (Fig. 1*F*).

For the remainder of this study that investigates the differential origin of pulmonary MΦ and DC, we therefore apply a stringent definition of the two cell types by considering $CD11c^+CD11b^+$ CX_3CR1/GFP^+ cells (Fig 1*A*; R1, R3, and R6 gated cells) as lung DC, and $CD11c^+CD11b^-CX_3CR1/GFP^-$ (Fig 1*A*; R1, R2, and R5 gated cells) as resting lung MΦ. Monocytes found in the lung parenchyma have previously been characterized as $CD11c^-$ $CD11b^+$ cells and are defined accordingly (23) (Fig. 1*A*; gates R1 and R4).

Blood monocytes can differentiate into lung DC in naive mice

The most direct way to study the fate of blood monocytes is arguably the adoptive transfer of these cells into recipient's bloodstream and subsequent tracking of graft descendants. To study the monocyte differentiation potential, we isolated the cells from donor blood according to surface expression of the monocyte-specific marker CD115 (M-CSF-R) using magnetic separation. Notably,

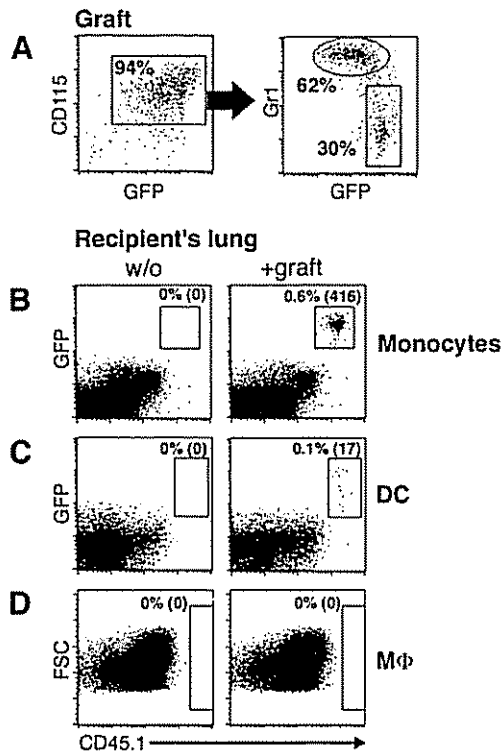

FIGURE 2. Grafted peripheral blood monocytes give rise to lung DC, but not MΦ in untreated recipient mice. *A*, FACS analysis of representative MACS-enriched $CD115^+$ cell graft isolated from *$cx_3cr1^{gfp/+}$*;CD45.1 donor blood. Note presence of $Gr1^{high}CX_3CR1/GFP^{int}$ and $Gr1^{low}CX_3CR1/GFP^{high}$ monocyte subsets. *B–D*, Lungs of untreated monocyte recipients, day 4 after transfer. CD45.2 wt recipients either received CX_3CR1/GFP^+ CD45.1 blood $CD115^+$ graft (10^6 cells, +graft) or no graft (w/o) on day 0. Lung monocytes (*B*, $CD11c^-CD11b^+$ cells gated according to Fig. 1*A* (R1 and R4)), DC (*C*, $CD11c^+CD11b^+$ cells gated according to Fig. 1*A* (R1 and R3)), and MΦ (*D*, $CD11c^+CD11b^-CX_3CR1/GFP^-$ cells gated according to Fig. 1*A* (R1, R2, and R5)) were analyzed on day 4 for graft-derived cells. Numbers indicate percentage of graft-derived cells ($CX_3CR1/GFP^+CD45.1^+$ or $CD45.1^+$) of total gated population and their absolute numbers (in parentheses). Data show one representative of three independent experiments involving one to two recipients per group.

this cell population included $Gr1^{high}$ and $Gr1^{low}$ monocyte subsets (Fig. 2*A*), both of which express CX_3CR1 (8). To distinguish between graft- and host-derived cells, donor monocytes were retrieved from blood of *$cx_3cr1^{gfp/+}$*;CD45.1 mice and transferred into congenic CD45.2 wt recipients. Graft-derived lung DC are therefore CD45.1 CX_3CR1/GFP positive (Fig. 1*C*), whereas host DC are CD45.1 GFP negative. The identification of graft-derived CX_3CR1/GFP-negative MΦ in recipient lungs relies solely on expression of the allotypic CD45 marker: whereas graft-derived MΦ will be CD45.1, host cells are CD45.2. Successful monocyte transfers were confirmed by detection of grafted monocytes in the recipients' lungs (Figs. 2*B* and 4*A*), blood, and spleens (data not shown).

We first transferred monocytes to untreated wt recipient mice, and analyzed their lung and alveolar space content 4 days later. We detected graft-derived cells in recipient's lung, most of which were undifferentiated $CD11c^-CD11b^+CX_3CR1/GFP^+$ monocytes (Fig. 2*B*). We also consistently observed few GFP-expressing $CD11c^+$ $CD11b^+$ lung DC (Fig. 2*C*), indicating differentiation of monocytes into DC in steady state. Despite the fact that MΦ outnumber DC by far in this tissue, we did, however, not detect donor-derived ($CD45.1^+$) lung MΦ (Fig. 2*D*). In addition, we could not detect graft-derived cells in recipients' alveolar space (data not shown).

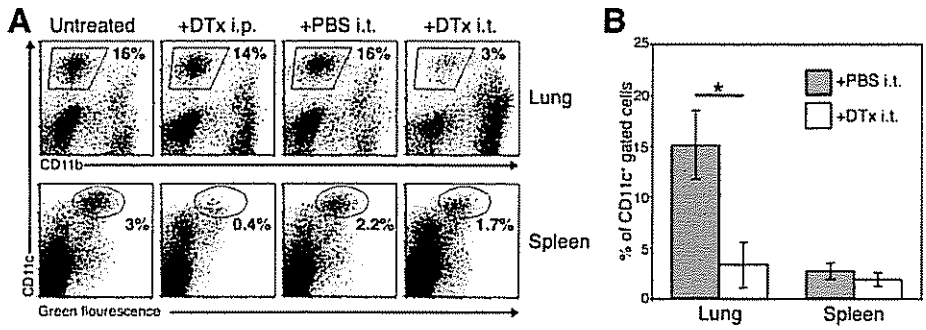

FIGURE 3. In vivo depletion of lung *CD11c*:DTR transgenic CD11c$^+$ cells, but not splenic CD11c$^+$ cells, upon i.t. instillation of DTx. *CD11c*:DTR mice were treated with DTx either i.p. (4 ng/gr, +DTx i.p.) or i.t. (100 ng, +DTx i.t.). Control littermates were either treated with PBS i.t. (+PBS i.t.) or left untreated. Lungs and spleens were analyzed 1 day after treatments. *A*, FACS analysis of lung cells for CD11c and CD11b expression (*upper panels*) and spleen cells for CD11c$^+$ and GFP expression (*lower panels*). Numbers indicate percentage of gated cells from total cells. *B*, Bar diagram summarizing percentages of CD11c$^+$ spleen and lung cells (gated as in *A*) of mice treated i.t. with either DTx (100 ng) or PBS. Mice were analyzed 1 day after treatments. $n = 4$. *, $p < 0.005$ (two-tailed Student's t test).

Blood monocytes can differentiate into lung DC and MΦ in mononuclear phagocyte-depleted mouse

The failure to detect graft-derived lung MΦ in untreated recipients could indicate that those cells do not originate from CD115$^+$ blood monocytes. Alternatively, the long-lived respiratory MΦ compartment might in steady state require only limited cellular input from the blood, which could be below our level of detection. To distinguish between these options, we decided to ablate lung MΦ before the monocyte transfer.

We took advantage of *CD11c*:DTR transgenic mice that allow the specific depletion of CD11c^{high} cells (24). The i.t. DTx instillation of *CD11c*:DTR transgenic mice results in the ablation of CD11c$^+$ lung mononuclear phagocytes, including DC and MΦ (34) (Fig. 3). Depletion of endogenous pulmonary MΦ by the DTx treatment of *CD11c*:DTR recipients might open otherwise closed niches to newly coming cells. Notably, in this strategy, grafted cells, which are not *CD11c*:DTR transgenic, are resistant to ablation.

We next transferred CX_3CR1^{GFP} CD45.1 monocytes to DTx-treated *CD11c*:DTR;CD45.2 recipients. Four days after transfer, recipient mice were analyzed by flow cytometry for the presence of graft-derived mononuclear phagocytes in their lung and alveolar space. We readily observed graft-derived parenchymal lung and alveolar CX_3CR1/GFP^+ DC in the recipient mice (Fig. 4, *B*, *D*, and *F*). Importantly, as opposed to the untreated recipients, we also could detect graft-derived CD45.1 MΦ in recipient's lung (Fig. 4*C*), suggesting that the ablation of endogenous lung MΦ promoted the seeding of the lung with graft-derived cells. Graft-derived monocytes, DC, and MΦ could also be detected upon perfusion of the recipients, indicating their location in the lung parenchyma (data not shown).

Taken together, these results show that adoptively transferred CD115$^+$ blood monocytes collectively have the capacity to differentiate into pulmonary DC and MΦ.

Monocyte-derived lung DC can prime naive T cells

DC are best defined by their unrivaled capacity to stimulate naive T cells (35, 36). Importantly, in the pulmonary mononuclear system, MΦ are established suppressors of T cell activation (20–22, 37). We therefore sought to study the functionality of graft-derived lung DC by transferring monocytes into mutant mice that lack the essential costimulatory molecules CD80 and CD86, and hence are incapable of naive T cell priming (26, 38).

We first tested the ability of grafted OVA-specific TCR transgenic T cells (OT-II) (27) to respond to i.t. OVA challenge in wt and *cd80*$^{-/-}$;*cd86*$^{-/-}$ recipient mice (Fig. 5*A*). Mice received an OT-II;CD45.1 CD4$^+$ T cell graft (day 0), followed by an i.t. challenge with OVA and LPS on the 3 subsequent days (days 1–3). Seven days after the initial immunization (day 8), mediastinal LNs were isolated and analyzed for the presence of OVA-specific

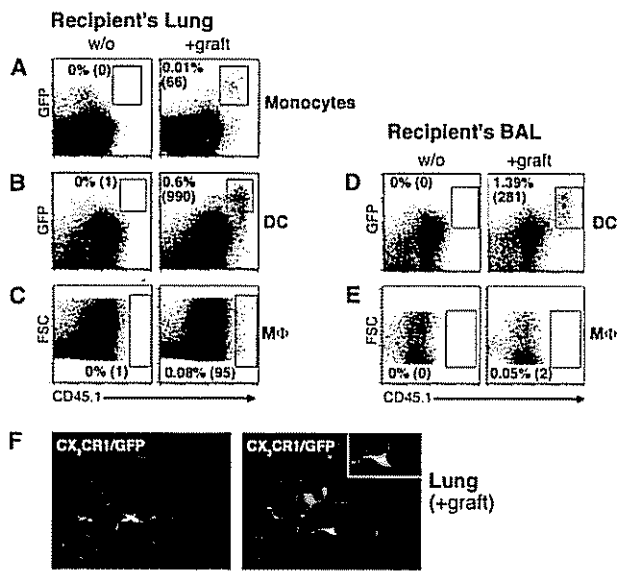

FIGURE 4. Grafted peripheral blood monocytes give rise to lung DC and MΦ in mononuclear phagocyte-depleted recipient mice. *A–E*, DTx-treated *CD11c*:DTR monocyte recipient lung, day 4 after transfer. *CD11c*:DTR;CD45.2 mice pretreated i.t. with DTx (100 ng, day 0) either received *cx*$_3$*cr1*$^{gfp/+}$;CD45.1 CD115$^+$ blood monocyte graft (10^6 cells, +graft) or no graft (w/o) 2 h after DTx treatment. Lung monocytes (*A*, CD11c$^-$CD11b$^+$ cells gated according to Fig. 1*A* (R1 and R4)), DC (*B*, CD11c$^+$CD11b$^+$ cells gated according to Fig. 1*A* (R1 and R3)), and MΦ (*C*, CD11c$^+$CD11b$^-$$CX_3CR1/GFP^-$ cells gated according to Fig. 1*A* (R1, R2, and R5)), as well as BAL DC (*D*, CD11c$^+$ CD11b$^+$ cells gated according to Fig. 1*A* (R1 and R3) and MΦ (*E*, CD11c$^+$CD11b$^-$$CX_3CR1/GFP^-$ cells gated according to Fig. 1*A* (R1, R2, and R5)) were analyzed on day 4 for graft-derived cells. Numbers indicate percentage of graft-derived cells (CX_3CR1/GFP^+CD45.1$^+$ or CD45.1$^+$) of total population and their absolute numbers (in parentheses). Data show representative results of three independent experiments involving one to two mice per group. *F*, Histological analysis of DTx-treated monocyte recipient lung. *CD11c*:DTR mouse was treated with DTx i.t. (100 ng, day 0) and received CX_3CR1^{GFP} blood monocyte graft 2 h later, as previously described. Pictures show green fluorescent cells with DC morphology in different areas of recipient lung.

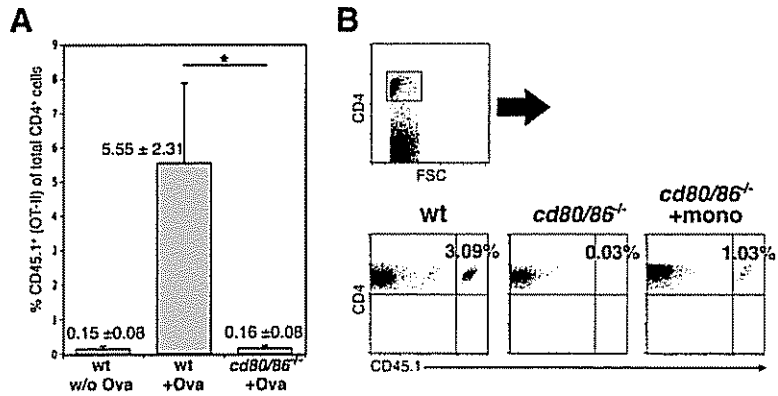

FIGURE 5. Rescue of *CD80/CD86* knockout phenotype by monocyte-derived APC. *A*, Impaired anti-OVA response of adoptively transferred OT-II $CD4^+$ T cells in mice lacking CD80 and CD86 molecules. The wt (CD45.2) and $cd80^{-/-};cd86^{-/-}$ (CD45.2) mice received an OT-II;CD45.1 OVA-specific T cell graft (10^6 cells) on day 0. Recipients were treated i.t. with either 10 μg of OVA and 100 ng of LPS (wt + Ova, $cd80/86^{-/-}$ + Ova) or LPS alone (wt w/o Ova) on days 1, 2, and 3. Mediastinal LNs were isolated on day 8 and analyzed for the presence of $CD45.1^+$ grafted T cells. Bar diagram shows percentage of $CD45.1^+CD4^+$ cells of the total $CD4^+$ T cell population (group size: $n = 5$ for OVA-treated groups, and $n = 3$ for LPS-treated group). Numbers indicate percentage of $CD45.1^+$ cells of total $CD4^+$ cells, followed by the appropriate SDs. *, $p < 0.01$ (two-tailed Student's t test). *B*, Monocyte transfer reconstitutes priming of OVA-specific CD4 T cells in $cd80^{-/-};cd86^{-/-}$ mice. The wt and $cd80^{-/-};cd86^{-/-}$ mice received OT-II grafts on day 0, as described in *A*. One day later, $cd80^{-/-};cd86^{-/-}$ mice also received either $cx_3cr1^{+/GFP};rag1^{-/-}$;CD45.2 $CD115^+$ blood monocyte graft (5×10^5 cells, $cd80/86^{-/-}$ +mono) or no graft ($cd80/86^{-/-}$). Three hours before monocyte transfer and on days 2 and 3, all mice were i.t. treated with OVA (10 μg) and LPS (100 ng), as described in *A*. Mediastinal LNs were collected on day 8, and the percentage of $CD45.1^+$ cells of total $CD4^+$ T cells was determined for each mouse. Data show one representative of three independent experiments involving one to two mice per group.

$CD4^+$ T cells ($CD45.1^+$). The levels of surviving grafted T cells in OVA/LPS-challenged $cd80^{-/-};cd86^{-/-}$ recipients were significantly lower than in OVA/LPS-challenged wt recipients and comparable to those of LPS-challenged control recipients (Fig. 5*A*). In conclusion, due to the absence of competent lung DC in these $cd80^{-/-}:cd86^{-/-}$ mice, grafted OVA-specific TCR transgenic

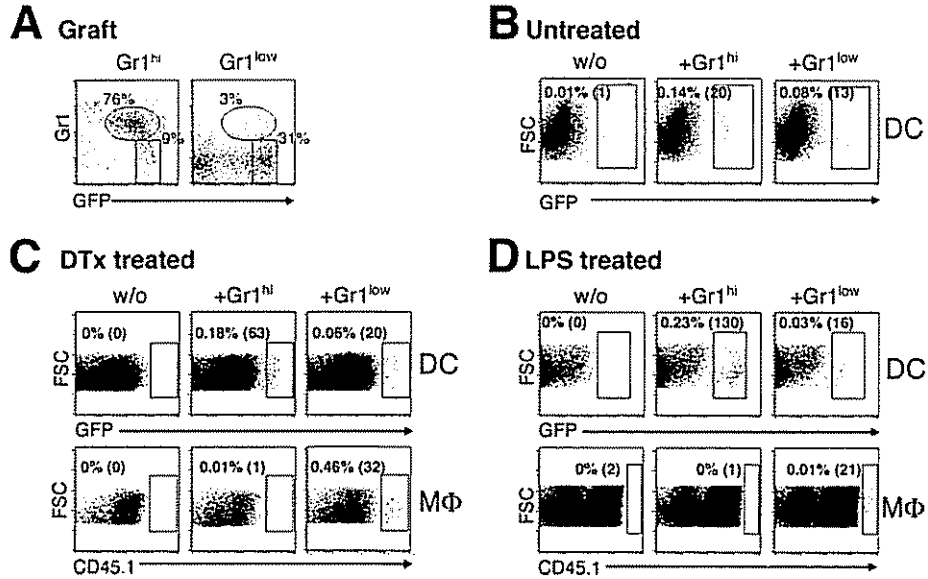

FIGURE 6. Distinct donor-derived mononuclear phagocyte populations in recipients of $Gr1^{high}$ and $Gr1^{low}$ monocyte grafts. *A*, FACS analysis of representative $cx_3cr1^{gfp/+};rag1^{-/-}$;CD45.1 monocyte grafts, MACS fractionated according to Gr1 expression. Dot plots show isolated $Gr1^{high}CX_3CR1/GFP^{int}$ (*left*) and $Gr1^{low}$ CX_3CR1/GFP^{high} (*right*) blood monocytes. *B*, Untreated wt mice received $Gr1^{high}$ (3×10^5 $CX_3CR1/GFP^{int}Gr1^{high}$ cells), $Gr1^{low}$ (3×10^5 $CX_3CR1/GFP^{high}Gr1^{low}$ cells) grafts, or no graft on day 0, as described in *A*. Lung DC were analyzed on day 4 for graft-derived (CX_3CR1/GFP^+) cells. DC are defined as $CD11c^+CD11b^+$ cells gated according to Fig. 1*A* (R1 and R3). Data show one representative of three independent experiments involving one to two mice per group. *C*, DTx-treated *CD11c*:DTR;CD45.2 mice were pretreated i.t. with DTx (100 ng) and received $Gr1^{high}$ (2.5×10^5 $CX_3CR1/GFP^{int}Gr1^{high}$ cells) graft, $Gr1^{low}$ (1×10^5 $CX_3CR1/GFP^{high}Gr1^{low}$ cells) graft, or no graft on day 0. Lung DC and MΦ were analyzed on day 4 for graft-derived cells. DC are defined as $CD11c^+CD11b^+$ cells gated according to Fig. 1*A* (R1 and R3). MΦ are defined as $CD11c^+CD11b^-CX_3CR1/GFP^-$ cells gated according to Fig. 1*A* (R1, R2, and R5). Data are representative of three independent experiments involving one to two mice per group. *D*, The wt recipients (CD45.2) pretreated i.t. with LPS (200 ng) received $Gr1^{high}$ (4×10^5 $CX_3CR1/GFP^{int}Gr1^{high}$ cells), $Gr1^{low}$ (2.5×10^5 $CX_3CR1/GFP^{high}Gr1^{low}$ cells), or no graft on day 0. Lung DC and MΦ compartments (defined as $CD11c^+CD11b^+$ cells gated according to Fig. 1*A* (R1 and R3) and $CD11c^+CD11b^-CX_3CR1/GFP^-$ cells gated according to Fig. 1*A* (R1, R2, and R5), respectively) were analyzed on day 4 for graft-derived cells. Data are representative of three independent experiments involving one to two mice per group. Numbers in *B–D* indicate percentage of graft-derived gated cells (CX_3CR1/GFP^+ or $CD45.1^+$) of total indicated population and their absolute numbers (in parentheses).

$CD4^+$ T cells failed to respond to i.t. OVA challenge (Fig. 5*A*). We then tested the ability of wt blood monocytes to reconstitute OT-II $CD4^+$ T cell response in $cd80^{-/-}$:$cd86^{-/-}$ mice. One day after OT-II T cell transfer, $cd80^{-/-}$;$cd86^{-/-}$ mice either received a monocyte graft or no graft. To exclude B cell contaminations, $CD115^+$ blood monocytes were retrieved from $cx_3cr1^{gfp/+}$;$rag1^{-/-}$; CD45.2 mice, which lack mature lymphocytes. Three hours before monocyte transfer, and on the 2 following days, all mice were challenged i.t. with OVA and LPS. Seven days after the initial immunization, we isolated the mediastinal LNs and analyzed them for the presence and proliferative expansion of OVA-specific $CD4^+$ T cells ($CD45.1^+$). As seen in Fig. 5*B*, monocyte-derived DC partially reconstituted the OVA-specific $CD4^+$ T cell response. This in vivo rescue of the CD80/CD86 deficiency confirms that adoptively transferred monocytes differentiated in the recipients into bona fide lung DC that are capable of priming naive T cells.

$Gr1^{high}$ and $Gr1^{low}$ blood monocyte subsets differ in their potential to become either DC or MΦ

The adoptive transfer of blood monocytes established that this heterogeneous population includes cells that can differentiate into both lung DC and MΦ (Fig. 4). We next decided to test whether the two $Gr1^{high}CX_3CR1^{int}$ and $Gr1^{low}CX_3CR1^{high}$ monocyte subsets (8) differ in their potential to give rise to pulmonary mononuclear phagocytes. To this end, we fractionated blood of $cx_3cr1^{gfp/+}$;$rag1^{-/-}$;CD45.1 donor mice by magnetic separation according to Gr1 expression (Fig. 6*A*) and injected the monocyte fractions into CD45.2 recipients.

To study the differentiation potential of $Gr1^{high}$ and $Gr1^{low}$ blood monocytes in steady state, we first transferred them into untreated wt recipients and analyzed their lungs 4 days later. In agreement with our previous data (Fig. 2*B*), both subsets failed to give rise to lung MΦ under these conditions (data not shown). Graft-derived CX_3CR1/GFP^+ DC could be detected in recipients that had received either $Gr1^{high}$ or $Gr1^{low}$ blood monocytes (Fig. 6*B*). This indicates that in steady state both monocyte subsets reach the lung and can give rise to DC.

We next examined the monocyte subset fate in recipients depleted of endogenous mononuclear phagocytes. To this end, we transferred Gr1-fractionated CX_3CR1^{GFP} CD45.1 blood cells into *CD11c*:DTR CD45.2 recipients that were pretreated i.t. with DTx. Also, under these conditions, we were able to detect graft-derived DC in recipients of either of the subsets (Fig. 6*C*). Interestingly, however, $CD45.1^+$ graft-derived lung MΦ were only observed in recipients of the $Gr1^{low}$ monocyte graft, but not in the lungs of $Gr1^{high}$ monocyte recipients (Fig. 6*C*). This suggests that $Gr1^{low}$ blood monocytes, but not $Gr1^{high}$ monocytes, have the potential to give rise to lung MΦ under the conditions studied.

It was shown recently that endotoxin exposure accelerates replacement of pulmonary MΦ by BM-derived cells as compared with noninflammatory conditions (39). In the DTx-induced cell ablation system, targeted cells die by apoptosis (24, 40) and their replenishment might therefore mimic noninflammatory conditions. To investigate the differentiation potential of the monocyte subsets under inflammation, we therefore transferred Gr1-fractionated CX_3CR1^{GFP} donor blood into wt recipients (CD45.2) pretreated i.t. with LPS. Both $Gr1^{low}$ and $Gr1^{high}$ monocyte subsets readily gave rise to DC (Fig. 6*D*). However, again only in recipients of $Gr1^{low}$ monocytes, we detected graft-derived lung MΦ (Fig. 6*D*).

In summary, our adoptive cell transfer experiments suggest that under inflammatory and noninflammatory conditions, both $Gr1^{high}$ and $Gr1^{low}$ blood monocytes can give rise to lung DC. Importantly, in our experimental system, only $Gr1^{low}$ monocytes, but not the $Gr1^{high}$ cells, gave rise to lung MΦ.

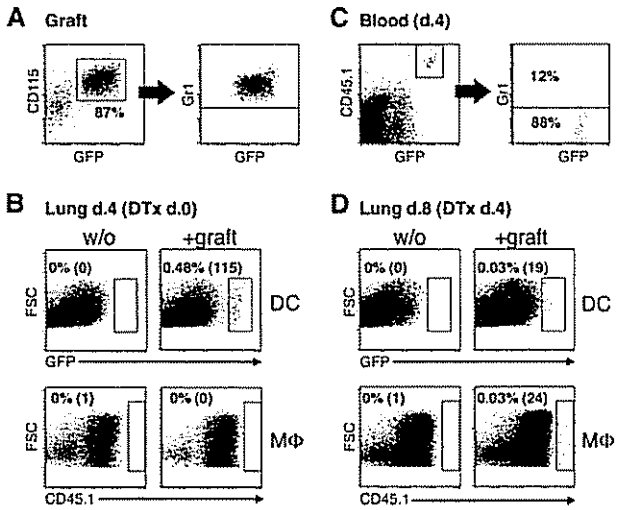

FIGURE 7. $Gr1^{high}$ monocytes give rise to lung MΦ after conversion into $Gr1^{low}$ monocytes. *A*, FACS analysis of $CD115^+CX_3CR1/GFP^{int}Gr1^{high}$ BM monocytes purified from $cx_3cr1^{gfp/+}$;CD45.1 mouse femora and tibiae using FACSAria cell sorter. *B* and *C*, *CD11c*:DTR mice pretreated i.t. with DTx (100 ng) received a $Gr1^{high}$ BM monocyte graft (10^6 cells) or no graft on day 0. *B*, Recipient lung MΦ and DC compartments (defined as $CD11c^+CD11b^+$ cells gated according to Fig. 1*A* (R1 and R3) and $CD11c^+CD11b^-CX_3CR1/GFP^-$ cells gated according to Fig. 1*A* (R1, R2, and R5), respectively) were analyzed on day 4 for graft-derived cells (CX_3CR1/GFP^+ or $CD45.1^+$). Numbers indicate percentage of gate cells of total indicated population and their absolute numbers (in parentheses). Data show one representative of three independent experiments involving one to two mice per group. *C*, Recipient blood was analyzed on day 4 for $CX_3CR1/GFP^+CD45.1^+$ graft-derived cells for Gr1 expression (*left panel*). Recovered population is equivalent to 10^3–10^4 total donor monocytes per recipient's bloodstream. *D*, *CD11c*:DTR recipients received a $Gr1^{high}$ monocyte graft (2×10^6 cells) or no graft on day 0, and were i.t. treated with DTx (100 ng) on day 4. Lung DC and MΦ (defined as $CD11c^+CD11b^+$ cells gated according to Fig. 1*A* (R1 and R3) and $CD11c^+CD11b^-CX_3CR1/GFP^-$ cells gated according to Fig. 1*A* (R1, R2, and R5), respectively) were analyzed on day 8 for graft-derived cells. Gates show and numbers indicate percentage of graft-derived cells (CX_3CR1/GFP^+ or $CD45.1^+$) of total population and their absolute numbers (in parentheses). Data show one representative of three independent experiments involving one to two mice per group.

Upon conversion into $Gr1^{low}$ monocytes, $Gr1^{high}$ BM monocytes gain the potential to generate lung MΦ

Recent studies have established that $Gr1^{high}$ monocytes are efficient precursors of $Gr1^{low}$ monocytes (12, 18, 19). This suggests that the failure of $Gr1^{high}$ blood monocytes to give rise to lung MΦ in our system (Fig. 6, *C* and *D*) might be due to the fact that the time window between transfer and analysis (4 days) was too short for both $Gr1^{high}/Gr1^{low}$ monocyte conversion and MΦ differentiation to occur.

To directly test whether grafted $Gr1^{high}$ monocytes can gain the ability to give rise to MΦ through a $Gr1^{low}$ monocyte intermediate, we investigated the ability of $Gr1^{high}$-derived $Gr1^{low}$ monocytes to give rise to lung MΦ. Isolation of cells from donor BM allows obtaining larger amounts of $Gr1^{high}$ monocyte as compared with the blood (~0.5×10^6 cells/femur vs ~0.5×10^5 cells/ml blood). We therefore isolated cells from BM of $cx_3cr1^{gfp/+}$;CD45.1 donor mice and purified $CD115^+CX_3CR1/GFP^+Gr1^{high}$ monocytes using a high-speed cell sorter (Fig. 7*A*). Purified cells were then

adoptively transferred to *CD11c*:DTR CD45.2 recipients, which were divided into two groups that were treated with DTx on different time points.

One group of recipient mice was treated with DTx i.t. on the day of BM monocyte transfer and analyzed 4 days later (Fig. 7, *B* and *C*). Confirming the results we had obtained with the $Gr1^{high}$ blood monocyte grafts (Fig. 6*C*), we readily observed graft-derived DC in the recipients' lungs, but failed to detect graft-derived MΦ (Fig. 7*B*).

A second group of mice was treated with toxin only 4 days after receiving $Gr1^{+}$ BM monocyte graft. At that time, the majority of graft-derived circulating blood monocytes had converted into $Gr1^{low}$ cells (Fig. 7*C*). Interestingly, the analysis of these recipient mice 4 days after DTx treatment (day 8) revealed the presence of both graft-derived DC and MΦ in their lungs (Fig. 7*D*).

Cumulatively, these results suggest that $Gr1^{high}$ monocytes lack the immediate potential to give rise to lung MΦ, but can gain this function upon conversion into $Gr1^{low}$ monocytes.

Discussion

In this study, we used adoptively transferred blood monocytes to investigate the precursor/progeny relationship between these circulating leukocytes and pulmonary mononuclear phagocytes, including DC and MΦ. Specifically, we studied the differentiation potential of two recently described murine monocyte subsets that can be differentiated according to expression of the Gr1 surface marker.

To study the differentiation potential of monocytes into lung mononuclear phagocytes, we made use of *CD11c*:DTR transgenic mice, which provided us with a tool to specifically ablate pulmonary $CD11c^{+}$ cells, without effecting undifferentiated monocytes (24, 34) (Fig. 3). Depletion of $CD11c^{+}$ cells, including MΦ and DC, promotes the seeding of the pulmonary mononuclear phagocyte system by blood-derived cells (L. Landsman and S. Jung, manuscript in preparation). Importantly, as opposed to other systems (41), our DTx-based depletion strategy is dependent on the genetic background of the mice (24), and non-DTR transgenic donor cells are therefore resistant to ablation upon differentiation into $CD11c^{+}$ cells. However, we cannot exclude that depletion of lung MΦ impairs lung homeostasis and as such provides proinflammatory conditions.

In agreement with studies on the rat intestinal LNs (17), we show that murine monocytes can give rise to lung DC in steady state (Fig. 2). Furthermore, we demonstrate differentiation of blood monocytes into lung DC under inflammation (Fig. 6), thus extending previous reports for skin and peritoneum (7–9). In addition, these monocyte-derived lung DC were capable of reconstituting $CD4^{+}$ T cell priming in an immunodeficient mouse model (Fig. 5). Importantly, we were able to show that both $Gr1^{high}CX_3CR1^{int}$ and $Gr1^{low}CX_3CR1^{high}$ blood monocyte subsets had the potential to give rise to lung DC under both inflammatory and noninflammatory conditions (Fig. 6).

Tissue MΦ are believed to arise from blood monocytes (1). However, direct proof for this connection is largely limited to serosal MΦ in the peritoneal cavity (5). In this study, we provide direct evidence that blood monocytes can give rise to parenchymal lung MΦ in MΦ-depleted recipients and under inflammation (Figs. 4 and 5). However, interestingly, the potential to become a lung MΦ is restricted to the $Gr1^{low}CX_3CR1^{high}$ monocyte subset.

Our results suggest that $Gr1^{high}CX_3CR1^{int}$ and $Gr1^{low}CX_3CR1^{high}$ monocyte subsets respond in the lung differently to the same environmental signal, indicating their commitment to acquire either DC or MΦ fate. Thus, the potential to give rise to lung MΦ was restricted to the $Gr1^{low}$ monocyte subset, whereas $Gr1^{high}$ monocytes seem destined to become lung DC. The latter can, however, gain the potential to become lung MΦ by conversion into $Gr1^{low}$ monocytes (Figs. 6 and 7). Upon differentiation into $Gr1^{low}CCR2^{-}$ cells, $Gr1^{high}CCR2^{+}$ monocytes are likely to lose their ability to respond to inflammatory signals, such as MCP-1 (CCL2) (16, 42). This scenario may reflect the need for DC during inflammation, in which $Gr1^{high}$ monocytes migrate to site of challenge and exclusively give rise to DC. It may ensure limitation of competition on precursor cells by steady-state tasks, such as the generation of tissue MΦ. Replenishment of the lung MΦ population under inflammation might be accomplished by proliferative expansion of local precursors in addition to monocyte differentiation (L. Landsman and S. Jung, manuscript in preparation).

Lung DC and MΦ play opposing roles in the initiation and maintenance of lung inflammations. Whereas DC activate T cells and thereby promote inflammation, pulmonary MΦ suppress these processes (20, 21, 37, 43). It has therefore been suggested that the balance of these two cell types influences the progression of lung inflammation, such as asthma (44, 45). The results presented in this study highlight the differential origins of MΦ and DC in the lung. Although lung DC can develop from both $Gr1^{high}CX_3CR1^{int}$ and $Gr1^{low}CX_3CR1^{high}$ monocyte subsets, lung MΦ originate from $Gr1^{low}$ monocytes. In-depth understanding of the origin of lung DC and MΦ might be of value for the development of cell therapies for respiratory disorders.

Acknowledgments

We thank our laboratory members for critical reading of the manuscript, and are grateful to Y. Chermesh and Y. Melamed for animal husbandry.

Disclosures

The authors have no financial conflict of interest.

References

1. Van Furth, R., and Z. A. Cohn. 1968. The origin and kinetics of mononuclear phagocytes. *J. Exp. Med.* 128: 415–435.
2. Gordon, S., and P. R. Taylor. 2005. Monocyte and macrophage heterogeneity. *Nat. Rev. Immunol.* 5: 953–964.
3. Sallusto, F., and A. Lanzavecchia. 1994. Efficient presentation of soluble antigen by cultured human dendritic cells is maintained by granulocyte/macrophage colony-stimulating factor plus interleukin 4 and down-regulated by tumor necrosis factor α. *J. Exp. Med.* 179: 1109–1118.
4. Wiktor-Jedrzejczak, W., and S. Gordon. 1996. Cytokine regulation of the macrophage (Mφ) system studied using the colony stimulating factor-1-deficient *op/op* mouse. *Physiol. Rev.* 76: 927–947.
5. Van Furth, R., M. C. Diesselhoff-den Dulk, and H. Mattie. 1973. Quantitative study on the production and kinetics of mononuclear phagocytes during an acute inflammatory reaction. *J. Exp. Med.* 138: 1314–1330.
6. Naito, M., S. Umeda, T. Yamamoto, H. Moriyama, H. Umezu, G. Hasegawa, H. Usuda, L. D. Shultz, and K. Takahashi. 1996. Development, differentiation, and phenotypic heterogeneity of murine tissue macrophages. *J. Leukocyte Biol.* 59: 133–138.
7. Randolph, G. J. 1999. Differentiation of phagocytic monocytes into lymph node dendritic cells in vivo. *Immunity* 11: 753–761.
8. Geissmann, F., S. Jung, and D. R. Littman. 2003. Blood monocytes consist of two principal subsets with distinct migratory properties. *Immunity* 19: 71–82.
9. Ginhoux, F., F. Tacke, V. Angeli, M. Bogunovic, M. Loubeau, X. M. Dai, E. R. Stanley, G. J. Randolph, and M. Merad. 2006. Langerhans cells arise from monocytes in vivo. *Nat. Immunol.* 7: 265–273.
10. Fogg, D. K., C. Sibon, C. Miled, S. Jung, P. Aucouturier, D. R. Littman, A. Cumano, and F. Geissmann. 2006. A clonogenic bone marrow progenitor specific for macrophages and dendritic cells. *Science* 311: 83–87.
11. Naik, S. H., D. Metcalf, A. van Nieuwenhuijze, I. Wicks, L. Wu, M. O'Keeffe, and K. Shortman. 2006. Intrasplenic steady-state dendritic cell precursors that are distinct from monocytes. *Nat. Immunol.* 7: 663–671.
12. Varol, C., L. Landsman, D. K. Fogg, L. Greenshtein, B. Gildor, R. Margalit, V. Kalchenko, F. Geissmann, and S. Jung. 2006. Monocytes give rise to mucosal, but not splenic conventional dendritic cells. *J. Exp. Med.* In press.
13. Passlick, B., D. Flieger, and H. W. Ziegler-Heitbrock. 1989. Identification and characterization of a novel monocyte subpopulation in human peripheral blood. *Blood* 74: 2527–2534.
14. Grage-Griebenow, E., H. D. Flad, and M. Ernst. 2001. Heterogeneity of human peripheral blood monocyte subsets. *J. Leukocyte Biol.* 69: 11–20.
15. Belge, K. U., F. Dayyani, A. Horelt, M. Siedlar, M. Frankenberger, B. Frankenberger, T. Espevik, and L. Ziegler-Heitbrock. 2002. The proinflammatory $CD14^{+}CD16^{+}DR^{++}$ monocytes are a major source of TNF. *J. Immunol.* 168: 3536–3542.

16. Palframan, R. T., S. Jung, G. Cheng, W. Weninger, Y. Luo, M. Dorf, D. R. Littman, B. J. Rollins, H. Zweerink, A. Rot, and U. H. von Andrian. 2001. Inflammatory chemokine transport and presentation in HEV: a remote control mechanism for monocyte recruitment to lymph nodes in inflamed tissues. *J. Exp. Med.* 194: 1361–1373.
17. Yrlid, U., C. D. Jenkins, and G. G. Macpherson. 2006. Relationships between distinct blood monocyte subsets and migrating intestinal lymph dendritic cells in vivo under steady-state conditions. *J. Immunol.* 176: 4155–4162.
18. Sunderkotter, C., T. Nikolic, M. J. Dillon, N. Van Rooijen, M. Stehling, D. A. Drevets, and P. J. Leenen. 2004. Subpopulations of mouse blood monocytes differ in maturation stage and inflammatory response. *J. Immunol.* 172: 4410–4417.
19. Qu, C., E. W. Edwards, F. Tacke, V. Angeli, J. Llodra, G. Sanchez-Schmitz, A. Garin, N. S. Haque, W. Peters, N. van Rooijen, et al. 2004. Role of CCR8 and other chemokine pathways in the migration of monocyte-derived dendritic cells to lymph nodes. *J. Exp. Med.* 200: 1231–1241.
20. Holt, P. G., J. Oliver, N. Bilyk, P. G. McMenamin, G. Kraal, and T. Thepen. 1993. Down-regulation of the antigen presenting cell function(s) of pulmonary dendritic cells in vivo by resident alveolar macrophages. *J. Exp. Med.* 177: 397–407.
21. Julia, V., E. M. Hessel, L. Malherbe, N. Glaichenhaus, A. O'Garra, and R. L. Coffman. 2002. A restricted subset of dendritic cells captures airborne antigens and remains able to activate specific T cells long after antigen exposure. *Immunity* 16: 271–283.
22. Lambrecht, B. N., B. Salomon, D. Klatzmann, and R. A. Pauwels. 1998. Dendritic cells are required for the development of chronic eosinophilic airway inflammation in response to inhaled antigen in sensitized mice. *J. Immunol.* 160: 4090–4097.
23. Gonzalez-Juarrero, M., T. S. Shim, A. Kipnis, A. P. Junqueira-Kipnis, and I. M. Orme. 2003. Dynamics of macrophage cell populations during murine pulmonary tuberculosis. *J. Immunol.* 171: 3128–3135.
24. Jung, S., D. Unutmaz, P. Wong, G. Sano, K. De los Santos, T. Sparwasser, S. Wu, S. Vuthoori, K. Ko, F. Zavala, et al. 2002. In vivo depletion of CD11c$^+$ dendritic cells abrogates priming of CD8$^+$ T cells by exogenous cell-associated antigens. *Immunity* 17: 211–220.
25. Jung, S., J. Aliberti, P. Graemmel, M. J. Sunshine, G. W. Kreutzberg, A. Sher, and D. R. Littman. 2000. Analysis of fractalkine receptor CX_3CR1 function by targeted deletion and green fluorescent protein reporter gene insertion. *Mol. Cell. Biol.* 20: 4106–4114.
26. Borriello, F., M. P. Sethna, S. D. Boyd, A. N. Schweitzer, E. A. Tivol, D. Jacoby, T. B. Strom, E. M. Simpson, G. J. Freeman, and A. H. Sharpe. 1997. B7-1 and B7-2 have overlapping, critical roles in immunoglobulin class switching and germinal center formation. *Immunity* 6: 303–313.
27. Barnden, M. J., J. Allison, W. R. Heath, and F. R. Carbone. 1998. Defective TCR expression in transgenic mice constructed using cDNA-based α- and β-chain genes under the control of heterologous regulatory elements. *Immunol. Cell Biol.* 76: 34–40.
28. Robertson, J. M., P. E. Jensen, and B. D. Evavold. 2000. DO11.10 and OT-II T cells recognize a C-terminal ovalbumin 323–339 epitope. *J. Immunol.* 164: 4706–4712.
29. Ho, W., and A. Furst. 1973. Intratracheal instillation method for mouse lungs. *Oncology* 27: 385–393.
30. Bergner, A., and M. J. Sanderson. 2003. Airway contractility and smooth muscle Ca^{2+} signaling in lung slices from different mouse strains. *J. Appl. Physiol.* 95: 1325–1332.
31. Vermaelen, K., and R. Pauwels. 2004. Accurate and simple discrimination of mouse pulmonary dendritic cell and macrophage populations by flow cytometry: methodology and new insights. *Cytometry A* 61: 170–177.
32. Havenith, C. E., A. J. Breedijk, P. P. van Miert, N. Blijleven, W. Calame, R. H. Beelen, and E. C. Hoefsmit. 1993. Separation of alveolar macrophages and dendritic cells via autofluorescence: phenotypical and functional characterization. *J. Leukocyte Biol.* 53: 504–510.
33. Vallon-Eberhard, A., L. Landsman, N. Yogev, B. Verrier, and S. Jung. 2006. Transepithelial pathogen uptake into the small intestinal lamina propria. *J. Immunol.* 176: 2465–2469.
34. Van Rijt, L. S., S. Jung, A. Kleinjan, N. Vos, M. Willart, C. Duez, H. C. Hoogsteden, and B. N. Lambrecht. 2005. In vivo depletion of lung CD11c$^+$ dendritic cells during allergen challenge abrogates the characteristic features of asthma. *J. Exp. Med.* 201: 981–991.
35. Steinman, R. M., and Z. A. Cohn. 1974. Identification of a novel cell type in peripheral lymphoid organs of mice. II. Functional properties in vitro. *J. Exp. Med.* 139: 380–397.
36. Steinman, R. M. 1999. Dendritic cells. In *Fundamental Immunology*, Vol. 1. W. E. Paul, ed. Lippincott-Raven, Philadelphia, pp. 547–573.
37. Pollard, A. M., and M. F. Lipscomb. 1990. Characterization of murine lung dendritic cells: similarities to Langerhans cells and thymic dendritic cells. *J. Exp. Med.* 172: 159–167.
38. Sharpe, A. H., and G. J. Freeman. 2002. The B7-CD28 superfamily. *Nat. Rev. Immunol.* 2: 116–126.
39. Maus, U. A., S. Janzen, G. Wall, M. Srivastava, T. S. Blackwell, J. W. Christman, W. Seeger, T. Welte, and J. Lohmeyer. 2006. Resident alveolar macrophages are replaced by recruited monocytes in response to endotoxin-induced lung inflammation. *Am. J. Respir. Cell Mol. Biol.* 35: 227–235.
40. Bennett, C. L., E. van Rijn, S. Jung, K. Inaba, R. M. Steinman, M. L. Kapsenberg, and B. E. Clausen. 2005. Inducible ablation of mouse Langerhans cells diminishes but fails to abrogate contact hypersensitivity. *J. Cell Biol.* 169: 569–576.
41. Van Rooijen, N. 1989. The liposome-mediated macrophage 'suicide' technique. *J. Immunol. Methods* 124: 1–6.
42. Maus, U., K. von Grote, W. A. Kuziel, M. Mack, E. J. Miller, J. Cihak, M. Stangassinger, R. Maus, D. Schlondorff, W. Seeger, and J. Lohmeyer. 2002. The role of CC chemokine receptor 2 in alveolar monocyte and neutrophil immigration in intact mice. *Am. J. Respir. Crit. Care Med.* 166: 268–273.
43. Careau, E., and E. Y. Bissonnette. 2004. Adoptive transfer of alveolar macrophages abrogates bronchial hyperresponsiveness. *Am. J. Respir. Cell Mol. Biol.* 31: 22–27.
44. Lambrecht, B. N., and H. Hammad. 2003. Taking our breath away: dendritic cells in the pathogenesis of asthma. *Nat. Rev. Immunol.* 3: 994–1003.
45. Peters-Golden, M. 2004. The alveolar macrophage: the forgotten cell in asthma. *Am. J. Respir. Cell Mol. Biol.* 31: 3–7.

Lung Macrophages Serve as Obligatory Intermediate between Blood Monocytes and Alveolar Macrophages[1]

Limor Landsman and Steffen Jung[2]

Alveolar macrophages are a unique type of mononuclear phagocytes that populate the external surface of the lung cavity. Early studies have suggested that alveolar macrophages originate from tissue-resident, local precursors, whereas others reported their derivation from blood-borne cells. However, the role of circulating monocytes as precursors of alveolar macrophages was never directly tested. In this study, we show through the combined use of conditional cell ablation and adoptive cell transfer that alveolar macrophages originate in vivo from blood monocytes. Interestingly, this process requires an obligate intermediate stage, the differentiation of blood monocytes into parenchymal lung macrophages, which subsequently migrate into the alveolar space. We also provide direct evidence for the ability of both lung and alveolar macrophages to proliferate. *The Journal of Immunology,* **2007, 179: 3488–3494.**

The constant exposure to environmental microbial challenges renders the respiratory tract one of the major sites of primary viral and bacterial infections (1). Highlighting this state of permanent alert, the lung, which comprises parenchyma and alveolar space, is seeded with numerous mononuclear phagocytes, including dendritic cells (DC)[3] and macrophages (MΦ) (1, 2). In steady state, MΦ are the major cell type in the alveolar space, representing ~90% of its hematopoietic cellular content (1) and playing a key role in its clearance from pulmonary pathogens and dying cells (3). Pulmonary MΦ, however, are poor T cell stimulators (4, 5), and have even been shown to suppress lung inflammations, probably by inhibiting DC function (4, 6–10).

Alveolar MΦ are bone marrow (BM)-derived cells (11, 12). Interestingly, however, after whole body irradiation and engraftment, their replacement by donor BM cells takes considerably longer than that of most other cells of the hematopoietic system (13, 14). Depending on the irradiation protocol used, the time required for the complete exchange of alveolar MΦ has been reported to vary from several weeks up to 1 year (11, 13–16). This delay in alveolar MΦ replacement by BM-derived cells is discussed as one of the critical causes for the sensitivity of BM transplantation patients to pulmonary infections (17, 18).

Monocytes are BM-derived circulating phagocytes that are considered to be the in vivo MΦ precursors (19, 20). However, specific MΦ populations, such as the brain microglia, have been shown to originate from local precursors, without persisting input from the BM (21). As for the origin of alveolar MΦ, although they clearly belong to the hemopoietic lineage, a direct connection to monocytic precursors remains to be shown (22). Moreover, several studies published during the 1970s and 1980s reported either circulating or local precursor for alveolar MΦ, depending on the method used (for review, see Ref. 22). Based on kinetic studies, Bowden and Adamson (23) suggested, for instance, a dual origin of alveolar MΦ: from blood-borne precursor and from proliferating cells in the lung parenchyma. With the discovery of alveolar DC (24), it became, however, unclear whether this study referred to two distinct cell types, i.e., alveolar DC and MΦ. In addition, the alveolar MΦ population was reported to remain unaffected by depletion of blood monocytes (25), leading to the conclusion that alveolar MΦ are not monocyte derived (26). Because alveolar MΦ are eventually replaced by BM-derived cells (11), the existence of circulating precursor was, however, not ruled out. Taken together, the identity of the alveolar MΦ precursor, as well as its own origin, remains to be revealed (22).

Through an adoptive monocyte transfer approach, we recently showed that parenchymal lung MΦ originate in vivo from blood monocytes (27). Furthermore, we reported that only one of the two major murine monocyte subsets, the $Gr1^{low}CX_3CR1^{high}CCR2^-$ cells (28), harbors the immediate potential to give rise to parenchymal lung MΦ (27). In this study, we extended these studies and investigated the in vivo origin of alveolar MΦ using a combination of conditional cell ablation and reconstitution. We show that grafted blood monocytes can give rise to alveolar MΦ. However, we provide evidence that alveolar MΦ do not originate directly from blood monocytes, but require a parenchymal lung MΦ intermediate. Lastly, we directly show that both lung and alveolar MΦ can undergo proliferation.

Materials and Methods

Mice

This study involved the use of the following C57BL/6 mouse strains: CD11c:diphtheria toxin (DTx) receptor (DTR) transgenic mice (B6.FVB-Tg(Itgax-DTR/GFP)57Lan/J) that carry a DTR transgene under the murine *cd11c* promotor (29); CX_3CR1^{GFP} mice harboring a targeted replacement of the *cx₃cr1* gene by a GFP reporter (30); and μMT mice (C57BL/6-*IgH-6tm1Cgn*) lacking the membrane exon of the Ig μ-chain gene, and therefore are B cell deficient (31). Mice were backcrossed with CD45.1 mice (B6.SJL-*Ptprca Pep3b*/BoyJ) when indicated. All mice were maintained

Department of Immunology, Weizmann Institute of Science, Rehovot, Israel

Received for publication April 17, 2007. Accepted for publication July 3, 2007.

The costs of publication of this article were defrayed in part by the payment of page charges. This article must therefore be hereby marked *advertisement* in accordance with 18 U.S.C. Section 1734 solely to indicate this fact.

[1] This study was supported by the MINERVA Foundation. S.J. is the incumbent of the Pauline Recanati Career Development Chair and a scholar of the Benoziyo Center for Molecular Medicine.

[2] Address correspondence and reprint requests to Dr. Steffen Jung, Department of Immunology, Weizmann Institute of Science, Rehovot 76100, Israel. E-mail address: s.jung@weizmann.ac.il

[3] Abbreviations used in this paper: DC, dendritic cell; BAL, bronchoalveolar lavage; BM, bone marrow; DTR, diphtheria toxin receptor; DTx, diphtheria toxin; int, intermediate; i.t., intratracheal; MΦ, macrophage; PCNA, proliferating cell nuclear Ag; wt, wild type.

under specific pathogen-free conditions and handled under protocols approved by the Weizmann Institute Animal Care Committee, according to international guidelines.

Cell isolations

Mice were sacrificed, and blood was collected from main artery and subjected to a Ficoll density gradient (Amersham) to remove erythrocytes and neutrophils. For bronchoalveolar lavage (BAL), the trachea was exposed to allow insertion of a catheter, through which the lung was filled and washed four times with 1 ml of PBS without Ca^{2+}/Mg^{2+}. Lung parenchyma was then collected and digested with 4 mg/ml collagenase D (Roche) for 1 h at 37°C, followed by incubation with ACK buffer to lyse erythrocytes. All isolated cells were suspended in PBS supplemented with 2 mM EDTA, 0.05% sodium azide, and 1% FCS.

Flow cytometric analysis

The following fluorochrome-labeled mAbs were purchased from eBioscience and used according to manufacturer's protocols: PE-conjugated anti-CD11c and anti-CD115 Abs, allophycocyanin-conjugated streptavidin and anti-CD11b Ab, and biotin-conjugated anti-CD45.1, CD11c, CD115, and MHC II Abs. PerCP-conjugated anti-CD11b Ab was purchased from BD Pharmingen. PE-labeled anti-proliferating cell nuclear Ag (PCNA) Ab was purchased from DakoCytomation and used according to the manufacturer's protocol for S phase-specific staining, with modifications. Before staining with the anti-PCNA Ab, cells were incubated with indicated biotin-conjugated Abs, followed by methanol fixation. Fixed cells were then incubated with streptavidin-fluorochrome conjugates and stained for PCNA. Cells were analyzed on a FACSCalibur cytometer (BD Biosciences) using CellQuest software (BD Biosciences).

Cell transfers

For blood monocyte transfers, ~20 mice were sacrificed and bled to collect an average of 18 ml of blood. Erythrocytes and neutrophils were removed by a Ficoll density gradient, and cells were washed and exposed to biotin-conjugated anti-CD115 Ab (eBioscience), followed by incubation with strepavidin-conjugated MACS beads (Miltenyi Biotec). Cells were then magnetically separated according to manufacturer protocol. The positive fraction was collected and i.v. injected to recipient mice. For mixed BM chimeras, recipient mice were irradiated with a lethal dose (950 rad) and 1 day later i.v. injected with 5×10^6 donor BM cells.

Intratracheal instillation

PBS (80 μl) containing either DTx (List Biological Laboratories; catalogue 150) or without addition was applied to the tracheae of mice, as previously described, with modifications (32). Briefly, mice were lightly anesthetized using isofluorane and placed vertically, and their tongues were pulled out. Using a long-nasal tip, liquid was placed at the top of trachea and actively aspirated by the mouse. Gasping of treated mice verified liquid application to the alveolar space.

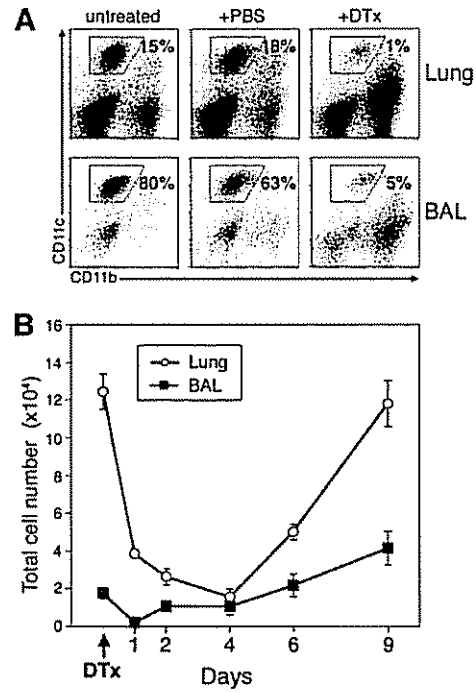

FIGURE 1. In vivo depletion and reconstitution of pulmonary MΦ. Flow cytometric analysis of collagenase-digested lung and BAL fluid of *CD11c*:DTR mice. *A*, Depletion of lung and alveolar MΦ of *CD11c*:DTR mice upon DTx treatment. On day 0, mice were treated i.t. with either PBS or DTx (100 ng) or left untreated. BAL and lung cells were isolated on day 1 and stained with PE-coupled anti-CD11c Ab and allophycocyanin-coupled anti-CD11b Ab. The percentage of MΦ (identified as $CD11c^+$ $CD11b^-$ cells, as indicated by gates) in the lung parenchyma and BAL of each mouse was determined. Numbers indicated the percentage of gated cells. *B*, Depletion of pulmonary MΦ is followed by their rapid reconstitution. *CD11c*:DTR mice were i.t. treated on day 0 with 100 ng of DTx and analyzed on days 0, 1, 2, 4, 6, and 9 for the number of $CD11c^+CD11b^-$ MΦ (as described in *A*) in their lung parenchyma (○) and BAL (■) fluids. Graph shows absolute lung and alveolar MΦ numbers on analyzed days. $n = 3$ for each time point. Data show one representative of two independent experiments.

Results

Depletion of lung and alveolar MΦ results in their rapid reconstitution

Murine pulmonary DC and MΦ, both in the lung parenchyma and the alveolar space, express the β-integrin CD11c. However, whereas pulmonary DC are also positive for MHC II, CD11b, and CX_3CR1, MΦ have been defined as low for MHC II and negative for CD11b and CX_3CR1 (5, 27, 33, 34).

CD11c:DTR transgenic mice allow for the conditional ablation of pulmonary DC and MΦ (27, 35). This ablation system exploits the fact that murine cells are generally resistant to DTx because they lack a high-affinity DTR required for toxin entry into the cell (36). *CD11c*:DTR transgenic mice express a primate DTR under the control of the *cd11c* promoter, resulting in sensitivity of CD11c-expressing cells to DTx-induced cell death (29). Hence, when applied intratracheally (i.t.) to *CD11c*:DTR transgenic mice, DTx causes the depletion of lung and alveolar $CD11c^+$ cells, including both DC and MΦ (27, 35) (Fig. 1*A*).

One day following DTx treatment, lung and alveolar MΦ numbers were dramatically reduced (Fig. 1*B*). The decrease in alveolar MΦ was followed by their rapid reconstitution, and 2 days after the treatment their amount almost reached initial levels. Lung MΦ, in contrast, continued to decline, reaching their lowest value on day 4, after which also their numbers recovered. By day 9, lung MΦ were restored to their initial levels, whereas at that time the size of the alveolar MΦ population was significantly enlarged over steady state (Fig. 1*B*).

These results indicate that, following their conditional depletion, both lung and alveolar MΦ populations are rapidly reconstituted, albeit with distinct kinetics.

Adoptively transferred blood monocytes can give rise to alveolar MΦ

Elsewhere, we have shown that grafted blood monocytes give rise to lung MΦ in MΦ-depleted, but not untreated, recipients (27). Four days after transfer, monocyte graft-derived MΦ could be readily observed in recipient lungs, whereas we failed to detect graft descendants in the alveolar space (27). This result could support the reported notion that blood monocytes do not give rise to alveolar MΦ (25). Alternatively, the kinetics of monocyte differentiation into alveolar MΦ might vary from their differentiation into lung MΦ, precluding detection of monocyte-derived alveolar

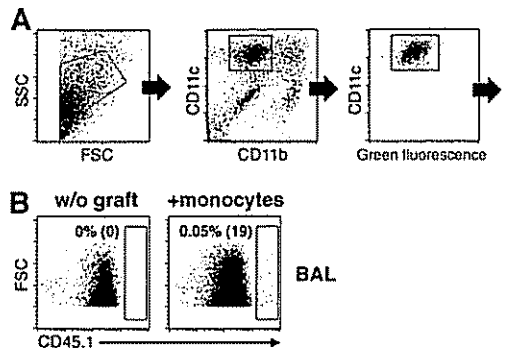

FIGURE 2. Grafted blood monocytes give rise to alveolar MΦ. DTx-treated *CD11c*:DTR mice were grafted with either CD115$^+$ monocytes (10^6 cells) isolated from blood of $cx_3cr1^{gfp/+}$;CD45.1 mice (+monocytes) or with no graft (w/o graft) on day 0. Fourteen days after transfer, BAL of recipient mice were analyzed for the presence of graft-derived alveolar MΦ. *A*, Alveolar MΦ were identified as CD11c$^+$CD11b$^-$CX$_3$CR1/GFP$^-$ cells, as indicated by *gates*. *B*, Graft-derived alveolar MΦ were further identified as CD45.1$^+$ cells, as indicated by *gate*. Numbers indicate percentage of graft-derived cells (CD45.1$^+$) of total gated population and their absolute numbers (in parentheses). Data show one representative of three independent experiments.

MΦ 4 days after transfer. To distinguish between these two options, we decided to extend our previous study and analyze monocyte recipients 14 days after transfer.

Monocytes, defined as positive for CD115 (also known as M-CSFR), were isolated from blood of $cx_3cr1^{gfp/+}$;CD45.1 mice and transferred into *CD11c*:DTR;CD45.2 transgenic mice, which had been pretreated by i.t. DTx installation. Two weeks after transfer, the BAL content of recipient mice was analyzed for graft-derived alveolar MΦ. The latter were identified as CD45.1$^+$CD11c$^+$ CD11b$^-$CX$_3$CR1/GFP$^-$ cells to discriminate them from CD45.1$^+$ CD11c$^+$CD11b$^+$CX$_3$CR1/GFP$^+$ graft-derived DC and CD45.2$^+$ recipient's cells (27) (Fig. 2*A*). As shown in Fig. 2*B*, 2 wk after transfer, we could detect graft-derived alveolar MΦ. This indicates that blood monocytes do have the capacity to give rise to alveolar MΦ.

Lung and alveolar MΦ show distinct reconstitution kinetics following irradiation and BM transfer

Together with our previous study (27), the above result shows that blood monocytes can give rise to both lung and alveolar MΦ, albeit with distinct kinetics. To further investigate the precursor/progeny relation of blood monocytes and pulmonary MΦ, we investigated the kinetics of their reconstitution after irradiation and total BM engraftment. To this end, we transferred syngeneic wild-type (wt) BM cells (CD45.1) into lethally irradiated recipients (CD45.2) and followed the regeneration of the blood monocyte compartment, as well as lung and alveolar MΦ, by donor-derived cells (Fig. 3*A*).

As expected from the literature (20), 1 wk following BM transfer, all blood monocytes were fully replaced by donor-derived (CD45.1$^+$) cells (Fig. 3*B*). In contrast, and in agreement with their earlier reported delayed reconstitution (14, 16, 37), alveolar MΦ began to be replaced by donor cells only 3 wk after transfer (Fig. 3*B*). Interestingly, the exchange of lung MΦ by donor BM-derived cells significantly preceded this event and showed intermediate kinetics, beginning at day 10, with full reconstitution being reached 3 wk after transfer (Fig. 3*B*).

In conclusion, all three cell types studied are reconstituted after irradiation by BM-derived cells, albeit with significantly distinct kinetics. Interestingly, our data suggest that lung MΦ begin to be replaced by donor BM cells only after exchange of the blood monocyte compartment, and alveolar MΦ start to be replaced only after full reconstitution of parenchymal lung MΦ (Fig. 3*B*).

Alveolar MΦ do not originate directly from blood monocytes

The DTx-induced ablation of alveolar MΦ in *CD11c*:DTR transgenic mice was followed by their rapid reconstitution (Fig. 1*B*). To investigate the origin of these newly generated alveolar MΦ, we transferred CD45.1 wt BM into irradiated *CD11c*:DTR transgenic recipients (CD45.2). The resulting wt→*CD11c*:DTR BM chimeras allow the conditional depletion of host lung and alveolar MΦ. On day 5 after BM transfer, i.e., at a time when some blood monocytes are of donor BM origin, but all lung and alveolar MΦ are still host derived (Fig. 3*B*), chimeras were either treated i.t. with DTx or left untreated. Mice were analyzed on day 8, 3 days after DTx treatment, when >90% of blood monocytes are donor derived (Figs. 3*B* and 4*A*). Whereas parenchymal lung MΦ of untreated chimeras were still host derived, in DTx-treated mice one-half of them were replaced by donor cells, most likely of blood monocyte origin (27) (Fig. 4*A*). Interestingly, in the same mice, >90% of newly generated alveolar MΦ were of host origin (CD45.1$^-$) (Fig. 4*A*). Hence, in our experimental setting, newly generated alveolar MΦ originated from a host-derived precursor, although all blood monocytes were donor derived (Figs. 3*B* and 4*A*). This result argues that alveolar MΦ do not originate directly from blood monocytes.

Lung MΦ serve as alveolar MΦ precursor

Depletion of both *CD11c*:DTR transgenic lung and alveolar MΦ by i.t. DTx treatment was followed by their rapid reconstitution (Fig. 1*B*). The kinetics of these processes was, however, different. Although alveolar MΦ numbers arose after 1 day, the number of parenchymal MΦ continuously declined for the first 4 days following the DTx treatment (Fig. 1*B*). The mean human serum $t_{1/2}$ of DTx has been estimated to be 18 h (38). Accordingly, the DTx treatment of *CD11c*:DTR transgenic mice generally induces a transient, short-term depletion of CD11c$^+$ cells (29). It is therefore unlikely that the persistent decline of lung MΦ from day 1 to day 4 (Fig. 1*B*) results from ongoing toxin-induced apoptosis, but rather suggests MΦ emigration from the lung parenchyma to the alveolar space. In addition, on day 5 after BM transfer, newly generated alveolar MΦ originated from host-derived precursors, whereas at that time lung MΦ were of host origin (Fig. 4*A*). Taken together, our results suggest that parenchymal lung MΦ act as immediate alveolar MΦ precursors.

To further investigate this option, we next studied the origin of alveolar MΦ at a time when parenchymal lung MΦ were reconstituted by donor-derived cells. To this end, wt→*CD11c*:DTR chimeras were treated 12 days after BM transfer with DTx i.t., and control chimeras were left untreated. At this time, all blood monocytes and a fraction of the parenchymal lung MΦ are of donor origin, but alveolar MΦ are still host derived (Fig. 3*B*). We analyzed the recipient mice 3 days later, i.e., on day 15, when all lung MΦ are donor derived (Figs. 3*B* and 4*B*). Although in untreated mice most alveolar MΦ were of host origin, following their DTx-induced depletion all newly generated alveolar MΦ were donor derived (Fig. 4*B*).

To conclude, the origin of newly generated alveolar MΦ correlated with the donor/host origin of lung MΦ (Fig. 4). Taken together with their differential reconstitution kinetics following depletion, these data support the notion that lung MΦ act as alveolar MΦ precursors.

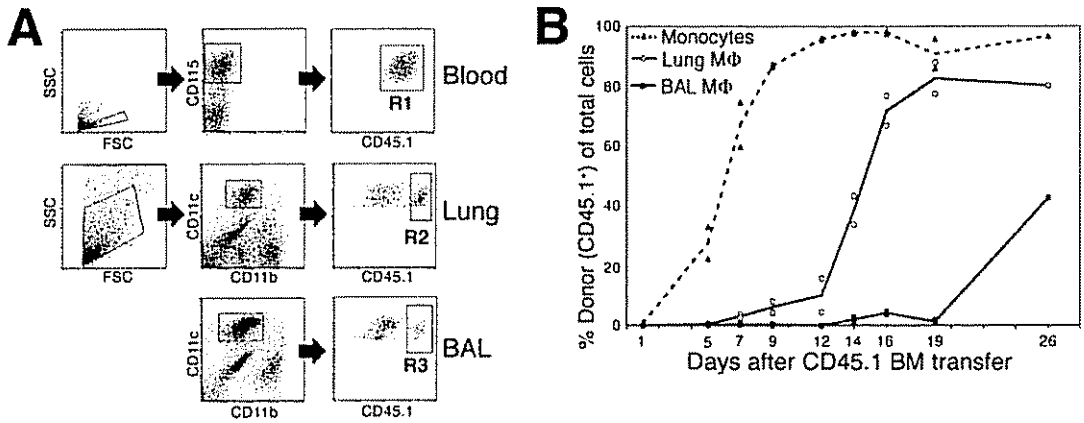

FIGURE 3. Different reconstitution kinetics of blood monocytes, lung MΦ, and alveolar MΦ follow irradiation and BM transfer. CD45.1 BM cells were transferred to CD45.2 wt recipient mice on day 0, and recipients' blood, digested lungs, and BAL fluids were analyzed on days 1, 5, 7, 9, 12, 14, 16, 19, and 26 for donor-derived monocytes and MΦ. *A*, Identification of donor BM-derived cells. Blood of recipient mice was stained with PE-coupled anti CD115 Ab and biotin-coupled anti CD45.1 Ab, followed by allophycocyanin-conjugated streptavidin. Cells isolated from lung parenchyma and BAL fluids were stained with PE-coupled anti-CD11c Ab, PerCP-coupled anti-CD11b Ab, and biotin-coupled anti-CD45.1 Ab, followed by allophycocyanin-conjugated streptavidin. R1 gate indicates $CD45.1^+$ donor-derived cells of total blood monocytes ($CD115^+$ cells). R2 and R3 gates indicate $CD45.1^+$ donor-derived cells of total lung and alveolar MΦ, respectively (identified as $CD11c^+CD11b^-$ cells, as indicated by gates). *B*, Kinetics of blood monocytes (▲), lung MΦ (○), and alveolar MΦ (■) reconstitution by donor BM-derived cells. Graph shows the percentage of donor-derived cells ($CD45.1^+$) of total blood monocytes (cells gated in R1, as indicated in *A*), lung MΦ (cells gated in R2, as indicated in *A*), and BAL MΦ (cells gated in R3, as indicated in *A*). n = 2 for each time point.

Proliferation of lung and alveolar MΦ

All blood monocytes are CX_3CR1 positive, and therefore express cytoplasmatic GFP in $cx_3cr1^{gfp/+}$ knockin mice (30), whereas pulmonary MΦ are CX_3CR1 negative (27) (Fig. 5*A*). Because GFP is stable for several days (39), all monocyte descendants inherit the cytoplasmic GFP label, even though expression of CX_3CR1/GFP might have ceased. Although they are monocyte derived and therefore expected to be GFP labeled, pulmonary MΦ of $cx_3cr1^{gfp/+}$ mice are GFP negative (27) (Fig. 5*A*). Because MΦ are long-lived cells (40), they most likely lost the GFP label over time. Alternatively, the rapid loss of the GFP label can be explained by cell divisions, which in the absence of GFP de novo synthesis will result in the dilution of the label between daughter cells. The latter is in agreement with previous studies suggesting that murine alveolar MΦ originate from proliferating precursors in the lung parenchyma (13, 23, 25).

To distinguish between those two options, we analyzed the GFP label of newly coming lung and alveolar MΦ. To this end, we

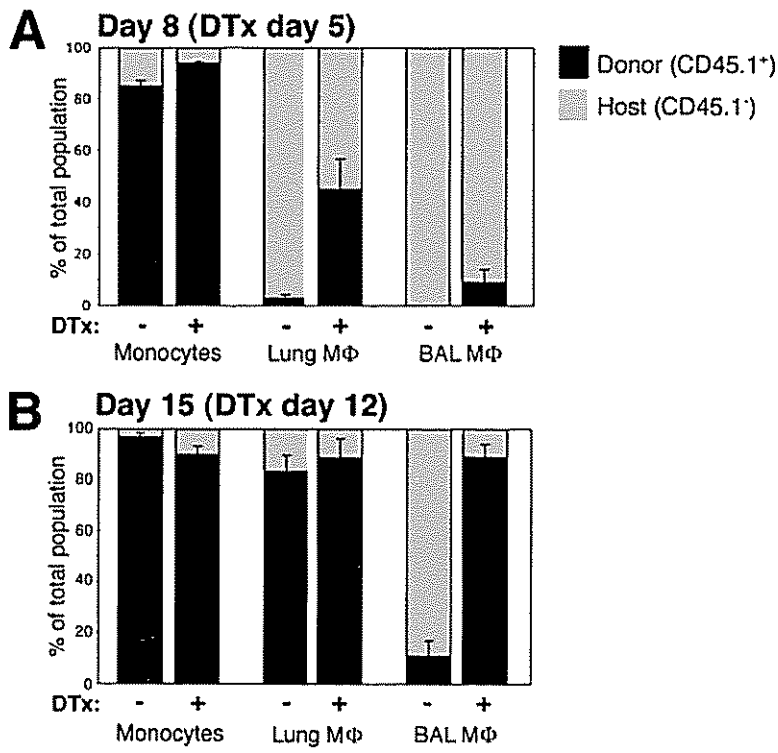

FIGURE 4. Alveolar MΦ do not originate directly from blood monocytes. BM cells of CD45.1 wt mice were adoptively transferred into irradiated *CD11c*:DTR CD45.2 transgenic recipients on day 0. Recipient mice were either treated i.t. with DTx on indicated days or left untreated and sacrificed 3 days later. Cells were then analyzed for CD45.1 expression, as described in Fig. 3*A*: donor-derived ($CD45.1^+$) blood monocytes, lung MΦ, and alveolar MΦ are cells gated in R1, R2, and R3, respectively, whereas host-derived ($CD45.1^-$) cells are cells outside those gates. *A*, Recipient mice were either treated i.t. with DTx on day 5 (+) or left untreated (−) and were sacrificed on day 8. Bar diagram shows percentage of donor ($CD45.1^+$, ■)- and host ($CD45.1^-$, □)-derived blood monocytes, lung MΦ, and alveolar MΦ of the total population. n = 5 for each group. One representative of three independent experiments. *B*, Recipient mice were either treated i.t. with DTx on day 12 (+) or left untreated (−) and were sacrificed on day 15. Bar diagram shows percentage of donor ($CD45.1^+$, ■)- and host ($CD45.1^-$, □)-derived blood monocytes, lung MΦ, and alveolar MΦ of the total population. n = 5 for each group. One representative of three independent experiments.

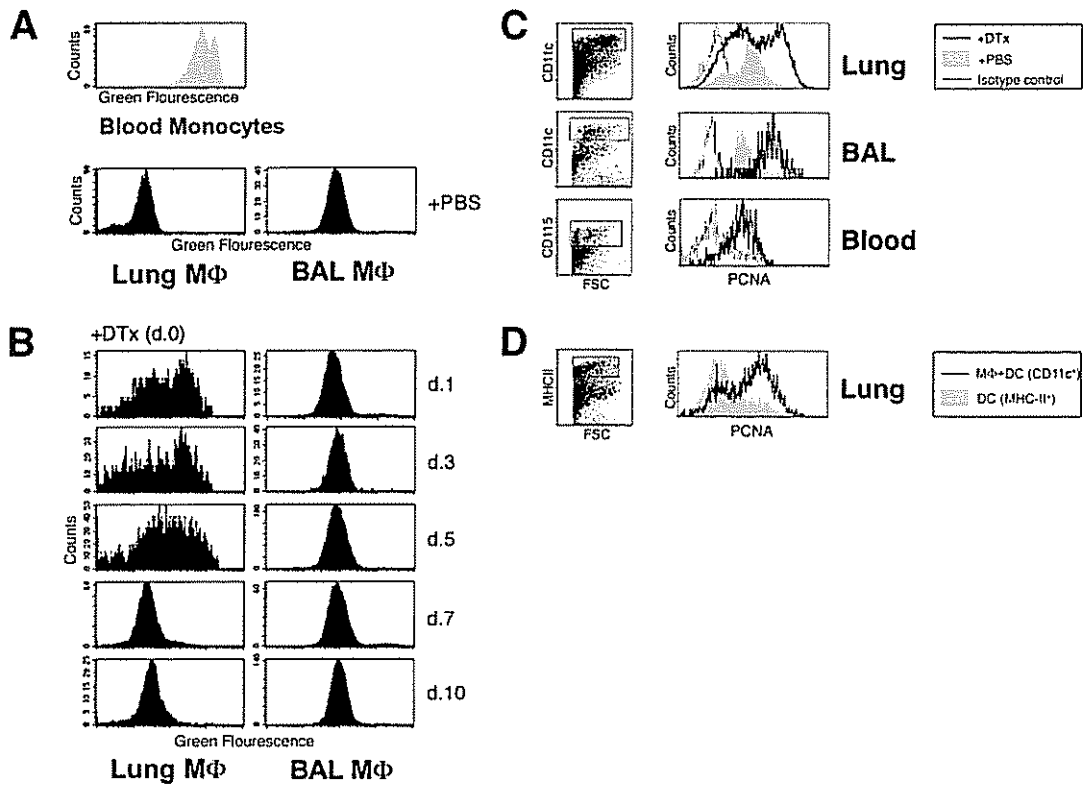

FIGURE 5. Lung and alveolar MΦ proliferate follow depletion. *A*, $Cx_3cr1^{gfp/+}$;*CD11c*:DTR double-transgenic mice were i.t. treated with PBS and sacrificed 1 day later. Blood monocytes (*upper panel*, identified as $CD115^+$ cells), lung MΦ (*left lower panel*, identified as $CD11c^+CD11b^-$ cells), and alveolar MΦ (*right lower panel*, identified as $CD11c^+CD11b^-$ cells) were analyzed for green fluorescence intensity. Data show one representative of three mice. *B*, $cx_3cr1^{gfp/+}$;*CD11c*:DTR mice were i.t. treated with DTx on day 0 and sacrificed on day 1, 3, 5, 7, or 10 following treatment. Lung (*left*) and alveolar (*right*) MΦ (identified as $CD11c^+CD11b^-$ cells) were analyzed for green fluorescence intensity. Note dilution of GFP label in CX_3CR1-negative MΦ with time. Data show one representative of three mice for each time point. *C*, *CD11c*:DTR were i.t. treated with either DTx or PBS on day 0 and sacrificed on day 3, and their blood, lungs, and BAL fluids were analyzed for PCNA expression. Lungs and BAL fluid cells were stained with biotin-coupled anti-CD11c Ab, followed by allophycocyanin-conjugated streptavidin and either PE-coupled anti-PCNA Ab or isotype control (broken line histogram). Histogram shows PCNA expression by $CD11c^+$ cells, as gated in dot plot, of DTx (solid line)- and PBS (gray filled)-treated mice. Blood cells were stained with biotin-coupled anti-CD115 Ab, followed by allophycocyanin-conjugated streptavidin and either PE-coupled anti-PCNA Ab or isotype control (broken line histogram). Histogram shows PCNA expression by $CD115^+$ cells, as gated in dot plot, of DTx (solid line)-treated mouse. Data show one representative of four mice for each group. *D*, *CD11c*:DTR;μMT mice, which are B cell deficient, were i.t. treated with DTx on day 0 and sacrificed on day 3, and their lungs were analyzed for PCNA expression. Half of lung cells were stained with biotin-coupled anti-CD11c Ab and half with biotin-coupled anti-MHC II Ab, both followed by allophycocyanin-conjugated streptavidin and PE-coupled anti-PCNA Ab. Histogram shows PCNA expression by $CD11c^+$ cells (solid line, as gated in *A*), including both MΦ and DC, and MHC II^+ cells (gray filled, as gated on dot plot), including only DC. Data show one representative of four mice.

generated a $cx_3cr1^{gfp/+}$;*CD11c*:DTR double-transgenic mouse line, treated the mice with DTx i.t., and investigated the green fluorescence intensities of their lung and alveolar MΦ on the following days (Fig. 5*B*). During the first 5 days after depletion, newly coming lung MΦ showed various green fluorescence intensities, ranging from high to low (Fig. 5*B*). This may result from differentiation of CX_3CR1/GFP-positive monocytes into CX_3CR1-negative MΦ and the division of the latter. From day 7 and on, lung MΦ fluorescence intensity was low and comparable to that of lung MΦ from PBS-treated mice (Fig. 5, *A* and *B*). This suggests there is no more input of monocytes at this stage, but because lung MΦ population increases (Fig. 1*B*), proliferation of differentiated lung MΦ most likely persists.

Throughout the experiment, alveolar MΦ showed similar green fluorescence intensities to those of PBS-treated mice (Fig. 5, compare *A* and *B*). This supports the notions that the differentiation of blood monocyte into alveolar MΦ is indirect and requires a lung MΦ intermediate. Furthermore, these data also suggest that the proliferation of lung MΦ (which allows the loss of the GFP label) preceded their migration into the alveolar space.

Next, we decided to directly study the proliferation status of lung and alveolar MΦ by determining their PCNA expression levels. The amount of PCNA increases during late G_1 phase at sites of DNA replication, reaches a maximum in S phase, and declines during G_2 phase (41, 42).

We therefore stained lung, BAL, and blood cells of *CD11c*:DTR mice 3 days after i.t. treatment with either DTx or PBS for PCNA. In PBS-treated mice, $CD11c^+$ lung cells were $PCNA^{int}$, indicating that they were in G_1 phase, and upon DTx treatment a majority of these cells became $PCNA^{high}$ (Fig. 5*C*), documenting S phase entry and proliferation (41). Because CD11c is expressed by both lung MΦ and DC (33, 34), the analyzed population includes both cell types. In contrast, MHC II is highly expressed by lung DC, but not by MΦ, and therefore allows the discrimination of the two cell types (34). To exclude a potential contamination with MHC II-expressing B cells, we crossed *CD11c*:DTR mice with B cell-deficient mice (μMT mice) (31), allowing the exclusive definition of lung MHC II^+ cells as DC. The comparison of PCNA expression levels of MHC II- and CD11c-positive lung cells of DTx-treated *CD11c*:DTR;μMT mice confirmed that the $PCNA^{high}$ cells were

lung MΦ ($CD11c^+MHC\ II^{low}$), whereas lung DC ($CD11c^+MHC\ II^+$) were $PCNA^{low\text{-}int}$ (Fig. 5*D*). This indicates that lung MΦ, but not lung DC, undergo proliferation.

Blood monocytes were $PCNA^{int}$ (Fig. 5*C*), in agreement with other studies showing that monocytes do not proliferate (28, 43). Interestingly, following the DTx treatment, alveolar MΦ became $PCNA^{high}$ (Fig. 5*C*), supporting the notion that they can proliferate, as previously reported in humans (44).

To conclude, both lung and alveolar MΦ have proliferative potential, which manifests itself upon their DTx-induced depletion and reconstitution. In addition, our results show that lung MΦ proliferation precedes their migration into the alveolar space.

Discussion

In this study, we provide direct evidence that alveolar MΦ originate from blood monocytes, and show that this process requires a lung-resident intermediate. We proposed that generation of alveolar MΦ involves the differentiation of blood monocytes into MΦ in the lung parenchyma, proliferative expansion of these cells, and their emigration into the alveolar space. In such a scenario, lung MΦ may serve as a local reservoir, from which alveolar MΦ can be generated whenever needed.

This model is in accordance with results of most previous studies on the alveolar MΦ origin. Our finding, suggesting an indirect connection of blood monocytes and alveolar MΦ, agrees, for example, with the finding of Sawyer et al. (25), showing that the alveolar MΦ population is unaffected by experimentally induced blood monocyte depletion. Furthermore, the derivation of alveolar MΦ from blood monocytes is in agreement with the previously reported replacement of these MΦ by donor cells upon BM transfer (11, 12), and the need for a lung intermediate can further explain the observed delayed reconstitution (13, 14). Bowden and Adamson (23) suggested a dual origin for alveolar MΦ, either directly from blood-borne precursor or from local proliferation. Our results suggest the steady-state derivation of alveolar MΦ from local proliferating precursor, i.e., lung MΦ, and therefore partially agree with the mentioned study. Alveolar DC had not been identified by that time Bowden's study was conducted (24), and our current data and previous reports suggest that they are derived from blood monocytes without local proliferation (27). We would therefore like to propose that the cells shown by Bowden and Adamson (23) to directly derive from blood monocyte are alveolar DC, potentially mistaken for alveolar MΦ. To conclude, our model offers a connection between works reporting local precursor (13, 23, 25, 45) and those indicating blood-borne precursor (11, 12, 40) for alveolar MΦ, previously thought to be contradictory.

We show that the pulmonary MΦ reservoir is maintained by MΦ proliferation in situ, in both lung parenchyma and alveolar space. In situ proliferating precursors were also suggested for other MΦ population, such as splenic MΦ and liver Kupffer cells (46, 47). Therefore, dependency on a local self-renewal capacity seems to be a general feature of MΦ populations, rather than unique to alveolar MΦ.

Because the main role of alveolar MΦ is the maintenance of the alveolar space by clearing dying cells, particles, and pathogens, there is a constant need for their presence in adequate numbers. By abolishing the dependency on recruitment of blood precursors, the existence of local precursor as reservoir for alveolar MΦ allows a tight control and prompt adjustment of their numbers. Consequently, the rate of monocyte differentiation into lung MΦ under steady state is likely to be low, precluding the detection of monocyte-derived alveolar MΦ (25, 45). In this study, we use a noninflammatory, experimentally induced MΦ depletion protocol to accelerate the MΦ turnover rate, allowing us to detect lung MΦ-derived alveolar MΦ in resting state.

Under conditions other than steady state, the dependency of alveolar MΦ population on input from the blood might differ. Inflammation is, for example, associated with an increase in alveolar MΦ levels (16, 37, 48), and i.t. LPS treatment of BM recipient mice accelerates the replacement of alveolar MΦ by donor cells (16). Interestingly, the rate of lung MΦ replacement by donor-derived cells was also promoted in these studies (16). In agreement with these findings, we have previously shown the differentiation of blood monocytes into lung MΦ in i.t. LPS-treated recipients, but not in untreated mice (27). We, however, had failed to detect graft-derived alveolar MΦ in these studies, which included the analysis of recipient mice 4 days following monocyte transfer (27). In addition, Adamson and Bowden's (48) kinetic studies (when interpreted as discussed above) suggest the existence of a lung intermediate for alveolar MΦ also during inflammation. We therefore suggest the kinetics of both monocyte differentiation into lung MΦ and the migration of the latter to the alveolar space to accelerate under inflammation. It thus remains possible that the differentiation of alveolar MΦ under inflammation also requires a lung MΦ intermediate.

The irradiation protocol used for the depletion of host BM may also affect the kinetic of alveolar MΦ differentiation from blood monocyte. In this respect, it is of note that different irradiation protocols before BM transfer resulted in distinct alveolar MΦ reconstitution kinetics (11, 13–15). Because irradiation primarily affects dividing cells, proliferating alveolar MΦ might become sensitive to irradiation. Therefore, the turnover of alveolar MΦ can be promoted by the stress caused by tissue damage (49), by a direct effect on pulmonary MΦ (13), or by a combination of the two.

One of the serious side effects of BM transplantation in humans is the increased susceptibility of patients to pulmonary infections (17, 18). It has been proposed that in addition to their lower number, alveolar MΦ of BM transplantation patients might be functionally impaired and therefore less reactive (37). The proliferative capacity of both lung parenchymal and alveolar MΦ might make both these cell types sensitive to irradiation. This can affect both the functionality of alveolar MΦ and the size of their reservoir in the lung parenchyma, reducing their capacity to efficiently combat pathogens. The indirect route from monocytes to alveolar MΦ might result in a delayed replacement of damaged alveolar MΦ with new and unaffected cells, maintaining the patient susceptibility to pathogen. Therefore, our results suggest that a strategy aiming at the active depletion of pulmonary MΦ might trigger an advantageous renewal from donor BM-derived monocytes, and could potentially reduce the period of patient vulnerability to pulmonary pathogens.

Acknowledgments

We thank our laboratory members for critical reading of the manuscript, and are grateful to Y. Chermesh and Y. Melamed for animal husbandry.

Disclosures

The authors have no financial conflict of interest.

References

1. Martin, T. R., and C. W. Frevert. 2005. Innate immunity in the lungs. *Proc. Am. Thorac. Soc.* 2: 403–411.
2. Lambrecht, B. N., and H. Hammad. 2003. Taking our breath away: dendritic cells in the pathogenesis of asthma. *Nat. Rev. Immunol.* 3: 994–1003.
3. MacLean, J. A., W. Xia, C. E. Pinto, L. Zhao, H. W. Liu, and R. L. Kradin. 1996. Sequestration of inhaled particulate antigens by lung phagocytes: a mechanism for the effective inhibition of pulmonary cell-mediated immunity. *Am. J. Pathol.* 148: 657–666.
4. Holt, P. G., J. Oliver, N. Bilyk, P. G. McMenamin, G. Kraal, and T. Thepen. 1993. Down-regulation of the antigen presenting cell function(s) of pulmonary

dendritic cells in vivo by resident alveolar macrophages. *J. Exp. Med.* 177: 397–407.
5. Julia, V., E. M. Hessel, L. Malherbe, N. Glaichenhaus, A. O'Garra, and R. L. Coffman. 2002. A restricted subset of dendritic cells captures airborne antigens and remains able to activate specific T cells long after antigen exposure. *Immunity* 16: 271–283.
6. Thepen, T., C. McMenamin, J. Oliver, G. Kraal, and P. G. Holt. 1991. Regulation of immune response to inhaled antigen by alveolar macrophages: differential effects of in vivo alveolar macrophage elimination on the induction of tolerance vs. immunity. *Eur. J. Immunol.* 21: 2845–2850.
7. Thepen, T., N. Van Rooijen, and G. Kraal. 1989. Alveolar macrophage elimination in vivo is associated with an increase in pulmonary immune response in mice. *J. Exp. Med.* 170: 499–509.
8. Careau, E., and E. Y. Bissonnette. 2004. Adoptive transfer of alveolar macrophages abrogates bronchial hyperresponsiveness. *Am. J. Respir. Cell Mol. Biol.* 31: 22–27.
9. Fainaru, O., E. Woolf, J. Lotem, M. Yarmus, O. Brenner, D. Goldenberg, V. Negreanu, Y. Bernstein, D. Levanon, S. Jung, and Y. Groner. 2004. Runx3 regulates mouse TGF-β-mediated dendritic cell function and its absence results in airway inflammation. *EMBO J.* 23: 969–979.
10. Takabayshi, K., M. Corr, T. Hayashi, V. Redecke, L. Beck, D. Guiney, D. Sheppard, and E. Raz. 2006. Induction of a homeostatic circuit in lung tissue by microbial compounds. *Immunity* 24: 475–487.
11. Godleski, J. J., and J. D. Brain. 1972. The origin of alveolar macrophages in mouse radiation chimeras. *J. Exp. Med.* 136: 630–643.
12. Thomas, E. D., R. E. Ramberg, G. E. Sale, R. S. Sparkes, and D. W. Golde. 1976. Direct evidence for a bone marrow origin of the alveolar macrophage in man. *Science* 192: 1016–1018.
13. Tarling, J. D., H. S. Lin, and S. Hsu. 1987. Self-renewal of pulmonary alveolar macrophages: evidence from radiation chimera studies. *J. Leukocyte Biol.* 42: 443–446.
14. Matute-Bello, G., J. S. Lee, C. W. Frevert, W. C. Liles, S. Sutlief, K. Ballman, V. Wong, A. Selk, and T. R. Martin. 2004. Optimal timing to repopulation of resident alveolar macrophages with donor cells following total body irradiation and bone marrow transplantation in mice. *J. Immunol. Methods* 292: 25–34.
15. Johnson, K. J., P. A. Ward, G. Striker, and R. Kunkel. 1980. A study of the origin of pulmonary macrophages using the Chediak-Higashi marker. *Am. J. Pathol.* 101: 365–374.
16. Maus, U. A., S. Janzen, G. Wall, M. Srivastava, T. S. Blackwell, J. W. Christman, W. Seeger, T. Welte, and J. Lohmeyer. 2006. Resident alveolar macrophages are replaced by recruited monocytes in response to endotoxin-induced lung inflammation. *Am. J. Respir. Cell Mol. Biol.* 35: 227–235.
17. Kruger, W., B. Russmann, N. Kroger, C. Salomon, N. Ekopf, H. A. Elsner, P. M. Kaulfers, D. Mack, N. Fuchs, M. Durken, et al. 1999. Early infections in patients undergoing bone marrow or blood stem cell transplantation: a 7 year single centre investigation of 409 cases. *Bone Marrow Transplant.* 23: 589–597.
18. Lossos, I. S., R. Breuer, R. Or, N. Strauss, H. Elishoov, E. Naparstek, M. Aker, A. Nagler, A. E. Moses, M. Shapiro, et al. 1995. Bacterial pneumonia in recipients of bone marrow transplantation: a five-year prospective study. *Transplantation* 60: 672–678.
19. Van Furth, R., and Z. A. Cohn. 1968. The origin and kinetics of mononuclear phagocytes. *J. Exp. Med.* 128: 415–435.
20. Van Furth, R., M. C. Diesselhoff-den Dulk, and H. Mattie. 1973. Quantitative study on the production and kinetics of mononuclear phagocytes during an acute inflammatory reaction. *J. Exp. Med.* 138: 1314–1330.
21. De Groot, C. J., W. Huppes, T. Sminia, G. Kraal, and C. D. Dijkstra. 1992. Determination of the origin and nature of brain macrophages and microglial cells in mouse central nervous system, using non-radioactive in situ hybridization and immunoperoxidase techniques. *Glia* 6: 301–309.
22. Gordon, S., and P. R. Taylor. 2005. Monocyte and macrophage heterogeneity. *Nat. Rev. Immunol.* 5: 953–964.
23. Bowden, D. H., and I. Y. Adamson. 1980. Role of monocytes and interstitial cells in the generation of alveolar macrophages. I. Kinetic studies of normal mice. *Lab. Invest.* 42: 511–517.
24. Pollard, A. M., and M. F. Lipscomb. 1990. Characterization of murine lung dendritic cells: similarities to Langerhans cells and thymic dendritic cells. *J. Exp. Med.* 172: 159–167.
25. Sawyer, R. T., P. H. Strausbauch, and A. Volkman. 1982. Resident macrophage proliferation in mice depleted of blood monocytes by strontium-89. *Lab. Invest.* 46: 165–170.
26. Naito, M., S. Umeda, T. Yamamoto, H. Moriyama, H. Umezu, G. Hasegawa, H. Usuda, L. D. Shultz, and K. Takahashi. 1996. Development, differentiation, and phenotypic heterogeneity of murine tissue macrophages. *J. Leukocyte Biol.* 59: 133–138.
27. Landsman, L., C. Varol, and S. Jung. 2007. Distinct differentiation potential of blood monocyte subsets in the lung. *J. Immunol.* 178: 2000–2007.
28. Geissmann, F., S. Jung, and D. R. Littman. 2003. Blood monocytes consist of two principal subsets with distinct migratory properties. *Immunity* 19: 71–82.
29. Jung, S., D. Unutmaz, P. Wong, G. Sano, K. De los Santos, T. Sparwasser, S. Wu, S. Vuthoori, K. Ko, F. Zavala, et al. 2002. In vivo depletion of $CD11c^+$ dendritic cells abrogates priming of $CD8^+$ T cells by exogenous cell-associated antigens. *Immunity* 17: 211–220.
30. Jung, S., J. Aliberti, P. Graemmel, M. J. Sunshine, G. W. Kreutzberg, A. Sher, and D. R. Littman. 2000. Analysis of fractalkine receptor CX_3CR1 function by targeted deletion and green fluorescent protein reporter gene insertion. *Mol. Cell. Biol.* 20: 4106–4114.
31. Kitamura, D., J. Roes, R. Kuhn, and K. Rajewsky. 1991. A B cell-deficient mouse by targeted disruption of the membrane exon of the immunoglobulin μ chain gene. *Nature* 350: 423–426.
32. Ho, W., and A. Furst. 1973. Intratracheal instillation method for mouse lungs. *Oncology* 27: 385–393.
33. Gonzalez-Juarrero, M., T. S. Shim, A. Kipnis, A. P. Junqueira-Kipnis, and I. M. Orme. 2003. Dynamics of macrophage cell populations during murine pulmonary tuberculosis. *J. Immunol.* 171: 3128–3135.
34. Vermaelen, K., and R. Pauwels. 2004. Accurate and simple discrimination of mouse pulmonary dendritic cell and macrophage populations by flow cytometry: methodology and new insights. *Cytometry A* 61: 170–177.
35. Van Rijt, L. S., S. Jung, A. Kleinjan, N. Vos, M. Willart, C. Duez, H. C. Hoogsteden, and B. N. Lambrecht. 2005. In vivo depletion of lung $CD11c^+$ dendritic cells during allergen challenge abrogates the characteristic features of asthma. *J. Exp. Med.* 201: 981–991.
36. Naglich, J. G., J. E. Metherall, D. W. Russell, and L. Eidels. 1992. Expression cloning of a diphtheria toxin receptor: identity with a heparin-binding EGF-like growth factor precursor. *Cell* 69: 1051–1061.
37. Ojielo, C. I., K. Cooke, P. Mancuso, T. J. Standiford, K. M. Olkiewicz, S. Clouthier, L. Corrion, M. N. Ballinger, G. B. Toews, R. Paine III, and B. B. Moore. 2003. Defective phagocytosis and clearance of *Pseudomonas aeruginosa* in the lung following bone marrow transplantation. *J. Immunol.* 171: 4416–4424.
38. Buzzi, S., D. Rubboli, G. Buzzi, A. M. Buzzi, C. Morisi, and F. Pironi. 2004. CRM197 (nontoxic diphtheria toxin): effects on advanced cancer patients. *Cancer Immunol. Immunother.* 53: 1041–1048.
39. Giuliano, K. A., P. L. Post, K. M. Hahn, and D. L. Taylor. 1995. Fluorescent protein biosensors: measurement of molecular dynamics in living cells. *Annu. Rev. Biophys. Biomol. Struct.* 24: 405–434.
40. Van oud Alblas, A. B., and R. van Furth. 1979. Origin, kinetics, and characteristics of pulmonary macrophages in the normal steady state. *J. Exp. Med.* 149: 1504–1518.
41. Landberg, G., and G. Roos. 1991. Antibodies to proliferating cell nuclear antigen as S-phase probes in flow cytometric cell cycle analysis. *Cancer Res.* 51: 4570–4574.
42. McCormick, D., and P. A. Hall. 1992. The complexities of proliferating cell nuclear antigen. *Histopathology* 21: 591–594.
43. Van Furth, R. 1989. Origin and turnover of monocytes and macrophages. *Curr. Top. Pathol.* 79: 125–150.
44. Nakata, K., H. Gotoh, J. Watanabe, T. Uetake, I. Komuro, K. Yuasa, S. Watanabe, R. Ieki, H. Sakamaki, H. Akiyama, et al. 1999. Augmented proliferation of human alveolar macrophages after allogeneic bone marrow transplantation. *Blood* 93: 667–673.
45. Sawyer, R. T. 1986. The ontogeny of pulmonary alveolar macrophages in parabiotic mice. *J. Leukocyte Biol.* 40: 347–354.
46. Van Furth, R., and M. M. Diesselhoff-den Dulk. 1984. Dual origin of mouse spleen macrophages. *J. Exp. Med.* 160: 1273–1283.
47. Crofton, R. W., M. M. Diesselhoff-den Dulk, and R. van Furth. 1978. The origin, kinetics, and characteristics of the Kupffer cells in the normal steady state. *J. Exp. Med.* 148: 1–17.
48. Adamson, I. Y., and D. H. Bowden. 1980. Role of monocytes and interstitial cells in the generation of alveolar macrophages. II. Kinetic studies after carbon loading. *Lab. Invest.* 42: 518–524.
49. Rubin, P., J. Finkelstein, and D. Shapiro. 1992. Molecular biology mechanisms in the radiation induction of pulmonary injury syndromes: interrelationship between the alveolar macrophage and the septal fibroblast. *Int. J. Radiat. Oncol. Biol. Phys.* 24: 93–101.

Transepithelial Pathogen Uptake into the Small Intestinal Lamina Propria[1]

Alexandra Vallon-Eberhard,[2*†] Limor Landsman,[2*] Nir Yogev,[*] Bernard Verrier,[†] and Steffen Jung[3*]

The lamina propria that underlies and stabilizes the gut lining epithelium is densely populated with strategically located mononuclear phagocytes. Collectively, these lamina propria macrophages and dendritic cells (DC) are believed to be crucial for tissue homeostasis as well as the innate and adaptive host defense. Lamina propria DC were recently shown to gain direct access to the intestinal lumen by virtue of epithelium-penetrating dendrites. However, the role of these structures in pathogen uptake remains under debate. In this study, we report that entry of a noninvasive model pathogen (*Aspergillus fumigatus* conidia) into the murine small intestinal lamina propria persists in the absence of either transepithelial dendrites or lamina propria DC and macrophages. Our results suggest the existence of multiple pathogen entry pathways and point at the importance of villus M cells in the uptake of gut lumen Ags. Interestingly, transepithelial dendrites seem altogether absent from the small intestine of BALB/c mice suggesting that the function of lamina propria DC extensions resides in their potential selectivity for luminal Ags, rather than in general uptake or gut homeostasis. *The Journal of Immunology*, 2006, 176: 2465–2469.

The surface of the gastrointestinal tract must protect the organism from harmful microorganisms while retaining permeability for nutrient absorption. The gut lumen-lining epithelium forms an efficient physical barrier. Exposure of the host to bacterial symbionts, commensals, and pathogens is further prevented through a number of nonspecific innate defense mechanisms. Local mucus production and a thick glycocalix reduce direct contact of the epithelium with the gut microflora and form a highly degradative microenvironment. Protection is also upheld through steady-state secretion of a broad spectrum of antimicrobial agents, such as α-defensins and secretory IgA Abs (1). Intestinal homeostasis is established and shaped by controlled host interaction with the commensal microflora through pathways allowing sensing and sampling of the gut content (2). The latter are likely to be also of crucial importance for immune protection against potential pathogens.

The luminal surface of the gut is lined with polarized, columnar epithelial cells. Joined by tight junctions dividing the apical and basolateral domains of neighboring cells, this single-cell layer restricts particle entry. Besides this barrier function, epithelial cells are actively involved in sensing of the gut microflora as indicated by prominent expression of membrane-bound and cytoplasmic "surveillance" proteins of the TLR and NOD/caspase recruitment domain superfamily (3). Triggering of these sensors potentially results in secretion of effector molecules and basolateral display of receptor ligands, such as CX_3CL1, thereby transducing information to underlying lamina propria cells (4, 5). Surveillance of the gut content is further supported by a distinctive type of epithelial cell, the so-called M cell, that fenestrates the epithelial layer and is specialized in transepithelial uptake of particulate and soluble molecules. M cell formation was reported to depend on lymphoepithelial cross-talk (6) and M cells are believed to remain intimately associated with the mucosal-associated lymphoid tissue. Accordingly, they were reported to be restricted to follicle-associated epithelium that colocalize with unique small intestinal lymphoid structures, the Peyer's patches. More recently, however, M cells were shown to be more widely distributed in the small intestine (7), suggesting extended exposure of the epithelium underlying lamina propria to the luminal content. A third mechanism that potentially enables immunosurveillance of the intestinal content is based on a cellular component of the immune system itself, the dendritic cells (DC).[4] These cells constitute a major cellular component of the intestinal lamina propria and have been shown to penetrate epithelial tight junctions by virtue of extended dendrites (8). The epithelial barrier integrity is retained through expression of tight junction proteins by the lamina propria DC (lpDC) (8). Transgenic mice harboring green fluorescent lpDC (CX_3CR1^{GFP} mice) allowed us recently to demonstrate the existence of transepithelial dendrites in live intestinal tissue (4). Although these extensions enable lpDC to sense the content of the intestinal lumen, their role in pathogen uptake remains under debate.

In this study, we report lamina propria entry of a noninvasive particulate pathogen, i.e., conidia of the fungus *Aspergillus fumigatus*, in the absence of transepithelial dendrites. Furthermore, we show that pathogen uptake persists after conditional in situ depletion of all lamina propria mononuclear phagocytes, including

*Department of Immunology, The Weizmann Institute of Science, Rehovot, Israel; and †Formation de Recherche en Evolution 2736, Centre National de la Recherche Scientifique, BioMérieux, Institut Fédératif de Recherche 128 Biosciences Lyon Gerland, Lyon, France

Received for publication August 4, 2005. Accepted for publication November 30, 2005.

The costs of publication of this article were defrayed in part by the payment of page charges. This article must therefore be hereby marked *advertisement* in accordance with 18 U.S.C. Section 1734 solely to indicate this fact.

[1] This work was supported by a European Molecular Biology Organization short-term fellowship (to A.V.-E.) and the MINERVA foundation. S.J. is an Incumbent of the Pauline Recanati Career Development Chair and a Scholar of the Benoziyo Center for Molecular Medicine.

[2] A.V.-E. and L.L. contributed equally to this work.

[3] Address correspondence and reprint requests to Dr. Steffen Jung, Department of Immunology, The Weizmann Institute of Science, Rehovot 76100, Israel. E-mail address: s.jung@weizmann.ac.il

[4] Abbreviations used in this paper: DC, dendritic cell; lpDC, lamina propria DC; lpMϕ, lamina propria macrophage; FKN, fractalkine; UEA, *Ulex europaeus* agglutinin; DTR, diphtheria toxin receptor; DTx, diphtheria toxin; $sPLA_2$, secretory group II phospholipase A2 gene.

0022-1767/06/$02.00

$CD11c^+CX_3CR1^+$ DCs (lpDC) and $CD11c^+CX_3CR1^-$ macrophages (lpMϕ). Together with the observation that transepithelial lpDC extensions seem absent from the small intestine of BALB/c mice, these findings argue against a general role of transepithelial dendrites in the maintenance of intestinal homeostasis, but suggest the existence of multiple pathogen entry routes.

Materials and Methods

Mice

This study involved the use of CD11c-diphtheria toxin receptor (DTR) transgenic mice (B6.FVB-Tg(Itgax-DTR/GFP)57Lan/J) (9) and CX_3CR1^{GFP} mice (10). C57BL/6 and BALB/c mice carrying the CX_3CR1^{GFP} allele were backcrossed >10 generations on the respective background. All mice were maintained under specific pathogen-free conditions and handled under protocols approved by The Weizmann Institute Animal Care Committee according to international guidelines.

Transformation of Aspergillus fumigatus *and conidia isolation*

A. fumigatus conidia (strain CBS 144.89) were provided by J.-P. Latgé (*Aspergillus* Unit, Pasteur Institute, Paris, France). Transformation was performed by electroporation using inflated spores. Briefly, conidia were incubated in yeast extract glucose 1% medium for 4 h at 37°C, washed, resuspended in yeast extract glucose 1% HEPES 20 mM (pH 8), and incubated for 1 h at 30°C. After centrifugation, spores were resuspended in electroporation buffer (10 mM Tris (pH 7.5), 270 mM sucrose, 1 mM lithium acetate). Plasmids (pAN7-1, pPgpd-DsRed) harboring a *hygB* resistance gene and DsRed gene, respectively (11) (provided by L. Mikkelsen, The Royal Veterinary and Agricultural University, Frederiksberg, Denmark) were added and electroporation was carried according the following conditions: 1 kV, 400 ω, 25 μF, in a 0.2-mm cuvette. Transformed spores were incubated for 15 min on ice in 1 ml of yeast extract glucose 1% medium, plated in minimum medium supplemented with 200 μg/ml hygromycin B (Invitrogen Life Technologies) and incubated at room temperature. For monosporic isolation, *A. fumigatus* spores were plated in sterilized water/Tween 20 0.1% at a final concentration of 10 spores/100 μl on malt agar 2% plates overlaid with 200 μg/ml hygromycin B. Single colonies were transferred to a new plate to allow production of conidia during 1wk at room temperature. The conidia stock was kept in sterile water at 4°C.

Isolation of small intestinal mononuclear phagocytes

Isolation of lamina propria cells was performed as previously described (4) with modifications. Briefly, following isolation from $Rag^{-/-}CX_3CR1^{GFP/+}$ mice, small intestine was inverted on a polyethylene tube (diameter 2.08 mm), incubated with RPMI 1640 for 30 min at 37°C to loosen the epithelium, washed, and treated with 1 mM DTT (Sigma-Aldrich) for 10 min at room temperature. After a wash, tissue was incubated twice with EDTA 30 mM for 10 min at room temperature, washed, and digested with 36 U/ml collagenase IV (Sigma-Aldrich) and 2000 U/ml DNase I (Roche) in PBS for 1 h at 37°C. The digested tissue was then sheared by repeated pipetting to release the lamina propria cells. The resulting cell suspension was passed through a mesh (70-μm nylon) and analyzed.

Pathogen uptake assay

Mice were sacrificed and 2- to 3-cm sections spanning the small intestinal terminal ileum were cut out, ligated at both ends, and placed in a petri dish. Pathogens were injected with a syringe into the loop and incubated for 10 min at 37°C in RPMI 1640. The loop was subsequently opened at both ends and extensively washed with PBS. This study involved two pathogens: DsRed-transformed *A. fumigatus* conidia and *Salmonella typhimurium* strain CS093 (provided by A. Porgador, Ben Gurion University, Beer Sheva, Israel). Conidia were added at a final concentration of 10^7 conidia/ml and 2×10^8 *S. typhimurium* bacteria/ml. Bacteria were used in their late logarithmic phase of growth, by diluting a colony in Luria broth containing 0.3 M NaCl and incubating overnight at 37°C.

FACS analysis

Fluorochrome-labeled mAbs were purchased from BD Pharmingen or eBioscience and used according to the manufacturer's protocols. CX_3CR1 staining was performed as previously described using an fractalkine (FKN)-Fc fusion protein (provided by Millennium Biotherapeutics) (10). Cells were analyzed on a FACSCalibur cytometer (BD Biosciences) using CellQuest software (BD Biosciences).

Staining and microscopy of the small intestinal mucosa

After pathogen or mock challenge, ligated small intestinal loops were opened at their end, intensively flushed with PBS, opened by longitudinal incision, and rinsed again. For M cell staining, the cut tissue was fixed in 4% paraformaldehyde for 1 h on ice, incubated with biotin-conjugated anti-*Ulex europaeus* agglutinin (UEA-1; Vector Laboratories) at 20 μg/ml for 2 h on ice followed by staining with streptavidin-allophycocyanin. Living tissues were imaged with a Zeiss Axioskop II fluorescent microscope for three-color imaging. Image acquisition was conducted with Simple PCI software.

Results

The murine small intestinal lamina propria harbors two distinct mononuclear phagocyte populations

To characterize the mononuclear phagocyte content of the murine small intestinal lamina propria, we isolated tissue samples from the small bowel, prepared single-cell suspensions, and analyzed them by flow cytometry. Taking advantage of a mouse strain that harbors a targeted replacement of the gene encoding the chemokine receptor CX_3CR1 by a reporter gene encoding GFP (10), we previously showed that the murine intestine harbors a distinct population of $CD11c^+CD11b^+$ DC that expresses CX_3CR1 (4). Flow cytometric analysis of unfractioned small intestinal single-cell suspensions revealed the presence of additional $CD11c^+$ mononuclear phagocytes that lack CX_3CR1 expression (Fig. 1). The two $CD11c^+$ populations differ with respect to maturation and activation markers, such as CD80, MHC class II, and the integrin CD11b, which show higher expression levels on the CX_3CR1-expressing cells. CX_3CR1^+ lpDC are further characterized by expression of the DC marker 33D1 (12) and high level expression of the α_{E2} integrin CD103, recently reported for rat intestinal DC (13). The classical macrophage marker F4/80 (14) did not consistently discriminate between the two populations (data not shown). However, absence of CD14, the primary receptor for LPS, on the CX_3CR1-negative $CD11c^+$ cell population suggests that these cells correspond to a population of lpMϕ, as described by Smythies et al. (15) for the human intestine. Interestingly, this mononuclear phagocyte dichotomy seems to be a characteristic general feature of the lamina propria because $CD11c^+$ lung mononuclear phagocytes can also be discriminated on the basis of

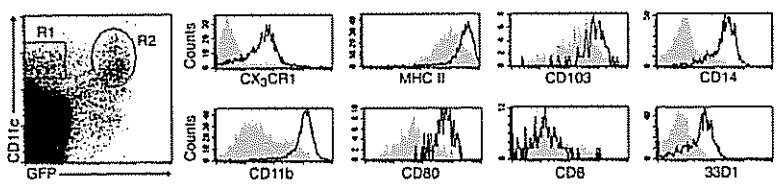

FIGURE 1. Phenotypic dichotomy of lamina propria mononuclear phagocytes. Isolated small intestinal lamina propria cells of $Rag^{-/-}$ $CX_3CR1^{GFP/+}$ mice were stained with Abs for CD11c and one of the indicated surface markers. CX_3CR1 was stained with FKN-Fc. Expression of surface markers of gated populations is shown in the *right histograms*. Gray-filled histograms: $CD11c^+$ CX_3CR1/GFP^- cells (lpMϕ) (Gate R1), open histograms: $CD11c^+$ CX_3CR1/GFP^+ (lpDC) (Gate R2).

CD11b and CX_3CR1 expression (16, 17) (L. Landsman, unpublished observation). Accordingly, we propose to refer to the $CD11c^+CD11b^+CX_3CR1^+$ population as lpDC and the $CD11c^+CD11b^-CX_3CR1^-$ cells as lpMϕ. Proximal and distal sections of the small intestine vary considerably in the microbial load. However, we did not observe significant differences between lamina propria cells isolated from the duodenum/jejunum and terminal ileum, for the markers analyzed (data not shown).

Neither transepithelial dendrites nor $CD11c^+$ lamina propria cells are required for quantitative pathogen uptake

C57BL/6 CX_3CR1^{GFP} mice allow the in situ detection of transepithelial dendrites in intact intestinal tissue (4). The latter allow strategically located lpDC to sense the content of the intestinal lumen. Supporting their role in immunosurveillance, lpDC extensions are restricted to the terminal ileum (4), a region characterized by increased bacterial load, a unique microflora as well as activated epithelium and lamina propria, suggesting constant exposure to bacterial stimuli (4, 18, 19). Furthermore, formation of transepithelial dendrites can be induced by challenge of intestinal villi with commensal and enteropathogenic bacteria (4). However, a direct role of lpDC and trans-epithelial dendrites in pathogen sampling, as originally suggested by Rescigno et al. (20) remains controversial (21, 22). Challenging the general accessibility of the lamina propria, Macpherson and Uhr (23) failed to detect bacteria-harboring lpDC after gavage with GFP-expressing *Escherichia coli*. In contrast, we reported that orally administered invasive *S. typhimurium* entered the lamina propria even in absence of transepithelial dendrites, while entry of a noninvasive *Salmonella* mutant to the lamina propria was CX_3CR1-dependent (4). To directly study dendrite/pathogen interactions at the intestinal surface, we investigated the potential of the noninvasive fungal pathogen, *Aspergillus fumigatus*, to induce transepithelial dendrites and enter the lamina propria. Both *Aspergillus* hyphae and conidia have been reported to interact with DC involving receptors of the IL-1R/TLR superfamily and C-type lectins (24, 25). To visualize the pathogen, we generated red fluorescent conidia by transforming *A. fumigatus* with an expression vector encoding DsRed protein (11). Using an ex vivo-ligated loop system that allows controlled pathogen exposure of intact tissue, we challenged intestinal villi of C57BL/6 $CX_3CR1^{GFP/+}$ mice with DsRed-expressing conidia. *Aspergillus* conidia readily induced the formation of transepithelial dendrites (Fig. 2*B*). Individual villi harbored extensions with previously reported globular endings (4) and extensions lacking the latter. *Aspergillus* conidia entered the $CX_3CR1^{GFP/+}$ lamina propria, where they seemed largely confined to GFP-expressing cells in the tip of the villi. Furthermore, we found transepithelial dendrites and globular structures to be associated with the conidia outside the epithelial cell layer (Fig. 2, *C* and *D*), suggesting their direct involvement in pathogen uptake. To further investigate this issue, we exposed conidia to villi of $CX_3CR1^{GFP/GFP}$ mice that lack lpDC extensions (4). As shown in Fig. 2*E*, CX_3CR1 deficiency did not impair pathogen entry as indicated by the abundance of noninvasive *Aspergillus* conidia in the lamina propria of $CX_3CR1^{GFP/GFP}$ mice.

Only a fraction of the $CD11c^+$ mononuclear phagocytes in the intestinal lamina propria expresses CX_3CR1 (Fig. 1) and is hence visible in CX_3CR1^{GFP} mice. The above experiments thus do not exclude an involvement of CX_3CR1-negative lamina propria $CD11c^+$ cells (lpMϕ) in pathogen uptake. Therefore, we investigated the uptake in a situation where all $CD11c^+$ mononuclear phagocytes are missing from the lamina propria. To this end, we took advantage of an animal model that allows the diphtheria toxin (DTx)-induced ablation of $CD11c^{high}$ cells in the intact organism (9). To visualize lpDC, the DTR transgene was crossed on the CX_3CR1^{GFP} background. Histological and flow cytometric analysis confirmed the rapid depletion of all $CD11c^+$MHC II^+ from the small intestine of toxin-treated CX_3CR1^{GFP}: CD11c-DTR tg mice (Fig. 3). We then prepared ligated intestinal loops from DTx-treated mice and challenged them with *Aspergillus* conidia. As seen in Fig. 2*F*, conidia uptake by the villi persisted in the absence of $CD11c^+$ lamina propria cells.

Taken together, there is unimpaired entry of our particulate model pathogen into the lamina propria of CX3CR1-deficient mice and mice depleted of both lpDC and lpMϕ. This suggests that transepithelial dendrites do not significantly contribute to quantitative gut content sampling, which is likely to proceed via alternative routes. Kiyono and coworkers (7) recently reported the existence of intestinal villus M cells that like Peyer's patch M cells can be identified on the basis of their display of (1-2)-fucose detected by UEA-1. Confirming these results, we could visualize numerous $UEA\text{-}1^+$ cells on villi of the terminal ileum of C57BL/6

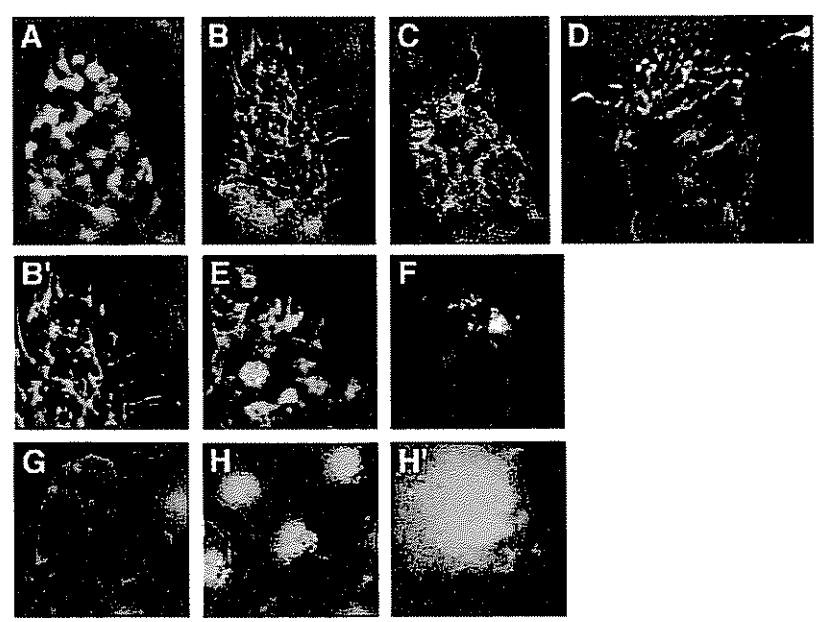

FIGURE 2. Pathogen entry into small intestinal lamina propria. Fluorescent microscopic analysis of DsRed-transduced *Aspergillus* conidia challenged villi of C57BL/6:CX_3CR1^{GFP} mice (green, lpDC; red, conidia; diameter 2–3 μm); original magnification, ×40). *A*, Unchallenged $CX_3CR1^{GFP/+}$ villus; *B–D*, *Aspergillus* conidia-challenged $CX_3CR1^{GFP/+}$ villi (note conidia in luminal globular structure (* in *D*); *E*, $CX_3CR1^{GFP/GFP}$ C57BL/6 mouse; and *F*, DTx-treated, lpDC and lpMϕ-depleted CD11c-DTR: $CX_3CR1^{GFP/+}$ C57BL/6 mouse. *G*, $UEA\text{-}1^+$ M cells in the villus epithelium; *H* and *H'*, colocalization of *Aspergillus* conidia with $UEA\text{-}1^+$ M cells on villi of $CX_3CR1^{GFP/+}$ mice.

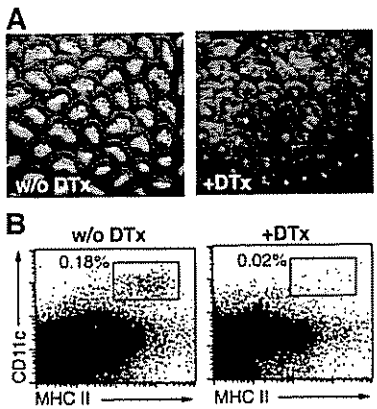

FIGURE 3. Conditional ablation of CD11c$^+$ lamina propria mononuclear phagocytes. *A*, Histological analysis of terminal ileum of DTx-treated (*left*) and untreated (*right*) $CX_3CR1^{GFP/+}$:CD11c-DTR transgenic mice 24 h after i.p. toxin injection (original magnification, ×10). *B*, Flow cytometric analysis of lamina propria cells of DTx-treated (*left*) and untreated (*right*) CD11c-DTR mice. Cells were stained with PE-conjugated anti-MHCII (I-A^b) and allophycocyanin-conjugated anti-CD11c Abs. Note quantitative ablation of all CD11c^{high} cells, including lpMϕ and lpDC.

CX_3CR1^{GFP} mice (Fig. 2*G*). Furthermore, analysis of pathogen-challenged ligated loops revealed conidia clusters in the epidermal layer that coincided with the M cell staining (Fig. 2, *H* and *H'*). These results support the notion that intestinal villus M cells are a major entry route for particulate pathogens to the lamina propria.

Transepithelial dendrite formation of CX_3CR1^+ lpDC is mouse strain dependent

Absence of lpDC extensions in CX_3CR1-deficient mice ($CX_3CR1^{GFP/GFP}$) (4) indicates a critical role of the CX_3CR1 chemokine receptor and its membrane-tethered ligand CX_3CL1 (FKN) in the penetration of the epithelial barrier. To test the general validity of this observation, we investigated the distribution of transepithelial extensions in another inbred mouse strain. Surprisingly, heterozygous mutant $CX_3CR1^{GFP/+}$ BALB/c mice lacked transepithelial dendrites in the terminal ileum both in steady state and after exposure to pathogens (*Aspergillus* conidia, *Salmonella*) (Fig. 4 and data not shown). GFP$^+$ lpDC of $CX_3CR1^{GFP/+}$ BALB/c mice express surface CX_3CR1 (data not shown). Furthermore, transepithelial dendrites are formed in F_1 hybrid $CX_3CR1^{GFP/+}$ mice that inherited their wild-type CX_3CR1 allele from the BALB/c and the mutant, CX_3CR1^{GFP} allele from the C57BL/6 parent (Fig. 4). The BALB/c allele thus encodes a functioning CX_3CR1 receptor capable of promoting dendrite formation. Absence of transepithelial dendrites in BALB/c mice is thus a recessive phenotype not linked to the CX_3CR1 locus but events upstream or downstream of CX_3CR1 action.

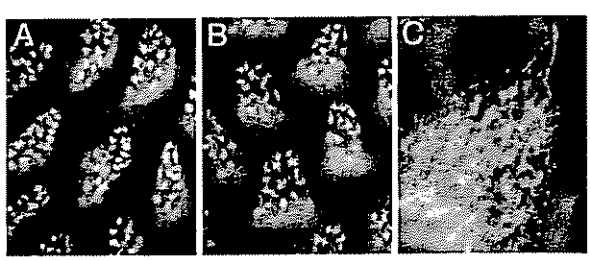

FIGURE 4. Absence of transepithelial dendrites in $CX_3CR1^{GFP/+}$ BALB/c mice. Fluorescent microscopic analysis of *Salmonella*-challenged small intestinal villi of $CX_3CR1^{GFP/GFP}$ C57BL/6 mouse (*A*), $CX_3CR1^{GFP/+}$ BALB/c mouse (*B*), and unchallenged $CX_3CR1^{GFP/+}$ F_1 (C57BL/6 × BALB/c) mouse (*C*).

The impact of the genetic background on the existence of transepithelial dendrites raised the question of whether their absence in C57BL/6 $CX_3CR1^{GFP/GFP}$ mice is indeed due to lack of the CX_3CR1 receptor, as we previously proposed (4). Alternatively, the phenotype of the C57BL/6 CX_3CR1-deficient mice could result from homozygosity of the chromosomal region (chromosome no. 9) flanking the CX_3CR1^{GFP} allele, which is derived from 129/sv mice (10). To this end, we tested whether transepithelial dendrites are present in mice homozygous for the respective chromosome or its subregion, i.e., F_1 hybrid mice resulting from the following crosses: $CX_3CR1^{GFP/GFP}$ B6 × 129/Sv and $CX_3CR1^{GFP/GFP}$ B6 × CCR2 $^{-/-}$ B6 (the CCR2 locus is adjacent to the CX_3CR1 locus and CCR2 mutant mice were generated using the same 129/sv ES cells as the CX_3CR1 mutation (10, 26)). In both hybrid strains, we observed transepithelial dendrites upon bacteria challenge (data not shown) confirming our original interpretation that the absence of transepithelial dendrites in C57BL/6 $CX_3CR1^{GFP/GFP}$ mice is due to their lack of the chemokine receptor CX_3CR1. However, absence of lpDC extensions in $CX_3CR1^{GFP/+}$ BALB/c mice suggests control of their formation by multiple genetic factors.

Discussion

Studies in the rat have established that lpDC sample enteric Ags and apoptotic epithelial cells in the lamina propria translocate to the mesenteric nodes and present their cargo to lymphocytes (27). The observation that lpDC can penetrate the epithelial tight junction barrier (8) thus led to speculations that besides Peyer's patch-associated M cells, lpDC might be a major route of luminal Ag transport to lamina propria-draining lymph nodes. Such a scenario would be of critical importance for our understanding of immunosurveillance and pathogen invasion. In the present study, we focus on the most proximal step of this cascade of events, i.e., pathogen entry into the lamina propria. Using hosts that either lack small intestinal transepithelial dendrites ($CX_3CR1^{GFP/GFP}$ mice; Ref. 4) or were depleted of lpDC (DTx-treated CD11c-DTR transgenic mice (9)) we show that entry of fungal conidia by in large relies on an alternative uptake route. These results suggest that lpDC extensions are dispensable for quantitative sampling of luminal Ags, which are readily accessible to the lamina propria through intestinal villus M cells (7). The study of $CX_3CR1^{GFP/+}$ BALB/c mice revealed that lpDC of this inbred mouse strain seem unable to form transepithelial dendrites. BALB/c and C57BL/6 mice differ in the kinetics of postnatal formation of isolated lymphoid follicles and cryptopatches (27). In addition, Kennedy et al. (28) reported that C57BL/6 mice harbor a natural disruption of the secretory group II phospholipase A2 gene ($sPLA_2$). Murine intestinal $sPLA_2$ has bactericidal activity (29) and the observed high expression of $sPLA_2$ in the intestine of BALB/c mice (28) might therefore affect the intestinal microflora. Furthermore, old BALB/c harbor more IgA$^+$ B cells in their lamina propria than C57BL/6 mice and have elevated IgA titers in fecal extracts (30). However, it remains to be shown whether and how these facts are related to differences in transepithelial dendrite formation. Differential lpDC access to the intestinal lumen is likely to contribute to the well-established observation that inbred mouse strains vary significantly in their susceptibility to pathogen infection known to be under mono- or multigenic control (31).

Absence of transepithelial dendrites in $CX_3CR1^{GFP/GFP}$ C57BL/6 and $CX_3CR1^{GFP/+}$ BALB/c mice impairs neither intestinal homeostasis, nor pathogen entry to the lamina propria. This

study thus seems to argue against the importance of these structures in intestinal pathogen uptake. However, lpDC extensions are likely decorated with DC-restricted pathogen receptors (for a recent review, see Ref. 32). Unlike the M cell route, the lpDC pathway might therefore allow for specific sensing and sampling of the intestinal lumen. Such a notion is also supported by our observation that some lpDC dendrites form upon epithelial penetration globular structures, i.e., an extended matrix for interaction with the gut content (4) (Fig. 2). The lpDC route could be an attractive target for the development of vaccination strategies. Furthermore, it could constitute a critical invasion path of pathogens targeting DC, such as HIV (33). However, a definitive answer on this topic will have to await experimental evidence showing lpDC-dependent entry of specific pathogens or Ag uptake by the transepithelial lpDC processes, migration of Ag-loaded lpDC to lymphoid organs, and activation of naive T cells.

Acknowledgments

We thank Drs. J.-P. Latgé, A. Porgador, and L. Mikkelsen for kindly providing the fungus *A. fumigatus*, *Salmonella*, and plasmids, respectively.

Disclosures

The authors have no financial conflict of interest.

References

1. Didierlaurent, A., J. C. Sirard, J. P. Kraehenbuhl, and M. R. Neutra. 2002. How the gut senses its content. *Cell. Microbiol.* 4: 61–72.
2. Hooper, L. V., and J. I. Gordon. 2001. Commensal host-bacterial relationships in the gut. *Science* 292: 1115–1118.
3. Philpott, D. J., and S. E. Girardin. 2004. The role of Toll-like receptors and Nod proteins in bacterial infection. *Mol. Immunol.* 41: 1099–1108.
4. Niess, J. H., S. Brand, X. Gu, L. Landsman, S. Jung, B. A. McCormick, J. M. Vyas, M. Boes, H. L. Ploegh, J. G. Fox, et al. 2005. CX3CR1-mediated dendritic cell access to the intestinal lumen and bacterial clearance. *Science* 307: 254–258.
5. Rimoldi, M., M. Chieppa, V. Salucci, F. Avogadri, A. Sonzogni, G. M. Sampietro, A. Nespoli, G. Viale, P. Allavena, and M. Rescigno. 2005. Intestinal immune homeostasis is regulated by the crosstalk between epithelial cells and dendritic cells. *Nat. Immunol.* 6: 507–514.
6. Golovkina, T. V., M. Shlomchik, L. Hannum, and A. Chervonsky. 1999. Organogenic role of B lymphocytes in mucosal immunity. *Science* 286: 1965–1968.
7. Jang, M. H., M. N. Kweon, K. Iwatani, M. Yamamoto, K. Terahara, C. Sasakawa, T. Suzuki, T. Nochi, Y. Yokota, P. D. Rennert, et al. 2004. Intestinal villous M cells: an antigen entry site in the mucosal epithelium. *Proc. Natl. Acad. Sci. USA* 101: 6110–6115.
8. Rescigno, M., M. Urbano, B. Valzasina, M. Francolini, G. Rotta, R. Bonasio, F. Granucci, J. P. Kraehenbuhl, and P. Ricciardi-Castagnoli. 2001. Dendritic cells express tight junction proteins and penetrate gut epithelial monolayers to sample bacteria. *Nat. Immunol.* 2: 361–367.
9. Jung, S., D. Unutmaz, P. Wong, G. Sano, K. De los Santos, T. Sparwasser, S. Wu, S. Vuthoori, K. Ko, F. Zavala, et al. 2002. In vivo depletion of CD11c$^+$ dendritic cells abrogates priming of CD8$^+$ T cells by exogenous cell-associated antigens. *Immunity* 17: 211–220.
10. Jung, S., J. Aliberti, P. Graemmel, M. J. Sunshine, G. W. Kreutzberg, A. Sher, and D. R. Littman. 2000. Analysis of fractalkine receptor CX_3CR1 function by targeted deletion and green fluorescent protein reporter gene insertion. *Mol. Cell. Biol.* 20: 4106–4114.
11. Mikkelsen, L., S. Sarrocco, M. Lubeck, and D. F. Jensen. 2003. Expression of the red fluorescent protein DsRed-Express in filamentous ascomycete fungi. *FEMS Microbiol. Lett.* 223: 135–139.
12. Nussenzweig, M. C., R. M. Steinman, M. D. Witmer, and B. Gutchinov. 1982. A monoclonal antibody specific for mouse dendritic cells. *Proc. Natl. Acad. Sci. USA* 79: 161–165.
13. Turnbull, E. L., U. Yrlid, C. D. Jenkins, and G. G. Macpherson. 2005. Intestinal dendritic cell subsets: differential effects of systemic TLR4 stimulation on migratory fate and activation in vivo. *J. Immunol.* 174: 1374–1384.
14. Austyn, J. M., and S. Gordon. 1981. F4/80, a monoclonal antibody directed specifically against the mouse macrophage. *Eur. J. Immunol.* 11: 805–815.
15. Smythies, L. E., M. Sellers, R. H. Clements, M. Mosteller-Barnum, G. Meng, W. H. Benjamin, J. M. Orenstein, and P. D. Smith. 2005. Human intestinal macrophages display profound inflammatory anergy despite avid phagocytic and bacteriocidal activity. *J. Clin. Invest.* 115: 66–75.
16. Julia, V., E. M. Hessel, L. Malherbe, N. Glaichenhaus, A. O'Garra, and R. L. Coffman. 2002. A restricted subset of dendritic cells captures airborne antigens and remains able to activate specific T cells long after antigen exposure. *Immunity* 16: 271–283.
17. Gonzalez-Juarrero, M., T. S. Shim, A. Kipnis, A. P. Junqueira-Kipnis, and I. M. Orme. 2003. Dynamics of macrophage cell populations during murine pulmonary tuberculosis. *J. Immunol.* 171: 3128–3135.
18. Uhlig, H. H., and F. Powrie. 2003. Dendritic cells and the intestinal bacterial flora: a role for localized mucosal immune responses. *J. Clin. Invest.* 112: 648–651.
19. Becker, C., S. Wirtz, M. Blessing, J. Pirhonen, D. Strand, O. Bechthold, J. Frick, P. R. Galle, I. Autenrieth, and M. F. Neurath. 2003. Constitutive p40 promoter activation and IL-23 production in the terminal ileum mediated by dendritic cells. *J. Clin. Invest.* 112: 693–706.
20. Rescigno, M., G. Rotta, B. Valzasina, and P. Ricciardi-Castagnoli. 2001. Dendritic cells shuttle microbes across gut epithelial monolayers. *Immunobiology* 204: 572–581.
21. Man, A. L., M. E. Prieto-Garcia, and C. Nicoletti. 2004. Improving M cell mediated transport across mucosal barriers: do certain bacteria hold the keys? *Immunology* 113: 15–22.
22. Milling, S. W., L. Cousins, and G. G. MacPherson. 2005. How do DCs interact with intestinal antigens? *Trends Immunol.* 26: 349–352.
23. Macpherson, A. J., and T. Uhr. 2004. Induction of protective IgA by intestinal dendritic cells carrying commensal bacteria. *Science* 303: 1662–1665.
24. Bozza, S., R. Gaziano, A. Spreca, A. Bacci, C. Montagnoli, P. di Francesco, and L. Romani. 2002. Dendritic cells transport conidia and hyphae of *Aspergillus fumigatus* from the airways to the draining lymph nodes and initiate disparate Th responses to the fungus. *J. Immunol.* 168: 1362–1371.
25. Serrano-Gomez, D., A. Dominguez-Soto, J. Ancochea, J. A. Jimenez-Heffernan, J. A. Leal, and A. L. Corbi. 2004. Dendritic cell-specific intercellular adhesion molecule 3-grabbing nonintegrin mediates binding and internalization of *Aspergillus fumigatus* conidia by dendritic cells and macrophages. *J. Immunol.* 173: 5635–5643.
26. Kuziel, W. A., S. J. Morgan, T. C. Dawson, S. Griffin, O. Smithies, K. Ley, and N. Maeda. 1997. Severe reduction in leukocyte adhesion and monocyte extravasation in mice deficient in CC chemokine receptor 2. *Proc. Natl. Acad. Sci. USA* 94: 12053–12058.
27. Hamada, H., T. Hiroi, Y. Nishiyama, H. Takahashi, Y. Masunaga, S. Hachimura, S. Kaminogawa, H. Takahashi-Iwanaga, T. Iwanaga, H. Kiyono, et al. 2002. Identification of multiple isolated lymphoid follicles on the antimesenteric wall of the mouse small intestine. *J. Immunol.* 168: 57–64.
28. Kennedy, B. P., P. Payette, J. Mudgett, P. Vadas, W. Pruzanski, M. Kwan, C. Tang, D. E. Rancourt, and W. A. Cromlish. 1995. A natural disruption of the secretory group II phospholipase A2 gene in inbred mouse strains. *J. Biol. Chem.* 270: 22378–22385.
29. Harwig, S. S., L. Tan, X. D. Qu, Y. Cho, P. B. Eisenhauer, and R. I. Lehrer. 1995. Bactericidal properties of murine intestinal phospholipase A2. *J. Clin. Invest.* 95: 603–610.
30. Kamata, T., F. Nogaki, S. Fagarasan, T. Sakiyama, I. Kobayashi, S. Miyawaki, K. Ikuta, E. Muso, H. Yoshida, S. Sasayama, and T. Honjo. 2000. Increased frequency of surface IgA-positive plasma cells in the intestinal lamina propria and decreased IgA excretion in hyper IgA (HIGA) mice, a murine model of IgA nephropathy with hyperserum IgA. *J. Immunol.* 165: 1387–1394.
31. Lam-Yuk-Tseung, S., and P. Gros. 2003. Genetic control of susceptibility to bacterial infections in mouse models. *Cell. Microbiol.* 5: 299–313.
32. Pulendran, B. 2005. Variegation of the immune response with dendritic cells and pathogen recognition receptors. *J. Immunol.* 174: 2457–2465.
33. Geijtenbeek, T. B., D. S. Kwon, R. Torensma, S. J. van Vliet, G. C. van Duijnhoven, J. Middel, I. L. Cornelissen, H. S. Nottet, V. N. KewalRamani, D. R. Littman, et al. 2000. DC-SIGN, a dendritic cell-specific HIV-1-binding protein that enhances trans-infection of T cells. *Cell* 100: 587–597.

CX_3CR1 Mediated Cell Survival in Monocyte Homeostasis and Atherogenesis

Limor Landsman[1*], Liat Bar-On[1*], Alma Zernecke[2], Ki-Wook Kim[1], Rita Krauthgamer[1], Sergio A. Lira[3], Irving L. Weissman[4], Christian Weber[2] and Steffen Jung[1]

*equal contribution

[1] Department of Immunology, The Weizmann Institute of Science, 76100 Rehovot, Israel

[2] Institute for Molecular Cardiovascular Research, RWTH University Hospital Aachen, 52074 Aachen, Germany.

[3] Immunobiology Center, Mount Sinai School of Medicine, New York, NY 10029.

[4] Stanford University School of Medicine, Pathology Department, Beckman Center B259, Stanford, CA 94305.

Corresponding author:

Steffen Jung, PhD

Department of Immunology

The Weizmann Institute of Science

Rehovot 76100, Israel

Tel: 00972 8 934 2787

FAX: 00972 8 934 4141

e.mail: s.jung@weizmann.ac.il

Abstract

CX_3CR1 is a chemokine receptor with a single ligand, the membrane-tethered chemokine CX_3CL1 (Fractalkine), whose *in vivo* function remains elusive. All blood monocytes express CX_3CR1, but the receptor levels differ between the main two subsets, with human $CD16^+$ and murine Ly6C/ $Gr1^{low}$ monocytes being CX_3CR1^{hi}. Here we show that absence of either CX_3CR1 or CX_3CL1 resulted in a significant reduction of $Gr1^{low}$ blood monocyte levels. Introduction of a bcl2 transgene restored this phenotype suggesting that the CX_3C axis provides an essential survival signal. Supporting this notion, CX_3CL1 specifically rescued cultured human monocytes from serum-deprivation induced cell death. CX_3CR1 was suggested to be involved in atherosclerosis, as human CX_3CR1 polymorphisms and murine CX_3CR1 deficiency protect from this disease. Here we show that enforced survival of monocytes and foam cells, a macrophage population unique to atherosclerotic plaques, restored atherogenesis in CX_3CR1-deficient mice. Our results therefore suggest that CX_3CL1-CX_3CR1 interactions provide an essential survival signal in whose absence increased death of monocytes and/or foam cells prevents disease progression. To conclude, we provide in vivo and in vitro evidence for the role of the CX_3C module in cell survival and offer a mechanistic explanation for its involvement in atherogenesis.

Introduction

Chemokines are a family of chemotactic cytokines that activate specific G-protein-coupled 7-transmembrane receptors (1) and been categorized into C, CC, CXC, and CX_3C families. CX_3CL1, also known as Fractalkine, is the only known CX_3C chemokine (1-3). Its expression has been reported for activated vascular endothelial cells (3), neurons (4), epithelial cells (5, 6), smooth muscle cells (7), dendritic cells (DC) (8) and macrophages (9). The single known CX_3CL1 receptor, CX_3CR1 (10), is expressed by T and NK cell subsets (10, 11), brain microglia (4, 12, 13), DC subsets (13-15) as well as blood monocytes (10, 13).

Classical small-molecular-weight chemokines are secreted proteins that are considered to form gradients by binding to extra cellular matrix proteoglycans. In contrast, CX_3CL1 is synthesized as a transmembrane protein with its chemokine domain presented on an extended mucin-like stalk (2, 3). In this form, CX_3CL1 promotes tight, integrin-independent adhesion of CX_3CR1-expressing leukocytes (7, 16). In addition, constitutive and inducible cleavage by metalloproteases can result in release of a soluble CX_3CL1 entity from the cell membrane (17-19). CX_3CL1 thus potentially acts as adhesion molecule and chemoattractant, albeit the importance of these activities for the physiological role of CX_3CL1 remains to be determined. Engagement of CX_3CR1 by its ligand triggers the PI3K/Akt signaling pathway in cell lines and cultured brain microglia, resulting in cell survival and proliferation (20-23). The significance of this activity for the *in vivo* role of the "CX_3C chemokine system remains however to be determined.

Interestingly, human CX_3CR1 gene polymorphisms were shown to be genetic risk factors for coronary artery diseases and atherosclerosis (24, 25). Furthermore, mice deficient for either CX_3CR1 or CX_3CL1 display a relative resistance to atherosclerosis development in the respective murine disease models (26-28). In

addition to ameliorated atherogenesis, CX_3CR1 KO mice display reduced cardiac allograft rejection (29). Furthermore, we have shown that their intestinal lamina propria DC lack trans-epithelial dendrite formation (14, 30). Importantly, the mechanistic explanations for all these phenotypes remain to be elucidated.

Monocytes are mononuclear phagocytes that are generated in the BM and released to the bloodstream (31, 32). From there they enter peripheral tissues, where they can give rise to macrophages and DC (15, 31-34). Undifferentiated monocytes represent a short-lived transitional state, with an estimated circulation half-life of ~71 hours in human (35) and ~17 hours in mice (31, 36). Monocytes are heterogeneous and can be divided into at least two main subpopulations (37), with human monocytes comprise a $CD14^{++}$ and a $CD14^{+}CD16^{+}$ subset (38). Murine monocytes have been divided into $Gr1^{hi}$ ($Ly6C^{hi}$) and $Gr1^{low}$ ($Ly6C^{low}$) monocyte subsets, which are functionally distinct; both with respect to their migration ability and differentiation potential (15, 34). All monocytes express CX_3CR1. The two subsets are however characterized by distinct surface levels, with human $CD14^{+}CD16^{+}$ and murine $Gr1^{low}$ monocyte subsets displaying significantly higher CX_3CR1 amounts (34). The role of this prominent CX_3CR1 expression for monocyte physiology remains unknown, although our original studies suggested that CX_3CR1-CX_3CL1 interactions might control monocyte levels (34) and others have suggested a role for CX_3CR1 in monocyte migration (39, 40).

Here we investigated the role of CX_3CL1-CX_3CR1 interaction on blood monocyte populations using mutant mice, as well as human blood monocyte isolates. We show that mice deficient for either CX_3CR1 or CX_3CL1 display a specific reduction in the frequency of circulating blood $Gr1^{low}$ monocytes, whereas $Gr1^{hi}$ monocytes remain unaffected. Using forced Bcl2 expression, we provide genetic evidence that the decrease of $Gr1^{low}$ monocytes results from enhanced cell death.

The protective CX_3C signal is direct and evolutionary conserved, as addition of soluble CX_3CL1 inhibits the serum deprivation-induced cell death of cultured human monocytes. Finally, we show that the absence of the CX_3C signal, resulting in impaired cell survival of monocytes or macrophages, is likely to explain the reported atherogenesis resistance of CX_3CR1 and CX_3CL1-deficient mice.

Results

Absence of CX_3CR1-CX_3CL1 interactions results in a specific reduction of $Gr1^{low}CX_3CR1^{hi}$ blood monocytes.

To study the physiological role of CX_3CR1 we took advantage of knock-in mice that carry a targeted replacement of the *cx3cr1* gene by a gene encoding green fluorescent protein (GFP) (13). Mice heterozygote for this mutation ($cx_3cr1^{gfp/+}$) express both CX_3CR1 and GFP, whereas homozygote mutant mice ($cx_3cr1^{gfp/gfp}$) express GFP under the control of the CX_3CR1 promoter, but lack CX_3CR1 expression. All circulating blood monocytes - as defined by expression of CD115 (MCSF receptor) express CX_3CR1 and are therefore GFP-positive in cx_3cr1^{gfp} mice (13). In order to study the role of CX_3CR1 expression on monocytes, we analyzed leukocytes of wt and $cx_3cr1^{gfp/gfp}$ mice. The comparative analysis revealed a slight, but consistent and significant reduction of the absolute number of monocytes in the absence of CX_3CR1 (Fig. 1B), also reflected in their reduced percentage among total non-granular white blood cells (ngWBC) (Fig. 1C). Blood monocyte levels of heterozygote mutant mice were comparable to wt mice (Fig. 1C).

Murine blood monocyte subsets differ in their level of CX_3CR1 surface expression with $Gr1^{hi}$ monocytes expressing intermediate levels of CX_3CR1 and $Gr1^{low}$ monocytes being CX_3CR1^{hi} (34). A subset specific monocyte analysis

revealed that $Gr1^{hi}$ monocyte levels remained unaffected by the CX_3CR1 deficiency (Fig. 1, B and C). In contrast, $Gr1^{low}$ monocytes of CX_3CR1 KO mice were found to be 3-fold reduced, as compared to wt and $cx_3cr1^{gfp/+}$ mice (Fig. 1, B and C).

To avoid indirect effects on these quantifications due to potential CX_3CR1 requirement by other CX_3CR1-expressing cell (such as NK and T cells (10, 11, 13)), we plotted the fraction of $Gr1^{low}$ monocytes among the total monocyte population in individual mice ($Gr1^{low}CD115^+$ cells out of total $CD115^+$ cells). While in wt and $cx_3cr1^{gfp/+}$ mice, approximately one third of the blood monocytes are $Gr1^{low}$, in $cx_3cr1^{gfp/gfp}$ mice the latter comprise only 15% of the total monocyte population (Figure 1C'). This way of presentation is used throughout the remainder of this study.

Mice deficient for CX_3CL1, the single known CX_3CR1 ligand (3, 10) display a reduction of their $F4/80^+$ blood monocyte population, as compared to wt littermates (41). We therefore next tested whether also the $cx_3cl1^{-/-}$ phenotype is restricted to the $Gr1^{low}CX_3CR1^{hi}$ monocyte subset. Indeed, $cx_3cr1^{gfp/gfp}$ and $cx_3cl1^{-/-}$ mice showed similar fractions of $Gr1^{low}$ monocytes (Fig. 2A), which were significantly lower than in wt controls (Fig. 1E).

To conclude, absence of either CX_3CR1 or CX_3CL1 results in a specific reduction in the level of circulating $Gr1^{low}$ blood monocytes.

Normal $Gr1^{low}$ monocytes levels require intrinsic CX_3CR1 expression

The observed $Gr1^{low}$ monocyte reduction could result from a systemic defect in CX_3CR1 and CX_3CL1-deficient mice. Alternatively, it could be a direct outcome of the absence of the receptor on $Gr1^{low}$ monocytes. To distinguish between these options, we generated mixed BM chimeras by reconstituting lethally irradiated wt mice with a 1:1 mixture of wt and $cx_3cr1^{gfp/gfp}$ BM cells. Eight weeks after transfer, the recipients' blood contained both GFP-positive ($cx_3cr1^{gfp/gfp}$) and GFP-negative (wt)

monocytes, allowing the comparison of cells of distinct genetic background ($cx_3cr1^{+/+}$; $cx_3cr1^{gfp/gfp}$) in the same environment. As shown in figure 2A, when compared to their wt counterpart, the level of CX_3CR1-deficient $Gr1^{low}$ monocytes was 3-fold reduced. Next, we transferred wt and $cx_3cr1^{gfp/gfp}$ BM cells into irradiated $cx_3cl1^{-/-}$ and wt recipients. The analysis of the resulting mixed BM chimeras revealed that in absence of CX_3CL1, wt $Gr1^{low}$ monocyte levels were significantly reduced, when compared to [wt > wt] chimeras and were similar to [$cx_3cr1^{gfp/gfp}$ > wt] mice (Fig. 2B). To conclude, our results indicate that the reduction of $Gr1^{low}$ monocytes in $cx_3cr1^{gfp/gfp}$ mice is a direct result of a monocyte-intrinsic CX_3CR1 requirement, whereas non-hematopoietic cells, presumably endothelial cells, serve as the source of CX_3CL1.

$Gr1^{low}$ monocytes require CX_3CR1 expression for their survival

We next investigated the cause for the $Gr1^{low}$ monocyte decrease in the absence of CX_3CL1-CX_3CR1 interactions. The reduction could result from impaired monocyte generation or increased cell death. Alternatively, absence of CX_3CR1 could impair monocyte egress from the BM to the bloodstream, as recently reported for another chemokine receptor, CCR2 (42). When comparing $cx_3cr1^{gfp/gfp}$ to their $cx_3cr1^{gfp/+}$ littermates, we could not detect a change in BM $Gr1^{low}$ monocyte levels (Fig 2C). This indicates that CX_3CR1 is not required for BM egress of monocytes and implies unimpaired monocyte production.

The adoptive co-transfer of wt and CX_3CR1-deficient $Gr1^{low}$ monocytes allows the comparison of monocyte fates bypassing differences in monocyte production. We previously reported such co-transfers, two days after which we analyzed the recipients for the presence of grafted cells. We observed a 2.5-fold reduction in the level of retrieved grafted $cx_3cr1^{gfp/gfp}$ monocytes as compared to co-transferred

cx3cr1$^{gfp/+}$ monocytes in recipient's blood and peripheral organs (34). The overall reduction in the level of grafted cx$_3$cr1$^{gfp/gfp}$ monocytes suggested impaired survival.

To directly address increased monocyte apoptosis as the cause of the CX$_3$CR1 KO phenotype, we took advantage of a transgenic mice, which carry a human gene encoding the anti-apoptotic Bcl2 factor under the control of the neutrophil- and monocyte-specific MRP8 promotor (hMRP8*bcl2* mice (43)). As expected, enforced Bcl2 expression resulted in an increase of blood monocyte levels ((43) and supp.1). Interestingly, although intra-cellular staining for human Bcl2 revealed that both monocyte subsets express the transgene at similar levels, the observed increment was significantly more pronounced for the Gr1^{low} subset as compared to Gr1^{hi} monocytes (supp. Fig.1). This might indicate Gr1^{low} monocyte are more prone to die as compared to Gr1^{hi} monocytes.

In order to study the influence of enforced Bcl2 expression on the CX$_3$CR1 KO phenotype, we generated double transgenic *cx3cr1*$^{gfp/gfp}$;hMRP6*bcl2* and *cx3cr1*$^{gfp/+}$;hMRP6*bcl2* mice. Interestingly, the analysis of the blood of these mice revealed that *bcl2* transgenic CX$_3$CR1 KO mice displayed Gr1^{low} monocyte levels comparable to *bcl2* transgenic *cx3cr1*$^{gfp/+}$ mice, comprising about 70% of their respective total blood monocytes (Fig. 2D). This was in contrast to the significant reduction in monocyte levels observed in non-transgenic *cx3cr1*$^{gfp/gfp}$ mice (Fig. 2D and 1C'). Hence, enforced monocyte survival restores Gr1^{low} cell numbers of CX$_3$CR1-deficient mice to the levels observed in CX$_3$CR1-proficient mice, thus rescuing their phenotype.

To conclude, our results suggest that the specific reduction of Gr1^{low} monocytes in *cx3cr1*$^{gfp/gfp}$ mice is due to their impaired survival, indicating an anti-apoptotic role for CX$_3$CR1-CX$_3$CL1 interaction *in vivo*.

CX_3CL1 has an anti-apoptotic effect on human blood monocytes

CX_3CL1 has been shown to act as a survival factor for transformed cell lines (20, 22), as well as cultured brain microglia (21). To directly study the role of CX_3CR1-CX_3CL1 interactions in monocyte survival, we resorted to an *ex vivo* system and probed the ability of recombinant soluble CX_3CL1 to rescue human blood monocytes from serum deprivation-induced cell death. Similarly to the mouse, human blood monocytes comprise two subsets, which are distinct in their CX_3CR1 expression levels (37). $CD14^{++}CD16^{-}$ monocytes express intermediate and $CD14^{+}CD16^{+}$ monocytes express high levels of CX_3CR1 (34).

We purified the two monocyte populations from human blood and cultured the cells in serum-free medium and medium supplemented with either serum or recombinant soluble CX_3CL1 (full length w/o TM anchor, aa 1-337; R&D systems). Four hours later we incubated the cells with propidium iodide (PI) to determine the percentage of dead cells in each group. As shown in Figure 3A, exposure to CX_3CL1-supplemented serum-free medium significantly reduced the level of PI^{+} dead cells, as compared to un-supplemented medium. As opposed to CX_3CL1, addition of BSA, ovalbumin or IgG to the cultures did not rescue monocytes from serum deprivation-induced death (Fig. 3B and data not shown). The percentage of dead cells decreased with the rising concentration of supplemented CX_3CL1 (Fig. 3C), indicating dose-dependency of its activity. Interestingly, both human monocyte subsets responded similarly to CX_3CL1, as indicated by comparable levels of surviving cells (Fig. 3A). In contrast to the murine *in vivo* data, the protective effect of CX_3CL1 on cultured human monocytes is therefore not restricted to the CX_3CR1^{hi} cells.

To conclude, CX_3CL1 acts as a human blood monocyte survival factor. Importantly, this activity does not require cell-cell interactions.

Reduced atherogenesis in the absence of CX_3CR1-CX_3CL1 interactions is due to impaired cell survival

Epidemological evidence suggests that the CX_3C chemokine family is involved in the development of human cardiovascular disorders. Thus human subjects harboring the $I_{249}M_{280}$ CX_3CR1 haplotype have a reduced risk to develop coronary artery disease and atherosclerosis (24, 25). The activities of this CX_3CR1 variant remain however a matter of debate (23, 44, 45). Mice deficient for apolipoprotein (*apoE*$^{-/-}$) develop atherosclerosis when subjected to western high fat diet (46). On a CX_3CR1-deficient genetic background, *apoE*$^{-/-}$ mice display reduced atherosclerotic plaque formation (26, 27). In addition, also CX_3CL1 deficient mice are relatively protected from atherosclerosis (28).

To test whether CX_3C-mediated cell survival signals provide a mechanistic explanation for these phenotypes, we asked whether enforced Bcl2 expression would restore atherosclerosis susceptibility of CX_3CR1-deficient mice. To this end we sublethally irradiated *apoE*$^{-/-}$ mice and reconstituted them with *cx*$_3$*cr1*$^{+/+}$, *cx*$_3$*cr1*$^{gfp/+}$ or *cx*$_3$*cr1*$^{gfp/gfp}$ BM, all either on wt or hMRP8*bcl2* transgenic background. Eight weeks after BM transfer, the mice were fed with high fat diet. Three months later their arteries were analyzed for the formation of atherosclerotic plaques. In agreement with the published data (26, 27), *apo*E$^{-/-}$ recipients of non-*bcl2* transgenic *cx*$_3$*cr1*$^{gfp/gfp}$ BM developed significantly reduced atherosclerotic plaques, when compared to recipients of either *cx*$_3$*cr1*$^{+/+}$ or *cx*$_3$*cr1*$^{gfp/+}$ BM (Fig. 4). This deficiency in plaque formation was however completely restored by the introduction of the *bcl2* transgene, as *apoE*$^{-/-}$ recipients of *cx*$_3$*cr1*$^{gfp/gfp}$;*bcl2* BM showed atherosclerosis levels comparable to recipients of CX_3CR1 proficient BM (Fig. 4).

To conclude, enforced cell survival promotes the generation of atherosclerotic plaques in the absence of CX_3CR1. These data suggest that increased cell death might be the cause for the observed protection of CX_3CR1 and CX_3CL1-deficient mice from atherosclerosis.

CX_3CR1 expression in atherosclerotic plaques

Constitutive CX_3C signals protect circulating blood monocyte from death under steady state conditions. However, these signals could also affect endurance and survival of other CX_3CR1-expressing myeloid cells, in particular within the atherosclerotic plaques - an inherently hostile environment due to the abundant presence of oxysterols (47). Both activated endothelium and neointimal smooth muscle cells could provide a protective CX_3CL1 source in the atheromas (3, 7, 48, 49). We next asked which cell types, other than monocytes, express CX_3CR1 in the lesions and thus could potentially receive the CX_3CL1 survival signal.

To this end we analyzed the atherosclerotic plaques of [$cx_3cr1^{gfp/+}$ > $apoE^{-/-}$] BM chimeras for the presence of GFP-expressing cells. Immunohistochemical analysis revealed numerous CX_3CR1/GFP^+ cells in the atheromas (Fig. 5A and supp. Fig. 2). Interestingly, this also included a distinct population of large Oil red^+ MOMA-2^+ cells, which likely represent characteristic foam cells (Fig. 5A), i.e. monocyte-derived macrophages that take up modified LDL and play a critical role in plaque formation (50). The level of plaque-resident CX_3CR1^+ cells, identified as GFP^+ cells in $cx_3cr1^{gfp/+}$ and $cx_3cr1^{gfp/gfp}$ mice, was reduced in the CX_3CR1-deficient mice (Fig 5B, supp. Fig 2). This is consistent with the notion of impaired foam cell survival in absence of CX_3CR1.

Human Bcl2 expression under the MRP8 promoter restored atherosclerosis development in CX_3CR1 deficient mice. Interestingly, immuno-histochemical analysis

revealed expression of the human Bcl2 transgene in the atherosclerotic plaques (Fig. 5C). Furthermore, it seems to be expressed by foam cells, as characterized by their typical large size (Fig. 5C). Mice harboring bcl2 transgene expression were further marked by increased levels of CX_3CR1-expressing cells in the plaque (Fig. 5B, supp. Fig 2). The increased atherosclerosis could thus result from the rescue of monocytes or/and foam cells in the plaques. Taken together these results suggest the lack of CX_3C-chemokine mediated survival of myeloid cells as the mechanistic cause underlying atherosclerosis resistance of CX_3CR1-deficient mice.

Discussion

The physiological function of the CX_3C chemokine family, as represented by the membrane-tethered ligand, CX_3CL1 (Fractalkine), and its sole receptor, CX_3CR1, remains poorly understood. Here we establish a novel role of CX_3CR1-CX_3CL1 interactions in the survival of blood monocytes. We could show that $Gr1^{low}$ monocytes levels are specifically reduced in the blood of both CX_3CL1 and CX_3CR1-deficient mice. Enforced monocytic expression of the anti-apoptotic factor Bcl2 reverted the phenotype, providing genetic evidence that this reduction results from impaired monocyte survival. In support of the *in vivo* data, recombinant CX_3CL1 specifically rescued cultured human monocytes from serum deprivation-induced death. This indicates a direct and evolutionary conserved role for CX_3CR1-CX_3CL1 interaction in cell survival. Finally we show that CX_3C survival signals provide the mechanistic explanation for one of the few known phenotypes of CX_3CR1 and CX_3CL1-deficient mice, i.e. their relative protection from diet-induced atherosclerois (26-28). Enforced survival of monocytes and foam cells in CX_3CR1 KO mice restored its atherogenesis levels to those found in wt mice, suggesting that CX_3CL1-CX_3CR1 interaction provides survival signals essential for disease progression.

Here we suggest a role for CX_3CL1 in promoting cell survival in vivo, during steady state conditions and atherosclerosis. Although chemokines were originally defined as chemoattractants, a growing body of evidence indicates their additional involvement in the control of cell survival (51). CX_3CL1 itself was reported to promote the survival of cancer cell lines (20, 22), as well as cultured microglia (21). Other chemokines, such as CXCL12/SDF1 and CXCL9/MIG protect CXCR4- and CXCR3-expressing cultured tumor cells from death (52, 53). Furthermore, CCL5/RANTES was shown to contribute to the *in vivo* survival of pulmonary macrophages during viral infection (54). Interestingly, our recent finding of impaired foam cells levels and atherosclerotic lesion formation in *ccr5*$^{-/-}$ mice (55, 56) might suggest a potential role of CCR5-mediated survival also under these conditions.

Our *in vitro* data show that CX_3CL1 can protect both human monocyte subsets from cell death. However, the survival of $Gr1^{hi}$ monocytes subset does not depend on CX_3CR1 engagement in the blood circulation. Their steady state maintenance might be ensured by other survival factors, including chemokines, that $Gr1^{low}$ cells might not respond to. Of note, $Gr1^{hi}$ monocytes, as well as their human $CD14^{++}$ counterpart, have an extensive chemokine receptor repertoire, as compared to $Gr1^{low}$ and $CD14^{+}CD16^{+}$ cells (34, 37). The differential sensitivity to CX_3CR1 deficiency of the monocyte subsets might also result from their distinct propensity to die, a notion supported by their differential response to Bcl2 over-expression in this study (Suppl. Figure 1B). This is of course might not be the case during inflammatory settings, when the dependency of $Gr1^{hi}$ monocytes on CX_3CL1 as a survival signal might grow. Furthermore, atherogenesis might primarily depend on local CX_3CL1-mediated cell survival in the atheroma, rather than on survival of circulating cells.

Monocytes are critical in the development, maintenance and resolution of atherosclerosis (50, 57). In the plaque, they are believed to give rise to foam cells, a

special macrophages subset found in those structures (58). Foam cell were shown to play a key role in the development of early atherosclerotic plaques and their maintenance (50). Accordingly, foam cell death during early disease stages has been shown to correlate with decreased atherogenesis, whereas their death during late stages leads to thrombosis and disease progression (47). CX_3CL1 is prominently expressed in the atherosclerotic lesion (5, 7). Here we suggest CX_3CL1 to play a critical role in the survival of CX_3CR1 expressing monocytes and foam cell in the atherosclerotic plaque. Accordingly, in their absence monocyte and foam cells undergo increased cell death, leading to reduced foam cell levels and the inhibition of plaque progression.

Our results suggest that inhibition of CX_3CR1-CX_3CL1 interactions during early atherogenesis stages might be beneficial in controlling this disease. However, since CX_3C signals are likely to be required for foam cell survival also during later atheroma stages, such inhibition could result in disease exacerbation. The development of therapeutic protocols based on interference with the CX_3CR1-CX_3CL1 axis will therefore require an in depth understanding of the system.

Materials and Methods

Mice. This study involved the use of the following C57BL/6 mouse strains: *Cx$_3$cr1*^{gfp} mice (13); *cx$_3$cl1*$^{-/-}$ mice (41); hMRP8*bcl2* mice (43) and *ApoE*$^{-/-}$ mice (B6.129P2-*Apoetm1Unc*/J, Jackson laboratories). Wt C57BL/6 mice were purchased from Harlan. Used mice were 7-10 weeks of age. All mice were maintained under specific pathogen-free conditions and handled under protocols approved by the Weizmann Institute Animal Care Committee according to international guidelines.

BM chimera generation. For blood cell analysis recipient mice were lethally irradiated with 950 rad dose and a day later were i.v. injected with $5{\cdot}10^6$ BM cells isolated from donor femora and tibiae. BM recipients were allowed to rest for eight weeks prior to analysis. *ApoE*$^{-/-}$ recipient mice were lethally irradiated with two 650 rad doses, a day later were i.v. injected with $5{\cdot}10^6$ donor BM, and were allowed to rest for three weeks before placed on high fat diet.

Mouse Cell isolation. Mice were bled from their tail veins, and subjected to a Ficoll density gradient (Amersham) for erythrocyte and neutrophil removal. BM cells were isolated from mouse femora, followed by erythrocyte lysis using ACK buffer. Cells were suspended in PBS supplemented with 2mM EDTA, 0.05% Sodium Azide and 1% FCS.

Human Blood Cell Isolation. Human blood monocytes were isolated from WBC-enriched blood (Israeli blood bank). Followed by erythrocytes and neutrophil removal through a Ficoll density gradient, monocyte subsets were magnetically separated using monocyte isolation kit II (Cat #130-091-153, Miltenyi Biotech) and CD16$^+$

monocyte isolation kit (Cat #130-091-765, Miltenyi Biotech), according to manufacturer protocols.

Flow cytometry Analysis. The following fluorochrome-labeled monoclonal antibodies and staining reagents were used according to manufacturers protocols: PE-conjugated anti-CD115 (eBioscience) and anti human Bcl2 (Cat # sc-509, Santa Cruz), APC-conjugated anti-Gr1 (Ly6C/G) (eBioscience) and Propidium Iodide (Sigma). Cells were analyzed on a FACSCalibur cytometer (Beckton-Dickinson) using CellQuest software (Beckton-Dickinson).

Human monocyte incubation. Isolated cells were washed with PBS to remove serum residues, and $5x10^4$ cells per well were plated in RPMI supplemented with non-essential amino acids. RPMI was further supplemented with FCS (10%, Beit Haemek industries), recombinant mouse CX_3CL1 (aa1-337 (Cat #472-FF), aa25-105 (Cat #571-MF); (R&D systems) or BSA (Sigma). Cells were incubated for four hours at 37^0C.

Mouse model of atherosclerotic disease progression. *ApoE*$^{-/-}$ mice were fed anatherogenic diet containing 21% fat (Altromine) and after 12 weeks were fixed by *in situ* perfusion. The extent of atherosclerosis was quantified by Oil-Red-O staining of throacoabdominal aortas prepared en face and computerized image analysis (MetaMorph v6.0, Universal Imaging Corporation or Diskus software), as previously described (56).

Immunohistochemistry. Plaque cellular composition was analyzed in transversal sections through the aortic root. Sections were stained with anti-MOMA-2 (MCA519,

Serotec) and anti- human Bcl2 (BD Biosciences) monoclonal antibodies, detected by alkaline phosphate substrate and the Vector Red Substrate Kit (Vector Laboratories). Nuclei are counterstained by 4`,6-Diamidino-2-pheylindol (DAPI). Images were recorded with a Leica DMLB fluorescence microscope and CCD camera.

Statistical analysis. All statistics were generated using a Students's *t*-test. All error bars in diagrams and numbers following a ± sign are standard deviations (s.d.).

Acknowledgements

This work was supported by the MINERVA Foundation and the Israeli Science Foundation (ISF) and the Deutsche Forschungsgemeinschaft. S.J. is the incumbent of the Pauline Recanati Career Development Chair. We thank members of the Jung laboratory for critical reading of the manuscript and are grateful to Y. Chermesh and O. Amram for animal husbandry.

References

1. Zlotnik, A., and Yoshie, O. 2000. Chemokines: a new classification system and their role in immunity. *Immunity* 12:121-127.
2. Pan, Y., Lloyd, C., Zhou, H., Dolich, S., Deeds, J., Gonzalo, J.A., Vath, J., Gosselin, M., Ma, J., Dussault, B., et al. 1997. Neurotactin, a membrane-anchored chemokine upregulated in brain inflammation. *Nature* 387:611-617.
3. Bazan, J.F., Bacon, K.B., Hardiman, G., Wang, W., Soo, K., Rossi, D., Greaves, D.R., Zlotnik, A., and Schall, T.J. 1997. A new class of membrane-bound chemokine with a CX3C motif. *Nature* 385:640-644.
4. Harrison, J.K., Jiang, Y., Chen, S., Xia, Y., Maciejewski, D., McNamara, R.K., Streit, W.J., Salafranca, M.N., Adhikari, S., Thompson, D.A., et al. 1998. Role

for neuronally derived fractalkine in mediating interactions between neurons and CX3CR1-expressing microglia. *Proc Natl Acad Sci U S A* 95:10896-10901.

5. Lucas, A.D., Chadwick, N., Warren, B.F., Jewell, D.P., Gordon, S., Powrie, F., and Greaves, D.R. 2001. The transmembrane form of the CX3CL1 chemokine fractalkine is expressed predominantly by epithelial cells in vivo. *Am J Pathol* 158:855-866.

6. Muehlhoefer, A., Saubermann, L.J., Gu, X., Luedtke-Heckenkamp, K., Xavier, R., Blumberg, R.S., Podolsky, D.K., MacDermott, R.P., and Reinecker, H.C. 2000. Fractalkine is an epithelial and endothelial cell-derived chemoattractant for intraepithelial lymphocytes in the small intestinal mucosa. *J Immunol* 164:3368-3376.

7. Ludwig, A., Berkhout, T., Moores, K., Groot, P., and Chapman, G. 2002. Fractalkine is expressed by smooth muscle cells in response to IFN-gamma and TNF-alpha and is modulated by metalloproteinase activity. *J Immunol* 168:604-612.

8. Papadopoulos, E.J., Sassetti, C., Saeki, H., Yamada, N., Kawamura, T., Fitzhugh, D.J., Saraf, M.A., Schall, T., Blauvelt, A., Rosen, S.D., et al. 1999. Fractalkine, a CX3C chemokine, is expressed by dendritic cells and is up-regulated upon dendritic cell maturation. *Eur J Immunol* 29:2551-2559.

9. Greaves, D.R., Hakkinen, T., Lucas, A.D., Liddiard, K., Jones, E., Quinn, C.M., Senaratne, J., Green, F.R., Tyson, K., Boyle, J., et al. 2001. Linked chromosome 16q13 chemokines, macrophage-derived chemokine, fractalkine, and thymus- and activation-regulated chemokine, are expressed in human atherosclerotic lesions. *Arterioscler Thromb Vasc Biol* 21:923-929.

10. Imai, T., Hieshima, K., Haskell, C., Baba, M., Nagira, M., Nishimura, M., Kakizaki, M., Takagi, S., Nomiyama, H., Schall, T.J., et al. 1997. Identification and molecular characterization of fractalkine receptor CX3CR1, which mediates both leukocyte migration and adhesion. *Cell* 91:521-530.

11. Combadiere, C., Salzwedel, K., Smith, E.D., Tiffany, H.L., Berger, E.A., and Murphy, P.M. 1998. Identification of CX3CR1. A chemotactic receptor for the human CX3C chemokine fractalkine and a fusion coreceptor for HIV-1. *J Biol Chem* 273:23799-23804.

12. Nishiyori, A., Minami, M., Ohtani, Y., Takami, S., Yamamoto, J., Kawaguchi, N., Kume, T., Akaike, A., and Satoh, M. 1998. Localization of fractalkine and CX3CR1 mRNAs in rat brain: does fractalkine play a role in signaling from neuron to microglia? *FEBS Lett* 429:167-172.

13. Jung, S., Aliberti, J., Graemmel; P., Sunshine, M.J., Kreutzberg, G.W., Sher, A., and Littman, D.R. 2000. Analysis of fractalkine receptor CX(3)CR1 function by targeted deletion and green fluorescent protein reporter gene insertion. *Mol Cell Biol* 20:4106-4114.

14. Niess, J.H., Brand, S., Gu, X., Landsman, L., Jung, S., McCormick, B.A., Vyas, J.M., Boes, M., Ploegh, H.L., Fox, J.G., et al. 2005. CX3CR1-mediated dendritic cell access to the intestinal lumen and bacterial clearance. *Science* 307:254-258.

15. Landsman, L., Varol, C., and Jung, S. 2007. Distinct differentiation potential of blood monocyte subsets in the lung. *J Immunol* 178:2000-2007.

16. Fong, A.M., Robinson, L.A., Steeber, D.A., Tedder, T.F., Yoshie, O., Imai, T., and Patel, D.D. 1998. Fractalkine and CX3CR1 mediate a novel mechanism of leukocyte capture, firm adhesion, and activation under physiologic flow. *J Exp Med* 188:1413-1419.

17. Garton, K.J., Gough, P.J., Blobel, C.P., Murphy, G., Greaves, D.R., Dempsey, P.J., and Raines, E.W. 2001. Tumor necrosis factor-alpha-converting enzyme (ADAM17) mediates the cleavage and shedding of fractalkine (CX3CL1). *J Biol Chem* 276:37993-38001.

18. Hundhausen, C., Misztela, D., Berkhout, T.A., Broadway, N., Saftig, P., Reiss, K., Hartmann, D., Fahrenholz, F., Postina, R., Matthews, V., et al. 2003. The disintegrin-like metalloproteinase ADAM10 is involved in constitutive cleavage of CX3CL1 (fractalkine) and regulates CX3CL1-mediated cell-cell adhesion. *Blood* 102:1186-1195.

19. Ludwig, A., and Weber, C. 2007. Transmembrane chemokines: versatile 'special agents' in vascular inflammation. *Thromb Haemost* 97:694-703.

20. Chandrasekar, B., Mummidi, S., Perla, R.P., Bysani, S., Dulin, N.O., Liu, F., and Melby, P.C. 2003. Fractalkine (CX3CL1) stimulated by nuclear factor kappaB (NF-kappaB)-dependent inflammatory signals induces aortic smooth muscle cell proliferation through an autocrine pathway. *Biochem J* 373:547-558.

21. Boehme, S.A., Lio, F.M., Maciejewski-Lenoir, D., Bacon, K.B., and Conlon, P.J. 2000. The chemokine fractalkine inhibits Fas-mediated cell death of brain microglia. *J Immunol* 165:397-403.

22. Brand, S., Sakaguchi, T., Gu, X., Colgan, S.P., and Reinecker, H.C. 2002. Fractalkine-mediated signals regulate cell-survival and immune-modulatory responses in intestinal epithelial cells. *Gastroenterology* 122:166-177.

23. Davis, C.N., and Harrison, J.K. 2006. Proline 326 in the C terminus of murine CX3CR1 prevents G-protein and phosphatidylinositol 3-kinase-dependent stimulation of Akt and extracellular signal-regulated kinase in Chinese hamster ovary cells. *J Pharmacol Exp Ther* 316:356-363.

24. Moatti, D., Faure, S., Fumeron, F., Amara Mel, W., Seknadji, P., McDermott, D.H., Debre, P., Aumont, M.C., Murphy, P.M., de Prost, D., et al. 2001. Polymorphism in the fractalkine receptor CX3CR1 as a genetic risk factor for coronary artery disease. *Blood* 97:1925-1928.

25. McDermott, D.H., Halcox, J.P., Schenke, W.H., Waclawiw, M.A., Merrell, M.N., Epstein, N., Quyyumi, A.A., and Murphy, P.M. 2001. Association between polymorphism in the chemokine receptor CX3CR1 and coronary vascular endothelial dysfunction and atherosclerosis. *Circ Res* 89:401-407.

26. Combadiere, C., Potteaux, S., Gao, J.L., Esposito, B., Casanova, S., Lee, E.J., Debre, P., Tedgui, A., Murphy, P.M., and Mallat, Z. 2003. Decreased atherosclerotic lesion formation in CX3CR1/apolipoprotein E double knockout mice. *Circulation* 107:1009-1016.

27. Lesnik, P., Haskell, C.A., and Charo, I.F. 2003. Decreased atherosclerosis in CX3CR1-/- mice reveals a role for fractalkine in atherogenesis. *J Clin Invest* 111:333-340.

28. Teupser, D., Pavlides, S., Tan, M., Gutierrez-Ramos, J.C., Kolbeck, R., and Breslow, J.L. 2004. Major reduction of atherosclerosis in fractalkine (CX3CL1)-deficient mice is at the brachiocephalic artery, not the aortic root. *Proc Natl Acad Sci U S A* 101:17795-17800.

29. Robinson, L.A., Nataraj, C., Thomas, D.W., Howell, D.N., Griffiths, R., Bautch, V., Patel, D.D., Feng, L., and Coffman, T.M. 2000. A role for fractalkine and its receptor (CX3CR1) in cardiac allograft rejection. *J Immunol* 165:6067-6072.

30. Vallon-Eberhard, A., Landsman, L., Yogev, N., Verrier, B., and Jung, S. 2006. Transepithelial pathogen uptake into the small intestinal lamina propria. *J Immunol* 176:2465-2469.

31. van Furth, R., and Cohn, Z.A. 1968. The origin and kinetics of mononuclear phagocytes. *J Exp Med* 128:415-435.

32. Varol, C., Landsman, L., Fogg, D.K., Greenshtein, L., Gildor, B., Margalit, R., Kalchenko, V., Geissmann, F., and Jung, S. 2007. Monocytes give rise to mucosal, but not splenic, conventional dendritic cells. *J Exp Med* 204:171-180.

33. Randolph, G.J. 1999. Differentiation of phagocytic monocytes into lynph node dendritic cells in vivo. *Immunity* 11:753-761.

34. Geissmann, F., Jung, S., and Littman, D.R. 2003. Blood monocytes consist of two principal subsets with distinct migratory properties. *Immunity* 19:71-82.

35. Whitelaw, D.M. 1972. Observations on human monocyte kinetics after pulse labeling. *Cell Tissue Kinet* 5:311-317.

36. van Furth, R. 1989. Origin and turnover of monocytes and macrophages. *Curr Top Pathol* 79:125-150.

37. Gordon, S., and Taylor, P.R. 2005. Monocyte and macrophage heterogeneity. *Nat Rev Immunol* 5:953-964.

38. Ziegler-Heitbrock, L. 2007. The CD14+ CD16+ blood monocytes: their role in infection and inflammation. *J Leukoc Biol* 81:584-592.

39. Ancuta, P., Rao, R., Moses, A., Mehle, A., Shaw, S.K., Luscinskas, F.W., and Gabuzda, D. 2003. Fractalkine preferentially mediates arrest and migration of CD16+ monocytes. *J Exp Med* 197:1701-1707.

40. Tacke, F., Alvarez, D., Kaplan, T.J., Jakubzick, C., Spanbroek, R., Llodra, J., Garin, A., Liu, J., Mack, M., van Rooijen, N., et al. 2007. Monocyte subsets differentially employ CCR2, CCR5, and CX3CR1 to accumulate within atherosclerotic plaques. *J Clin Invest* 117:185-194.

41. Cook, D.N., Chen, S.C., Sullivan, L.M., Manfra, D.J., Wiekowski, M.T., Prosser, D.M., Vassileva, G., and Lira, S.A. 2001. Generation and analysis of mice lacking the chemokine fractalkine. *Mol Cell Biol* 21:3159-3165.

42. Serbina, N.V., and Pamer, E.G. 2006. Monocyte emigration from bone marrow during bacterial infection requires signals mediated by chemokine receptor CCR2. *Nat Immunol* 7:311-317.

43. Lagasse, E., and Weissman, I.L. 1994. bcl-2 inhibits apoptosis of neutrophils but not their engulfment by macrophages. *J Exp Med* 179:1047-1052.

44. McDermott, D.H., Fong, A.M., Yang, Q., Sechler, J.M., Cupples, L.A., Merrell, M.N., Wilson, P.W., D'Agostino, R.B., O'Donnell, C.J., Patel, D.D., et al. 2003. Chemokine receptor mutant CX3CR1-M280 has impaired adhesive function and correlates with protection from cardiovascular disease in humans. *J Clin Invest* 111:1241-1250.

45. Daoudi, M., Lavergne, E., Garin, A., Tarantino, N., Debre, P., Pincet, F., Combadiere, C., and Deterre, P. 2004. Enhanced adhesive capacities of the naturally occurring Ile249-Met280 variant of the chemokine receptor CX3CR1. *J Biol Chem* 279:19649-19657.

46. Plump, A.S., Smith, J.D., Hayek, T., Aalto-Setala, K., Walsh, A., Verstuyft, J.G., Rubin, E.M., and Breslow, J.L. 1992. Severe hypercholesterolemia and atherosclerosis in apolipoprotein E-deficient mice created by homologous recombination in ES cells. *Cell* 71:343-353.

47. Tabas, I. 2005. Consequences and therapeutic implications of macrophage apoptosis in atherosclerosis: the importance of lesion stage and phagocytic efficiency. *Arterioscler Thromb Vasc Biol* 25:2255-2264.

48. Zeiffer, U., Schober, A., Lietz, M., Liehn, E.A., Erl, W., Emans, N., Yan, Z.Q., and Weber, C. 2004. Neointimal smooth muscle cells display a

proinflammatory phenotype resulting in increased leukocyte recruitment mediated by P-selectin and chemokines. *Circ Res* 94:776-784.

49. Volger, O.L., Fledderus, J.O., Kisters, N., Fontijn, R.D., Moerland, P.D., Kuiper, J., van Berkel, T.J., Bijnens, A.P., Daemen, M.J., Pannekoek, H., et al. 2007. Distinctive Expression of Chemokines and Transforming Growth Factor-{beta} Signaling in Human Arterial Endothelium during Atherosclerosis. *Am J Pathol.*

50. Libby, P. 2002. Inflammation in atherosclerosis. *Nature* 420:868-874.

51. Tanaka, T., Bai, Z., Srinoulprasert, Y., Yang, B.G., Hayasaka, H., and Miyasaka, M. 2005. Chemokines in tumor progression and metastasis. *Cancer Sci* 96:317-322.

52. Zhou, Y., Larsen, P.H., Hao, C., and Yong, V.W. 2002. CXCR4 is a major chemokine receptor on glioma cells and mediates their survival. *J Biol Chem* 277:49481-49487.

53. Kawada, K., Sonoshita, M., Sakashita, H., Takabayashi, A., Yamaoka, Y., Manabe, T., Inaba, K., Minato, N., Oshima, M., and Taketo, M.M. 2004. Pivotal role of CXCR3 in melanoma cell metastasis to lymph nodes. *Cancer Res* 64:4010-4017.

54. Tyner, J.W., Uchida, O., Kajiwara, N., Kim, E.Y., Patel, A.C., O'Sullivan, M.P., Walter, M.J., Schwendener, R.A., Cook, D.N., Danoff, T.M., et al. 2005. CCL5-CCR5 interaction provides antiapoptotic signals for macrophage survival during viral infection. *Nat Med* 11:1180-1187.

55. Zernecke, A., Liehn, E.A., Gao, J.L., Kuziel, W.A., Murphy, P.M., and Weber, C. 2006. Deficiency in CCR5 but not CCR1 protects against neointima formation in atherosclerosis-prone mice: involvement of IL-10. *Blood* 107:4240-4243.

56. Braunersreuther, V., Zernecke, A., Arnaud, C., Liehn, E.A., Steffens, S., Shagdarsuren, E., Bidzhekov, K., Burger, F., Pelli, G., Luckow, B., et al. 2007. Ccr5 but not Ccr1 deficiency reduces development of diet-induced atherosclerosis in mice. *Arterioscler Thromb Vasc Biol* 27:373-379.

57. Swirski, F.K., Libby, P., Aikawa, E., Alcaide, P., Luscinskas, F.W., Weissleder, R., and Pittet, M.J. 2007. Ly-6Chi monocytes dominate hypercholesterolemia-associated monocytosis and give rise to macrophages in atheromata. *J Clin Invest* 117:195-205.

58. Bobryshev, Y.V. 2006. Monocyte recruitment and foam cell formation in atherosclerosis. *Micron* 37:208-222.

Figure Legends

Figure 1: Reduced numbers of Gr1^{low} monocytes in CX$_3$CR1-deficient mice

A) Flow cytometry analysis of blood monocytes. Left dot plot shows total ficoll-fractionated wt blood cells. Cells gated in region R1 are living, non-granular white blood cells (ngWBC). Middle and right dot plots show CD115 and Gr1 staining of blood cells gated in R1. Region R2 gates monocytes, as indicated by their CD115 expression. Cells gated in R3 and R4 regions are Gr1^{hi} and Gr1^{low} monocytes, respectively.

B) Comparison of blood monocyte population size of wt and *cx$_3$cr1*$^{gfp/gfp}$ mice. Diagram shows number of monocytes, identified as CD115$^+$ cells (R2 gated cells), in 1 ml of blood.

C, C') Comparison between monocyte population size of wt , *cx$_3$cr1*$^{gfp/+}$ and *cx$_3$cr1*$^{gfp/gfp}$ mice. Bar diagram (C) shows for each group of mice the percentage of total blood monocytes (R2 gated cells), Gr1^{hi} monocytes (R3) and Gr1^{low} monocytes (R4) out of WBC gated in R1. (C') Alternative presentation of the data showed in C. Bar diagram shows the percentage of Gr1^{low} monocytes (R4) among total monocytes p (R2) for each of the mouse strains. n=5 for each group.

D) Comparison between blood monocytes of wt, cx$_3$cr1$^{gfp/gfp}$ and cx$_3$cl1$^{-/-}$ mice. Bar histogram shows for each group the percentage of Gr1^{low} monocytes (R4 gated cells) out of total monocytes (R2 gated cells) for each mouse strain. n=5. *pValue<0.05, **p Value<0.005, **p Value<5x10^{-5}, all as compared to wt mice.

Figure 2: Reduction of Gr1^{low} monocytes in absence of CX$_3$CR1 is due impaired cell survival

A) Comparison of wt and *cx$_3$cr1*$^{gfp/gfp}$ monocytes in mixed BM chimera blood. BM cells were isolated from wt and *cx$_3$cr1*$^{gfp/gfp}$ donors, mixed to 1:1 ratio from each genotype and transferred into irradiated wt recipients. Eight weeks after transfer recipient mice were bled and their blood content was analyzed. Dot plot shows discrimination between GFP-positive *cx$_3$cr1*$^{gfp/gfp}$ monocytes (R5 gated cells) and GFP-negative wt monocytes (R6 gated cells). Bar diagram shows percentage of Gr1^{low} monocytes (as gated in R4, Fig. 1A) out of either total wt (R6, black-filled bar) or *cx$_3$cr1*$^{gfp/gfp}$ (R5, gray filled bars) monocytes. n=8.

B) Comparison of monocyte levels in presence and absence of CX$_3$CL1. Wt and *cx$_3$cl1*$^{-/-}$ irradiated mice received BM cells of wt and *cx$_3$cr1*$^{gfp/gfp}$ mice, and were bled eight weeks later. Bar histogram shows percentage of Gr1^{low} monocytes (R4 in Fig.1*A*) out of total monocytes (R2 in Fig.1*A*) of wt and *cx$_3$cl1*$^{-/-}$ recipients of either wt or *cx$_3$cr1*$^{gfp/gfp}$ BM cells. n=5.

C) Comparison of blood and BM monocytes of *cx$_3$cr1*$^{gfp/+}$ and *cx$_3$cr1*$^{gfp/gfp}$ littermates. Bar diagram shows the percentage of Gr1^{low} cells (gated in R4, Fig. 1*A*) out of total blood or BM monocytes (cells gated in R2, Fig. 1*A*). n=4 for each group.

D) Comparison of monocytes of hMRP8bcl2 transgenic *cx$_3$cr1*$^{gfp/gfp}$ and *cx$_3$cr1*$^{gfp/+}$ mice. Bar histogram shows percentage of Gr1^{low} monocytes (cells gated in R4, Fig. 1*A*) out of total monocytes (cells gated in R2, Fig. 1*A*) of *cx$_3$cr1*$^{gfp/+}$ and *cx$_3$cr1*$^{gfp/gfp}$ mice, either hMRP8bcl2 transgenic on non-transgenic. n=3.*pValue<5x10^{-8} as compared to wt **pValue<5x10^{-5} as compared to wt recipient ***p Value<0.005 as compared to cx$_3$cr1$^{gfp/+}$ mice.

Figure 3: CX$_3$CL1 rescues human blood monocytes from serum deprivation-induced death

A) $CD14^{++}CD16^{-}$ and $CD14^{+}CD16^{+}$ human blood monocytes incubated in RPMI (Medium) or RPMI supplemented with either 10% FCS (+FCS) or 10nM soluble CX_3CL1 (+CX_3CL1). Bar diagram shows percentage of PI-positive dying cells. n=3.

B) $CD14^{+}CD16^{+}$ monocytes incubated with RPMI (Medium) or RPMI supplemented with 10% FCS (+FCS), 10nM soluble CX_3CL1 (+CX_3CL1 10nM) or 10nM BSA (+BSA 10nM). Bar diagram shows percentage of PI- positive cells. n=4.

C) $CD14^{++}CD16^{-}$ monocytes incubated with RPMI supplemented with 1nM, 5nM, 10nM or 100nM CX_3CL1. Diagram shows percentage of PI- positive cells. n=3.

*pValue<0.01, **pValue<0.001. Results are representative example of 3 independent experiments.

Figure 4: Enforced cell survival promotes atherogenesis in the absence of CX_3CR1

A) Aortas and aorta roots of *ApoE*$^{-/-}$ recipients of wt, *cx*$_3$*cr1*$^{gfp/gfp}$ and *cx*$_3$*cr1*$^{gfp/gfp}$;hMRP8Bcl2 (*cx*$_3$*cr1*$^{gfp/gfp}$ bcl2 tg) BM cells. Orange oil O^{+} staining is shown in red.

B) Quantitative analysis of atherosclerotic lesion area in *apoE*$^{-/-}$ recipients of wt (black circles), *cx*$_3$*cr1*$^{gfp/+}$ and *cx*$_3$*cr1*$^{gfp/gfp}$ BM cells, either from hMRP8Bcl2 transgenic (hBcl2 tg) or non-transgenic (non tg) donors. Atherosclerotic plaques were analyzed in aortic roots and en face prepared aortas by Oil-red-O staining. Each group represents either five or six *apoE*$^{-/-}$ recipients of three distinct BM donors. *pValue<0.01, **pValue<0.05.

Figure 5: Foam cells express CX_3CR1 and hBcl2 transgene

A) Histology of atherosclerotic plaque analyzing CX_3CR1/GFP expression by foam cell. Irradiated *ApoE*$^{-/-}$ recipients of *cx*$_3$*cr1*$^{gfp/+}$ BM were analyzed for Orange Oil

deposition, as well as MOMA-2 and CX_3CR1/GFP expression. Arrow indicates GFP-labeled foam cells identified by MOMA-2 expression and orange oil deposit and size.

B) Irradiated *ApoE*$^{-/-}$ recipients of *cx*$_3$*cr1*$^{gfp/+}$;hMRP8*bcl2*, *cx*$_3$*cr1*$^{gfp/+}$, *cx*$_3$*cr1*$^{gfp/gfp}$ and *cx*$_3$*cr1*$^{gfp/gfp}$;hMRP8*bcl2* BM cells were analyzed for plaque CX_3CR1/GFP expression. Bar diagram represents the percentage of GFP$^+$ area out of total plaque area. n=6 mice. *pValue<0.05, **pValue<0.005.

C) Aortic root plaques of irradiated *ApoE*$^{-/-}$ recipients of wt or hMRP8bcl2 transgenic BM were analyzed for bcl-2 expression. Arrow indicate hBcl2-stained foam cells, identified by typical size.

Supplementary 1: Differential effect of enforced bcl2 expression on the two monocyte subsets.

A) Expression of hBcl2 transgene by monocyte subsets. MACS purified CD115$^+$ blood cells from *cx*$_3$*cr1*$^{gfp/+}$;hMRP8Bcl2 and *cx*$_3$*cr1*$^{gfp/+}$ littermates were stained with anti-Gr1 and anti-human Bcl2 antibodies. Dot plot shows Gr1^{hi} (R7 gated cell) and Gr1^{low} (R8 gated cell) monocyte populations. Histograms show hBcl2 expression by the subsets of hMRP8Bcl2 transgenic and non-transgenic mice.

B) Comparison of blood monocyte populations of wt and hMRP8bcl2 mice. Diagram shows the numbers of total Gr1^{hi} and Gr1^{low} monocytes (identified as indicated in Fig. 1A) in 1 ml of blood. Note that bcl2 expression rescues more Gr1^{low} than Gr1^{hi} monocytes.

Supplementary 2: Immunohistochemical analysis of atherosclerotic plaques of *ApoE*$^{-/-}$ BM chimeras

Irradiated *ApoE*$^{-/-}$ recipients of *cx*$_3$*cr1*$^{+/+}$;hMRP8*bcl2*, *cx*$_3$*cr1*$^{gfp/+}$, *cx*$_3$*cr1*$^{gfp/gfp}$ and *cx*$_3$*cr1*$^{gfp/gfp}$;hMRP8*bcl2* BM cells were analyzed for MOMA-2 and CX_3CR1/GFP expression. One representative of six mice.

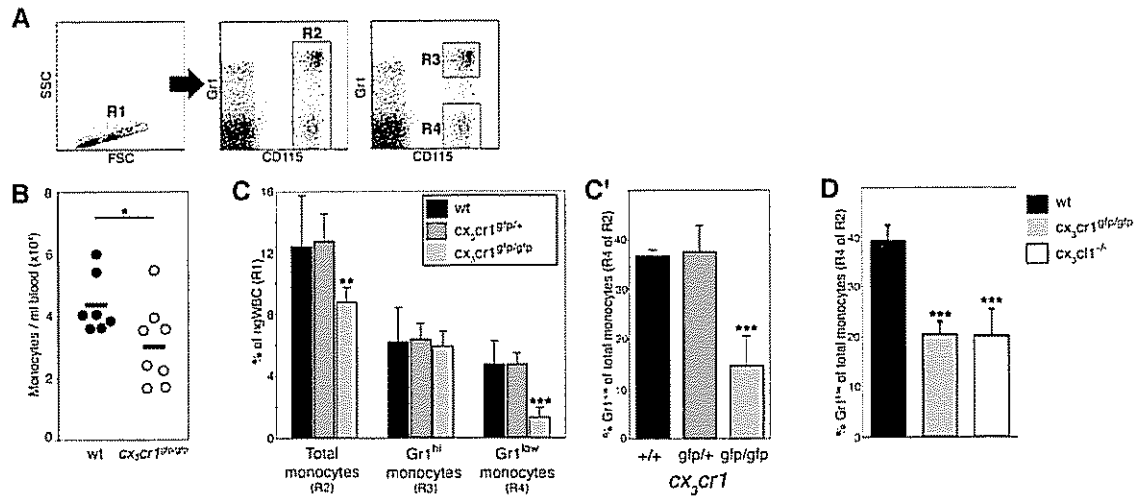
A
SSC
R1
FSC
Gr1
R2
CD115
Gr1
R3
R4
CD115
B
Monocytes / ml blood (x10³)
wt
cx3cr1gfp/gfp
C
wt
cx3cr1gfp/+
cx3cr1gfp/gfp
% of hgWBC (R1)
Total monocytes (R2)
Gr1hi monocytes (R3)
Gr1low monocytes (R4)
C'
% Gr1+/- of total monocytes (R4 of R2)
+/+
gfp/+
gfp/gfp
cx3cr1
D
wt
cx3cr1gfp/gfp
cx3cl1-/-
% Gr1low of total monocytes (R4 of R2)

Figure 1

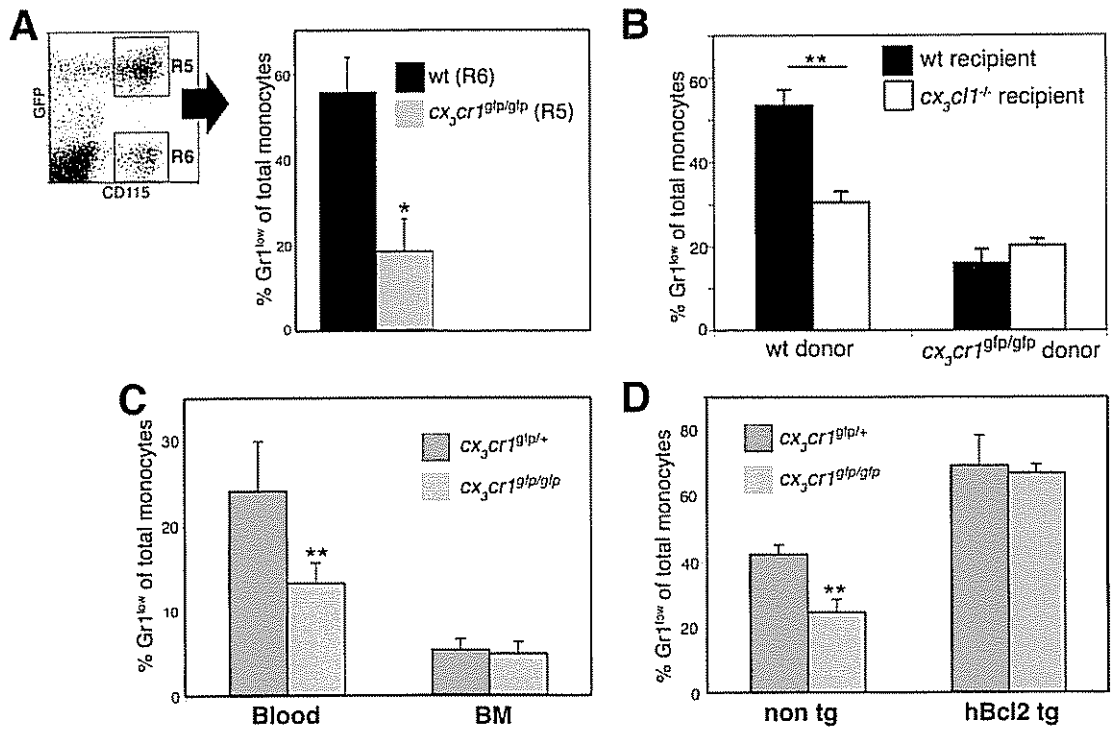
A
GFP
CD115
R5
R6
% Gr1low of total monocytes
wt (R6)
cx3cr1gfp/gfp (R5)
B
wt recipient
cx3cl1-/- recipient
wt donor
cx3cr1gfp/gfp donor
C
cx3cr1gfp/+
cx3cr1gfp/gfp
Blood
BM
D
non tg
hBcl2 tg

Figure 2

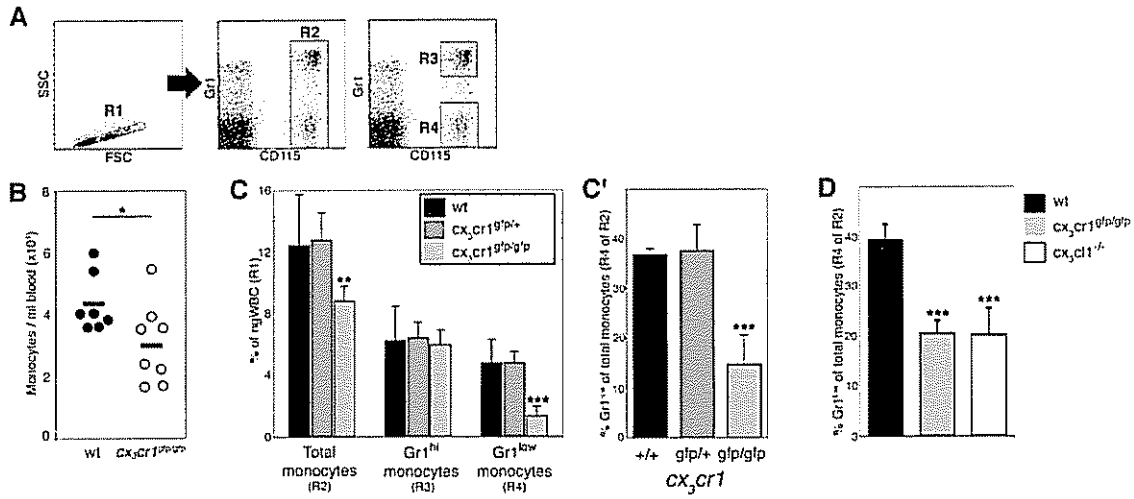
A
SSC
R1
FSC
Gr1
R2
CD115
R3
R4
B
Monocytes / ml blood (x10³)
wt
cx3cr1gfp/gfp
C
wt
cx3cr1gfp/+
cx3cr1gfp/gfp
% of rg/WBC (R1)
Total monocytes (R2)
Gr1hi monocytes (R3)
Gr1low monocytes (R4)
C'
% Gr1low of total monocytes (R4 of R2)
+/+
gfp/+
gfp/gfp
cx3cr1
D
wt
cx3cr1gfp/gfp
cx3cl1-/-
% Gr1low of total monocytes (R4 of R2)

Figure 1

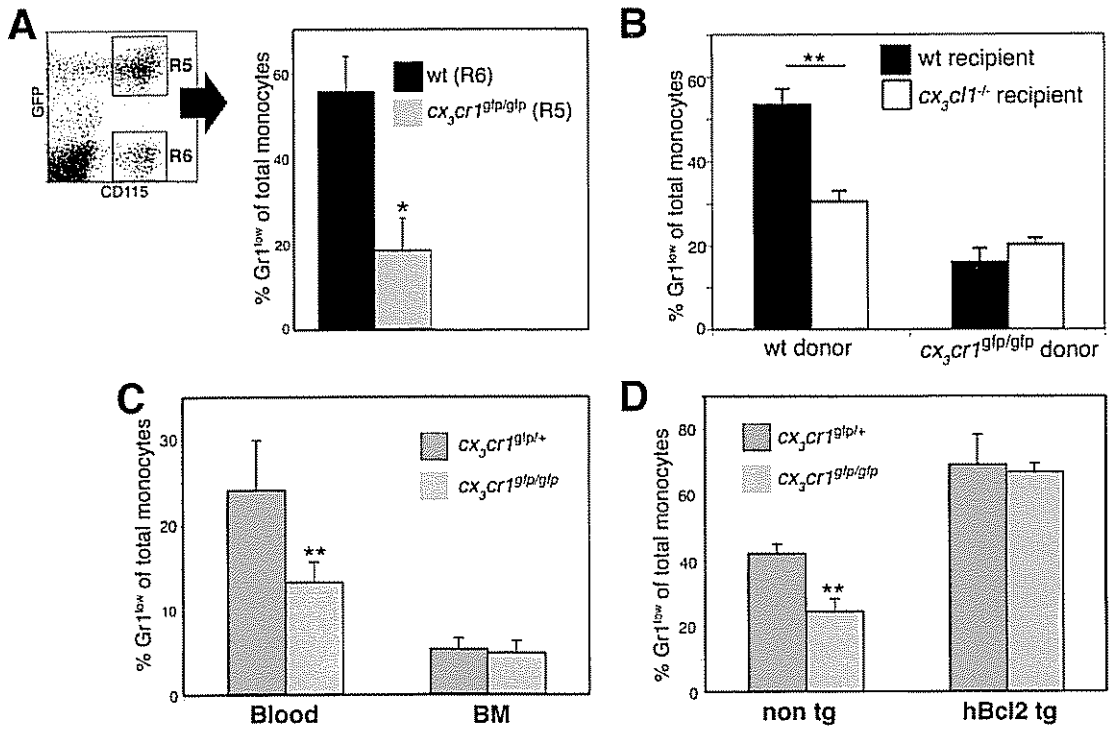
A
GFP
CD115
R5
R6
% Gr1low of total monocytes
wt (R6)
cx3cr1gfp/gfp (R5)
B
wt recipient
cx3cl1-/- recipient
wt donor
cx3cr1gfp/gfp donor
C
cx3cr1gfp/+
cx3cr1gfp/gfp
Blood
BM
D
non tg
hBcl2 tg

Figure 2

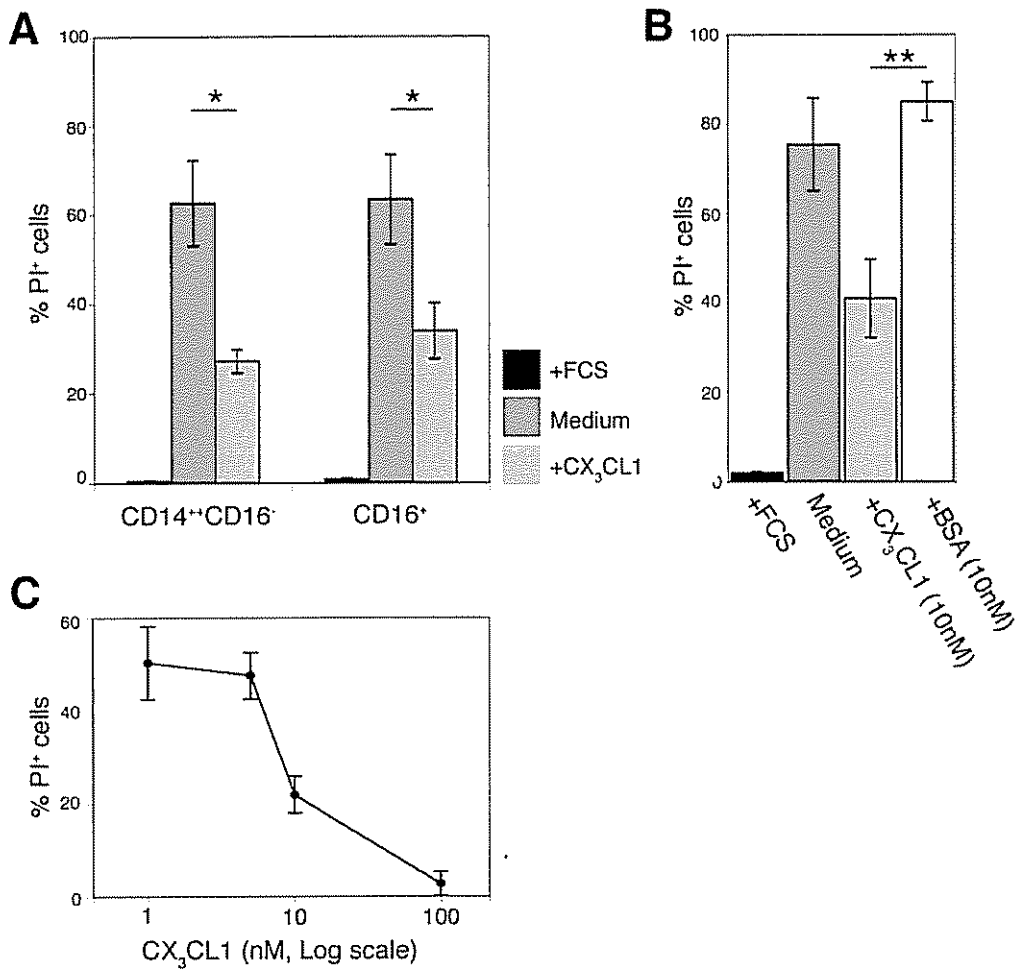
A
100
80
60
40
20
0
% PI+ cells
*
*
CD14++CD16-
CD16+
+FCS
Medium
+CX3CL1
B
100
80
60
40
20
0
% PI+ cells
**
+FCS
Medium
+CX3CL1 (10nM)
+BSA (10nM)
C
60
40
20
0
% PI+ cells
1
10
100
CX3CL1 (nM, Log scale)

Figure 3

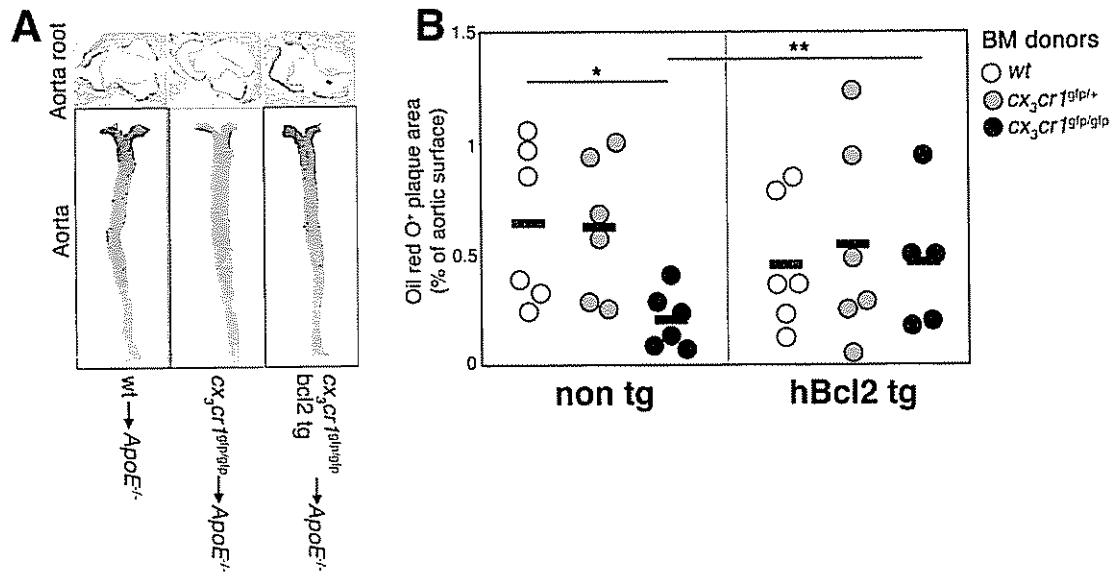

Figure 4

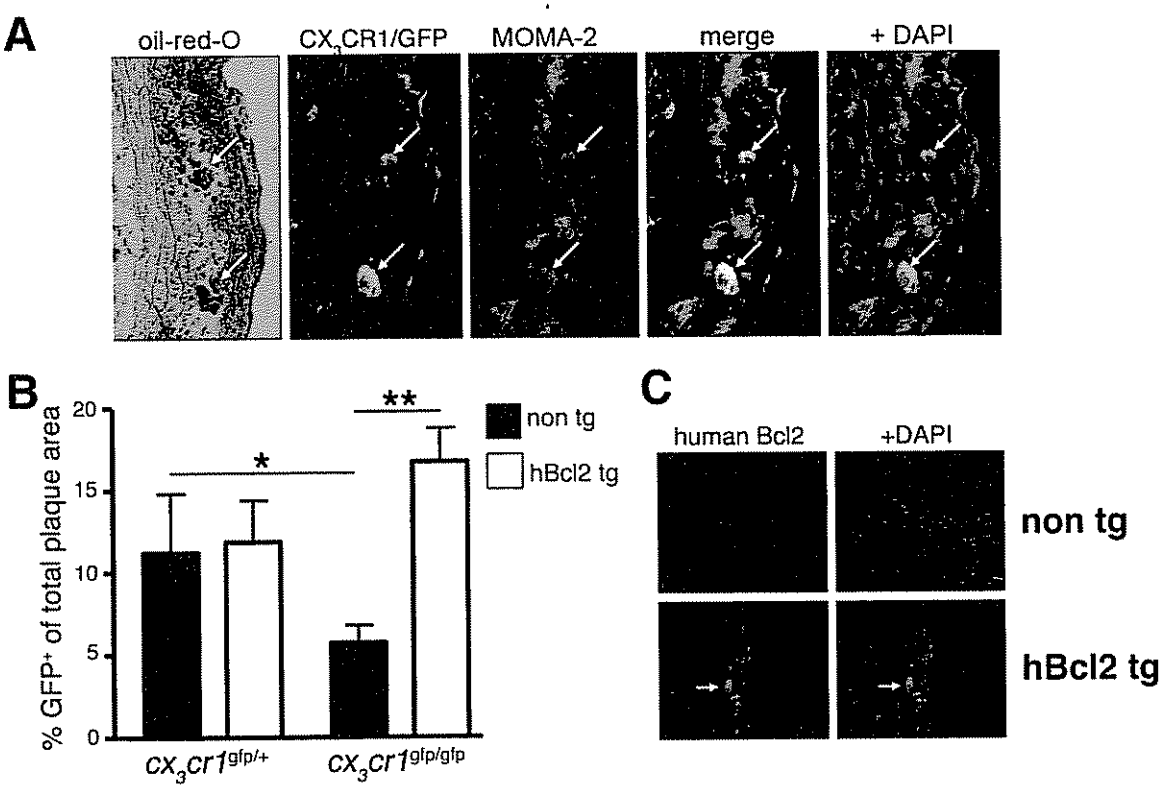

Figure 5

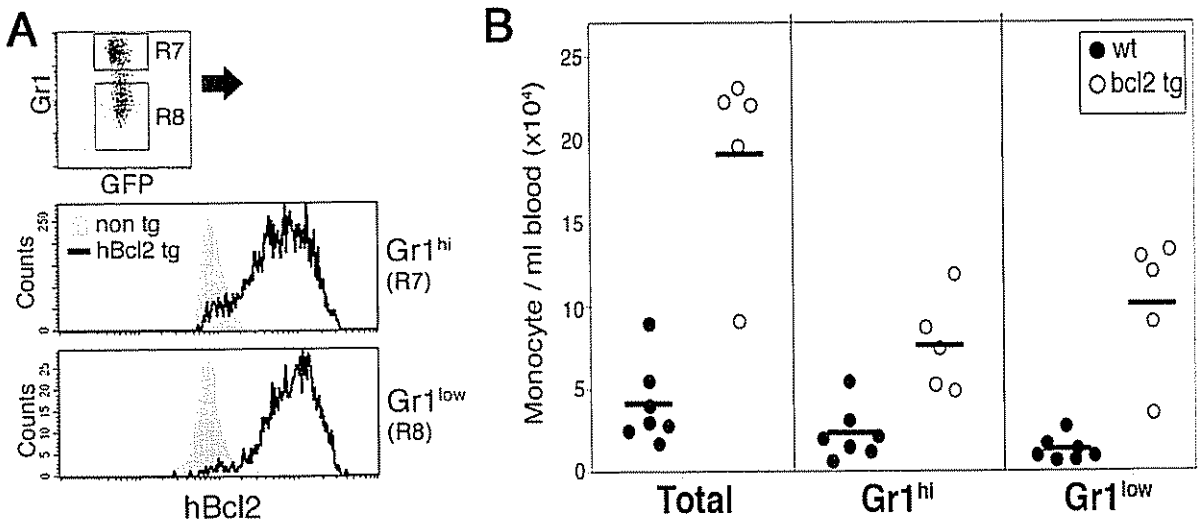

Supplementary 1

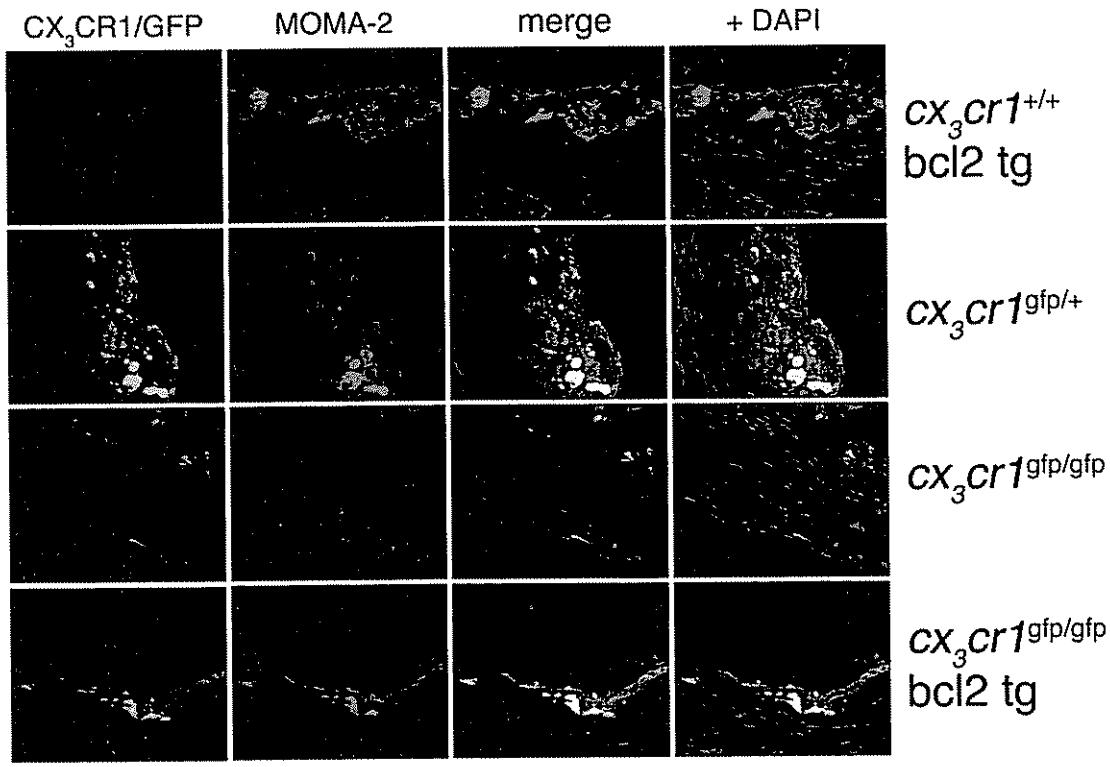

Supplementary 2

Contribution

In two of the attached manuscripts I am a shared leading author

The manuscript entitles **"Trans-Epithelial Pathogen Uptake into the Small Intestinal Lamina Propria"** summarizes a study done together with a visiting student from France, Alexandra Vallon-Eberhard. In this project I performed some of the experiments and participated in the research design and analysis.

The manuscript entitles **"CX_3CR1 mediated cell survival signals in monocyte homeostasis and atherogenesis"** summarizes a study done together with Liat Bar-On, a PhD student in the lab. In this work I designed the experiments, helped in the execution and participated in data analysis. In addition, I wrote the manuscript summarizing our result, which is currently submitted for publication.